

***Development of Specifications and Performance Criteria
for Surface Preparation
Based on Issues Related to Bond Strength***

CRC Cooperative project

Report prepared

by

B. Bissonnette (Laval University, Canada)
L. Courard (University of Liège, Belgium)
A. Garbacz (Warsaw University of Technology, Poland)
B. Robertson (Bureau of Reclamation, U.S.A.)
A.M. Vaysburd (Vaycon Consulting, U.S.A.)
K.F. von Fay (Bureau of Reclamation, U.S.A.)

June 2016

Executive summary

Table of contents

Executive summary	i
Table of contents	ii
List of figures	iii
Section 1 – Introduction.....	1
1.1 Background Bond in Repair / Overlay Composite Systems	4
1.2 Objective and Scope	8
1.3 References	11

List of figures

Figure 1-1: Schematics of mechanical shear and tensile bond between substrate and repair, resulting from interlock mechanisms	5
Figure 1-2: Weak zone between substrate and repair system	6
Figure 1-3: Idealized model of a surface repair system.....	7

Section 1 – General introduction

1.1 Background

The aim of concrete repair or overlay¹ is to prolong the service life of the deteriorated/distressed structure or its element, to restore the load-carrying capacity and the stiffness or to strengthen the structure or its member. Consequently, monolithic action in the produced composite repair system is critical. A prerequisite for monolithic action is sufficient lasting bond between existing substrate and the new-cast repair/overlay material.

The long-term performance of concrete repairs and overlays can be to a large degree linked to their resistance to debonding and cracking.

The mechanisms of cracking and debonding are complex and mainly depend on material characteristics, environmental influences and degree of restraint. The most important repair/overlay material characteristics with respect to the bond are tensile strength and extensibility properties of the viscoelastic repair materials and volume changes caused by shrinkage. Development and magnitude of interface bond strength and most importantly bond durability further greatly depend on substrate surface preparation and workmanship during repair/overlay application.

The mechanisms and characteristics of bond between existing concrete and repair materials with respect to various factors and influences have been the object of a many studies in the

¹ In ICRI Concrete Repair Terminology (2010), an overlay is defined as *a bonded or unbonded layer of material placed on a concrete surface to either restore or improve the function of the previous surface*. From this point of view, an overlay can thus be considered as a repair, since its performance and durability are depending essentially on the same considerations.

recent years. The number of ongoing research projects in the field, the current state of knowledge, the codes of practice, and especially in-situ repair performances, however show that many questions still remain unresolved. As a result, guidelines and project specifications for the design and implementation of repairs are often deficient in scope, performance criteria and detailing.

The scope of existing guidance and specifications concerning concrete repair bond issues is presently limited. Existing standards and specifications can basically be divided in design specifications for concrete repairs and structural design procedures for load-bearing concrete overlays.

This is mainly due to the need of further understanding of factors and conditions affecting bond strength and durability as affected by concrete surface preparation for repair/overlay [1]. A number of research projects have been documented in the literature, discussing aspects of bond properties and characteristics in terms of material properties, concrete substrate surface texture and condition, curing procedures, as well as some environmental factors of influence. However, despite the relatively large pool of theoretical knowledge, the practical issues related to surface preparation of existing concrete for repair in order to systematically achieve a lasting interfacial coexistence in a composite repair system are still inadequately addressed; unfortunately, as a result, repair and overlay debonding is still quite often observed.

The need for more practical design and application recommendations has widely been recognized by designers, materials specialists and contractors [2, 3].

Regardless of the cost, complexity and quality of repair material or application method employed, the quality surface preparation of the substrate prior the repair will often determine

whether a repair project is a success or a failure and whether a repaired structure meets the design objectives [4].

The durability, in this context, may be defined as the lasting interfacial coexistence of two composite materials combined in a composite system. Although most of the specified requirements and engineers' considerations tend to focus on the achievement of the prescribed initial bond strength, it must be noted that this parameter can be only considered as a necessary condition, but certainly not a sufficient one. The most critical aspect is the durability of the bond, which is governed to a large extent by the service conditions of the repaired structure.

The concrete substrates are different, one from the other, in age, quality and service exposure: from the relatively new concrete to the most deteriorated one, exposed to various temperatures, relative humidity, chemically aggressive interior (inside the concrete substrate) and exterior environments, electrochemical status and mechanical loads.

At the time this project was undertaken, published data and information allowed for the following characterization of the concrete substrate to be repaired/overlaid:

- it is physically and chemically very complex;
- such complexity is also very variable from case to case;
- the complexity has to be considered on the basis of scale, which is relevant and dependent on the particular situation;
- practical answers and guidance/performance criteria at the present time, as well as the problem of achieving optimum bond in the repair/overlay composite systems, depend more upon broad judgment and experience than detailed knowledge.

An in-depth literature survey on concrete repair bond issues carried out at the onset of this project have revealed that many critical details and parameters are still little known. Research is thus needed in order to develop or improve field test characterization methods, in order to

enable the identification and field assessment of dependable performance criteria (QA & QC) for practical repair applications.

1.2 Bond in repair and overlay composite systems

The characteristics of adhesion or “bond” can be studied from two opposite perspectives. On the one hand, it can be addressed based upon the conditions and nature of the contact between two materials, taking into account different bond mechanisms. On the other hand, it can be appraised through a quantitative measurement of the magnitude of adhesion, usually expressed in terms of stress or energy required to separate the two materials. In practice, available information on repair adhesion commonly refers to the equivalent average tensile stress required to separate the concrete substrate and the repair material [5].

The term “adhesion” describes the condition in the boundary layer between two bonded materials with a common interface. Adhesion mechanisms can be divided basically into thermodynamic mechanisms, chemical bonding and mechanical interlocking.

Mechanical adhesion in repaired concrete members relies on the penetration and hardening of the repair material inside the open cavities and asperities at the surface of the concrete substrate and the physical anchorage resulting therefrom. Capillary absorption plays an important role in the anchorage effect, as it draws cement paste (or any other binding system being used) into small cavities of the substrate. The extent of this effect is dependent on the moisture condition of the substrate (mainly the surface moisture) and the viscosity of the repair product.

It is important to note that mechanical adhesion in tension differs significantly from that in shear: for instance, a high interface roughness may improve shear bond strength, whereas tensile mechanical bond strength primarily depends on vertical anchorage in pores and voids (Figure 1-1).

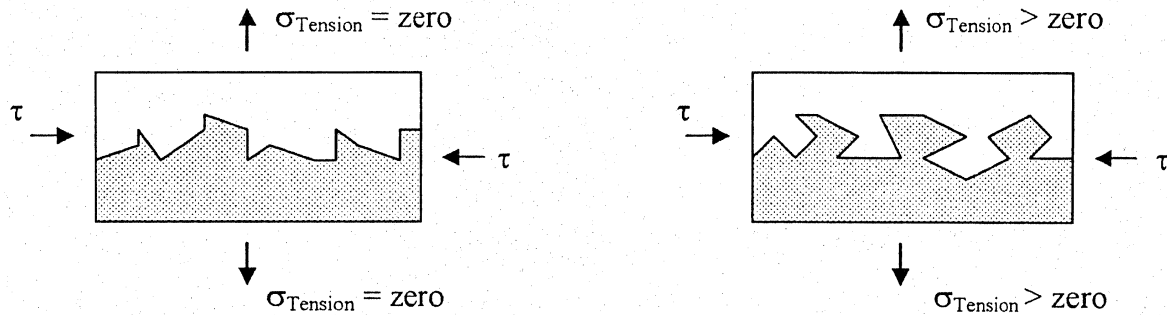


Figure 1-1: Schematics of mechanical shear and tensile bond between substrate and repair, resulting from interlock mechanisms [6]

The above is important for the correct choice of bond strength test methods and for appraising the relationship between the measured shear and pull-off (tensile) bond strengths. Usually, differential volume changes resulting from drying shrinkage or temperature gradients cause both shear and tensile stresses at the interface. In structural design, tensile stresses perpendicular to the interface are rare. By contrast, interface shear stresses occur frequently in composite systems such as repairs and overlays. Standards, specifications and established practice in concrete repair field define bond strength commonly in relation to tensile strength (pull-off bond test) alone which, according to the above considerations, may be insufficient. Still today, the pull-off test is the only method commonly applied in the testing of bond strength on real structures.

Pigeon and Saucier [7] consider the interface between old and new concrete to be very similar to the well-known ITZ (interfacial transition zone) developing between the

the cementitious matrix in the bulk concrete. According to them, its formation is deeply by the “wall effect”, which leads to the presence of a weak layer within the resulting transition zone (Figure 1-2: Weak zone between substrate and repair system [7])

). Many will argue that the presence and extent of such a weak zone is dependent on the surface preparation performed prior to repair.

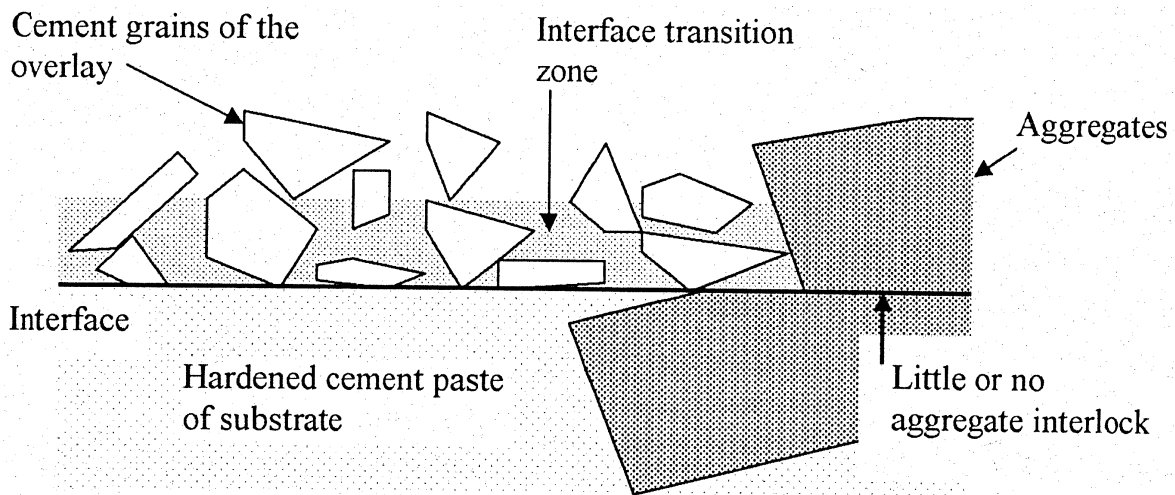


Figure 1-2: Weak zone between substrate and repair system [7]

Emmons and Vaysburd [8] presented an idealized model of a surface repair as a three-phase composite system, consisting of the existing concrete, the repair material and a transition zone between them (Figure 1-3). The authors stated that the characteristics of the transition zone are a function of the properties of the substrate (adherent), the properties of the repair material (adhesive) and the substrate surface preparation. Environmental factors, such as temperature or moisture, also play an important role on the properties of the interface region and on interfacial bond development.

A possible macroscopic characterization of the quality or degree of adhesion is obtained by the introduction of a transition zone along the geometrical interface between the adhesive and adherent phases. The thickness of the transition zone is the sum of the lengths in the adherent and the adhesive, where interactive forces of any nature change the mechanical nature of the original continuum [9]. This explains why the authors are referring to the so-called “*interphase zone*” [10].

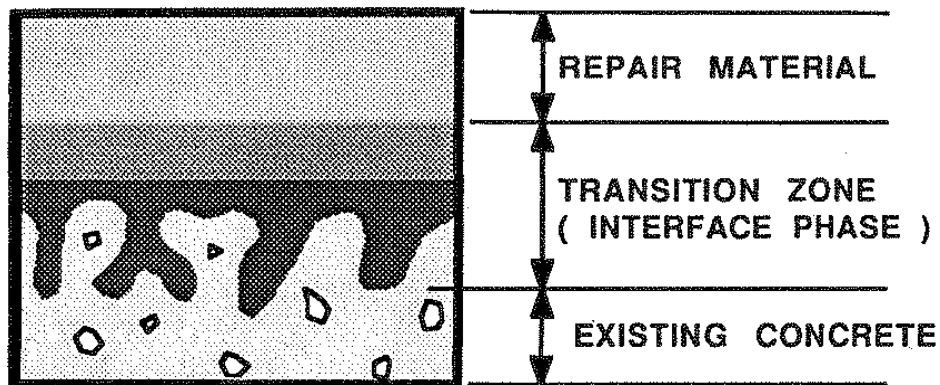


Figure 1-3: Idealized model of a surface repair system [8]

Adherence between a repair layer and the existing concrete is a case of adhesion between two solids, as a result of setting and hardening of an initially semi-liquid substance (repair material mixture) poured on a solid substrate (existing concrete).

The following factors exert primary influence the development of the transition zone and the resulting bond durability:

- physical and chemical properties of the concrete substrate;
- characteristics and condition of the prepared surface;
- physical and chemical properties of the repair material;
- environmental conditions (notably moisture and temperature).

The repair material and concrete substrate, similar to a variety of glued connections, can be considered as a contact connection where the constitutive binder in the repair material acts as the glue. In this case, the bond strength can be considered to be the result of mechanical interlocking, specific adhesion, and cohesion.

Mechanical anchorage of the repair develops within the roughness and the porosity of the substrate surface. When estimating the effect of the existing substrate, not only its roughness, but also the size and form of protrusions must be taken into account. In the case of extended and gentle unevenness, an increase of the bond strength only comes essentially with an increase in the effective contact area. The specified properties of the repair material (e.g. consistency, method of compaction, etc.) may have a considerable influence on mechanical anchorage and adhesion. The bond strength developing between existing concrete and a repair layer also depends to a great extent on cohesion of the repair material, which itself is determined by the actual strength of the constitutive binder, its mineralogical components and the conditions prevailing during the period of curing.

Adhesion and cohesion are closely interconnected in the overall formation process of the contact zone. It is assumed that ultimately, adhesion is the most important aspect in the overall bond strength make up.

1.3 Objective and scope

Of critical importance to the long term useful performance of the composite repair/overlay system is the existing concrete surface preparation prior to application of the repair material. Proper surface conditioning is essential for the durability of the repaired structure. The repair

material is often blamed for “*not sticking*”, but the source of the trouble usually stems from inadequate surface preparation.

Therefore, the primary objective of this research study is to identify the fundamental factors and characteristics of concrete substrates prepared for repair/overlay and to develop guideline specifications for surface preparation of existing concrete. The research activities include both laboratory and field testing and evaluation.

The scope of the study include the following:

- to evaluate existing methods for assessment of the roughness parameters of a prepared surface;
- to establish correlations between shear bond strength, pull-off tensile strength, and surface roughness;
- to estimate the effect of load eccentricity in a tensile pull-off test on the bond strength;
- to develop a field test to evaluate the optimum moisture conditioning of the particular concrete substrate;
- to evaluate the effect of concrete carbonation on bond strength;
- to develop performance criteria and guide specifications for surface preparation.

As limitations, even if the scope of the title of the project “*Development of Specifications and Performance Criteria for Surface Preparation Based on Issues Related to Bond Strength*” suggests a wide scope, not all relevant aspects are being dealt with in the research program. In particular, the investigation is limited to normal weight concrete substrates and ordinary cement-based repair/overlay materials (resin-based and lightweight concrete substrates and repair materials are beyond the scope of investigation).

A number of factors have to be considered when addressing the influence of the concrete surface on bond in a composite repair/overlay system, notably the macro- and micro-roughness

of the substrate surface, its mechanical integrity, its absorptivity and moisture content, its porosity characteristics that will dictate the contact angle with the binding phase, chemical and mineralogical make up of the existing concrete, condition of the substrate and exposure conditions.

The experimental plan is divided into the following six tasks:

- Task 1 : Evaluate existing techniques for characterisation of concrete surface roughness parameters.
- Task 2 : Establish relationships between tensile bond, shear bond and surface roughness parameters.
- Task 3 : Evaluate the effect of load eccentricity in a tensile pull-off test on bond strength results.
- Task 4 : Develop a field test to evaluate the optimum moisture conditioning of the particular concrete substrate.
- Task 5 : Evaluate the effect of carbonated concrete substrate on bond strength.
- Task 6 : Develop performance criteria for achieving adequate bond in composite repair systems and guide specifications for concrete surface preparation prior to repair based on the results of the study.

In those tasks the following surface treatment techniques are investigated:

- jackhammering;
- sandblasting;
- scarifying;
- shotblasting;
- water jetting.

Supported by experimental test results and theoretical background, this research aims at a better understanding of strength and long-term performance of repairs and bonded overlays. Experimental procedures and test parameters were chosen based on the literature review and the related experience gained by the investigators (research, design and practice).

1.4 References

1. Courard, L., Garbacz, A. (2006) Failure of concrete repair: how to avoid it?, *Proceedings of the 2nd International Symposium on Advances in Concrete through Science and Engineering* (Ed. J. Marchand, B. Bissonnette, R. Gagné, M. Jolin, F. Paradis), Quebec, Canada, 167-191.
2. Vaysburd, A.M., Emmons P.H., Mailvaganam, N.P., McDonald, J.E., Bissonnette, B. (2004), Concrete Repair Technology – A revised approach is needed, *Concrete International*, 1: 59-65.
3. Granju, J.-L. (2004) 193-RLS RILEM TC Bonded Cement-based Material overlays for the Repair, the Lining or the Strengthening of Slabs or Pavements, *State-of-the-Art Report*, France, 114 p.
4. Vaysburd A.M., Sabnis, G.M., Emmons, P.H., McDonald, J.E. (2001) Interfacial Bond and Surface Preparation in Concrete Repair, *Indian Concrete Journal*, 15: 27-33.
5. Courard, L. (1999) How to analyse thermodynamic properties of solids and liquids in relation with adhesion?, *Proceedings of the 2nd International RILEM Symposium ISAP' 99*, 9-19.
6. Beushausen H.D. (2005) Long-term Performance of Bonded Concrete Overlays Subjected to Differential Shrinkage, Ph.D. Thesis, University of Cape Town, South Africa, 265 pp.
7. Pigeon, M., Saucier, F. (1992) Durability of repaired Concrete Structures, *Proceedings of International Symposium on Advances in Concrete Technology*, Athens, 741-773.
8. Emmons, P.H., Vaysburd, A.M. (1993) Factors Affecting Durability of Concrete Repair, *Proceedings of Fifth International conference on Structural Faults and Repair – 93*, Edinburgh, UK, 253-267.
9. Cardon, A.H., Hiel, C.C. (1986) Durability Analysis of Adhesive Joints, *RILEM Symposium on Resin Adherence to Concrete*, Paris, 3-7.

10. Courard, L., Darimont, A. (1998) Appetency and adhesion: analysis of the kinetics of contact between concrete and repairing mortars, *RILEM International Conference, Interfacial Transition Zone in Cementitious Composites* (Eds. A. Katz, A. Bentur, M. Alexander and G. Arliguie, E&FN Spon), Haifa, Israël, 185-194.

Table of contents

Table of contents	i
List of tables	iii
List of figures	iv

Section 2 – Evaluation of existing techniques for the characterization of concrete surface roughness (CRC Proposal Task 1) 1

2.1	Introduction	1
2.2	Concrete surface profile (CSP).....	4
2.3	Sand patch test	5
2.4	Mechanical profilometry	6
2.5	Laser profilometry	8
2.6	Interferometric surfometry.....	10
2.7	Profile description	11
2.8	Profile description with advanced methods.....	16
2.9	Experimental comparison and analysis of the techniques	17
2.9.1	Concrete substrates and surface treatments.....	17
2.9.2	Evaluation of concrete surface texture with sand patch test	19
2.9.3	Mechanical vs. laser profilometry	23
2.9.4	Surface roughness characterization with the microscopic observation method	27
2.9.5	Concrete surface texture evaluated with mechanical and interferometric methods.....	30
2.9.6	CSP profiles vs. interferometric measurements	34

2.10 Conclusions	35
2.11 References.....	37
2.12 Standards and test methods.....	40

List of tables

Table 2-1:	Comparison of various methods of concrete surface geometry characterization	3
Table 2-2:	Concrete surface treatment methods and corresponding CSP's.....	4
Table 2-3:	Vertical amplitude parameters of surface profile as per EN ISO 4287	7
Table 2-4:	Horizontal amplitude parameters of surface profile as per EN ISO 4287	8
Table 2-5:	Surface profile make up.....	14
Table 2-6:	Abbott curve parameters	15
Table 2-7:	Composition and compressive strength of tested concrete substrates	19
Table 2-8:	Results of the sand patch test for the various surface treatment techniques	20
Table 2-9:	SEM observations of concrete surfaces after various treatments	21
Table 2-10:	The examples for concrete surface roughness representation with mechanical (left) and laser (right) profilometry	24
Table 2-11:	Stereological parameters evaluated with the microscopic method for various types of surface preparation	28
Table 2-12:	Surface preparation of specimens tested through interferometric and mechanical profilometry.....	31
Table 2-13:	Surface profile characteristics determined through mechanical profilometry – waviness (<i>W</i>), roughness (<i>R</i>) and Abbot parameters (<i>C</i>).....	32
Table 2-14:	Surface profile characteristics determined through interferometric profilometry – overall shape (<i>F</i>), meso-waviness (<i>M</i>) and Abbot parameters (<i>C</i>).....	34

List of figures

Figure 2-1:	Measurement of surface macrotexture with the sand patch test procedure.....	5
Figure 2-2:	Mechanical profilometer developed at the University of Liège – a) scheme of the measuring device; b) stylus used in concrete surface roughness evaluation; c) influence of the stylus geometry on the recorded profile.....	7
Figure 2-3:	Examples of 3D representation with surfometry, waviness and roughness profiles after different surface treatments, as determined through mechanical profilometry (University of Liège).....	9
Figure 2-4:	Laser profilometry with optical displacement meter – a) experimental setup; b) 3D representation of a shotblasted concrete substrate (Warsaw University of Technology).....	10
Figure 2-5:	Examples of 3D representation of specimen surfaces obtained by laser profilometry after waviness and roughness filtering	12
Figure 2-6:	Optomorphological profilometry – a) principle of measurement; b) relationship between form and level line; c) testing equipment; d) example of 3D representation of concrete surface (University of Liège).....	13
Figure 2-7:	Laser profilometry – a) schematic representation of the laser profiling testing device; b) line laser; c) laser image of a concrete surface	13
Figure 2-8:	Effect of scale on profile decomposition.....	14
Figure 2-9:	The Abbott curve and its interpretation	15
Figure 2-10:	Illustration of a) sampling for microscopic observation; and b) surface geometry characterization with laser and mechanical profilometry.....	18
Figure 2-11:	a) Significance of the R_S and R_L parameters; b) evaluation of the R_S value using grid of cycloids.....	18
Figure 2-12:	Influence of the sand volume used in the sand patch test	23
Figure 2-13:	Waviness parameters a) W_t and b) W_a ; microroughness parameters c) R_t and d) R_a ; as determined through laser and mechanical profilometry.....	25
Figure 2-14:	Relationships between waviness parameters a) W_a , b) W_t and W_v and c) Abbott parameters, determined through laser (Δ) and mechanical (\bullet) profilometry; d) relationship of W_{as} and W_{ap} vs. SRI.....	27
Figure 2-15:	Relationships a) R_S vs. SRI and b) R_S vs. arithmetic mean deviation of waviness profile, as determined through laser (W_{as}) and mechanical (W_{ap}) profilometry	30
Figure 2-16:	Concrete surface profiles obtained with selected surface preparation methods ...	31

Figure 2-17: 3D representation of surfaces and corresponding roughness and waviness
À profiles for three different types of treatment 33

Figure 2-18: Use of an interferometric measuring device for concrete surface
characterization 34

Figure 2-19: ICRI CSP evaluation (Guideline No. 310.2R–2013) – a) photographs of the nine
replicates ordered from 1 to 9; b) characterization of the CSP replicates
performed by Perez et al. using an interferometric method [5] 35

Section 2 – Evaluation of existing techniques for the characterization of concrete surface roughness (CRC Proposal Task 1)

This section of the report is related to Task 1 of the project, which is devoted to the evaluation of existing techniques for the characterization of concrete surface roughness. For the most part, the research operations have been performed in the laboratories of the Department of Building Materials Engineering (DBME) at the Warsaw University of Technology (Poland), GeMMe Building Materials in the ArGEnCo Department at the University of Liège (Belgium), and Laval University, Quebec (Canada).

2.1 Introduction

The roughness of the substrate is one of the parameters often considered to affect adhesion strength between repair material and existing concrete.

Nevertheless, this has been controversial for a number of years: some reported bond test results have shown that surface roughness exerts only a minor influence on the tensile bond. For instance, in the tests performed by Silfwerbrand [1], adhesion to rough, water-jetted surfaces was compared with bond to smooth sandblasted surfaces. It was concluded that there could be a roughness “threshold value” beyond which further improvement of the substrate roughness would not enhance bond strength. According to these test results, the “threshold value” ought to be close to the surface roughness of typical sandblasted surfaces. However, it remains the opinion of many specialists in the industry that a rougher surface is beneficial to bond strength. Given that roughness depends directly on the surface preparation method, the investigations

presented here are intended to shed new light on the subject and ultimately resolve the controversy.

According to American National Standards Institute (ANSI) [2], the methods for measuring roughness and surface texture can be classified into three types: contacting methods, taper sectioning and optical (non-contacting) methods. Taper sectioning is used in metallurgy and involves cutting across a surface at a low angle α to physically amplify asperity heights by $\text{ctg } \alpha$ [3]. Among the contacting methods there are stylus-type profilometers, tactile tests, measurement of kinetic friction, measurement of static friction, rolling ball measurements, and measurement of the compliance of a metal sphere with a rough surface. Optical (non-contacting) methods include laser profilometry, interferometry and optical reflecting instruments. Light microscopy and scanning electron microscopy may be counted in this group of methods.

A state-of-the-art review on roughness quantification methods for concrete surfaces was recently presented by P. Santos et al. [4] (Table 2-1).

A variety of approaches have been used over the years to characterize the surface roughness of concrete: evaluation of the proportion of the surface occupied by aggregates, measurement of the maximum roughness amplitude, adhesion tests, calculation of surface parameters based on image analysis or on microscopy observations, etc. However, many of these methods are unable to provide a sufficiently detailed representation of the actual surface profile for the calculation of morphological and statistical parameters and are not user-friendly under field conditions. In order to achieve a reliable quantitative analysis of superficial concrete morphology after surface preparation, different profilometry and surfometry techniques can be used [4–10]. The data obtained through such techniques makes it possible to conduct a real quantitative assessment of the surface profile by means of statistical parameters calculated from

the total superficial profile [11] and from the filtered waviness (low frequency/macroroughness) and roughness (high frequency/microroughness) profiles [12]. Some of these parameters, e.g., the arithmetic mean profile and the flatness coefficient, are particularly effective, both for the shape of valleys and peaks, as well as for their amplitude and frequency [13].

Table 2-1: Comparison of various methods of concrete surface geometry characterization [4]

Roughness quantification method	Quantitative evaluation	Non-destructive	Cost	Portable	Work intensive	Contact with the surface
Concrete surface profile (CSP)	No	Yes	Low	Yes	No	No
Sand patch test	Yes	Yes	Low	Yes	No	Yes
Outflow meter	Yes	Yes	Low	Yes	No	Yes
Mechanical stylus	Yes	No	Moderate	No	Yes	Yes
Circular track meter	Yes	Yes	Moderate	Yes	No	No
Digital surface roughness meter	Yes	Yes	Moderate	Yes	No	No
Microscopy	Yes	No	High	No	Yes	No
Ultrasonic method	No	Yes	Moderate	Yes	No	No
Slit-island method	Yes	No	Low	No	Yes	Yes
Roughness gradient method	Yes	No	Low	No	Yes	Yes
Photogrammetric method	Yes	Yes	Moderate	Yes	Yes	No
Shadow profilometry	Yes	Yes	Low	Yes	Yes	Yes
Air leakage method	No	Yes	Low	Yes	No	Yes
PDI method	Yes	No	Low	No	Yes	Yes
2D LRA method	Yes	Yes	Moderate	Yes	No	No
3D laser scanning method	Yes	Yes	High	Yes	No	No

The selected characterization techniques were compared for effectiveness, accuracy, consistency and field applicability. The following techniques were analyzed on a comparative basis:

- *Concrete surface profile* (CSP), in accordance with ICRI Guideline No. 310.2R-2013.
- *Sand patch test*, in accordance with ASTM E965 (similar to EN 13036-1:2010) and EN 1766.

- *Mechanical profilometry*, in which a high-precision extensometer is moved over the entire surface to obtain a 3D map (with x, y and z coordinates) from which morphological parameters are computed.
- *Laser technique*, in which the superficial elevation (distance from the laser beam source to the object) of each point is calculated on the basis of the laser beam transit time.
- *Interferometric profilometry*, based on observation and analysis of the shadow produced by the superficial roughness of the surface (moiré fringe pattern principle).

The aim of this task is to identify the most suitable techniques for both laboratory and field use, as well as the most relevant quantitative roughness characteristics [14].

2.2 Concrete surface profile (CSP)

The visual observation of surface roughness is the simplest evaluation method, but it is rather subjective. The systematic approach for visual surface qualification was proposed by ICRI (ACI 562 Repair Code). The reference replicates that make up the CSP (Table 2-2) represent concrete surfaces after typical surface treatments commonly used in the field: details are given in the ICRI Guideline No. 03732. The range of evaluation is, however, limited to gentle surface treatments.

Table 2-2: Concrete surface treatment methods and corresponding CSP's

Profile reference replicates	Surface preparation methods	CSP
	Detergent scrubbing	1
	Low-pressure water cleaning	1
	Acid etching	1-3
	Grinding	1-3
	Abrasive blasting (sand)	2-5
	Steel shotblasting	3-8
	Scarifying	4-9
	Needle scaling	5-8
	Water jetting	6-9
	Scabbling	7-9
	Flame blasting	8-9
	Milling/rotomilling	9

2.3 Sand patch test

The sand patch tests described in ASTM E965 (very similar to EN 13036-1:2002) is one of the most commonly used methods for examining the macrotexture depth of concrete surfaces, mainly for road and airfield pavements. This method consists in careful application of a specific volume and grading of particles (glass spheres or sand) onto a surface and subsequent measurement of the total area covered (Figure 2-1).



Figure 2-1: Measurement of surface macrotexture with the sand patch test procedure

The surface roughness is characterized by the mean texture depth (MTD), calculated in accordance with Equation 2-1:

$$MTD = \frac{4V}{\pi D^2} [mm] \quad (2-1)$$

where: V = volume of granular material [mm^3]

D = diameter of circle covered by granular material [mm]

A similar method for evaluating surface roughness is proposed in the European standard EN 1766:2000 in the case of concrete substrate preparation prior to repair. Silica sand with a 100/50 μm grading size is recommended for evaluation. The surface roughness index (SRI) is calculated in accordance with Equation 2-2:

$$SRI = \frac{V}{D^2} \cdot 1272 \quad (2-2)$$

where the symbols are the same as in Equation 1-1; $V = 25$ mL is recommended.

The advantages of the sand patch method are its speed, non-destructive character and applicability in situ; a disadvantage is that the surface has to be protected from wind and rain. The main limitations are the range of validity (from 0.25–5 mm only) and the fact that it can be used only on horizontal surfaces.

2.4 Mechanical profilometry

In this method, deviations of the surface geometry are detected by a sensor (stylus) that moves along the surface [3, 4]. The gauge turns vertical deflections of the stylus position into electrical signals which are recorded by the computer, thus creating a surface profile (Figure 2-1a). It is possible to regulate the distance between measurement points for better precision [4]. The geometry (round or conical) and size (radius) of the extremity of the stylus are of prime significance for the profile to record: some profiles characterized by small wavelengths will not be detected if the diamond cone radius is too large (Figure 2-2b, c).

Roughness measurements usually yield images of the profile. To analyze the influence of the treatment on the surface, it is necessary to mathematically and statistically quantify the shape of the surface by means of several parameters (Table 2-3 and Table 2-4). Another approach is surfometry, a surface metrology of the profile rendered in 3D: in this case, the profilometer is used to obtain several profiles in parallel. The results are analyzed in two orthogonal directions (x,y) to generate a 3D representation of the surface (Figure 2-3). This method yields a quantification of the surface geometry, irrespective of its anisotropy [15].

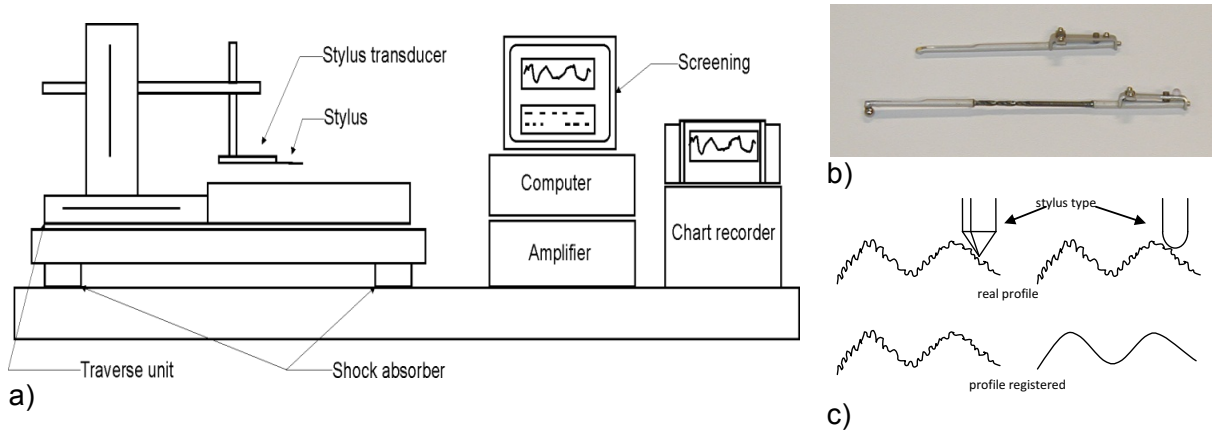
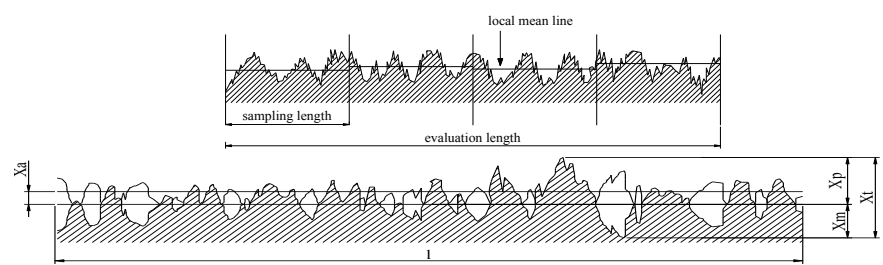


Figure 2-2: Mechanical profilometer developed at the University of Liège – a) scheme of the measuring device; b) stylus used in concrete surface roughness evaluation; c) influence of the stylus geometry on the recorded profile

Table 2-3: Vertical amplitude parameters of surface profile as per EN ISO 4287

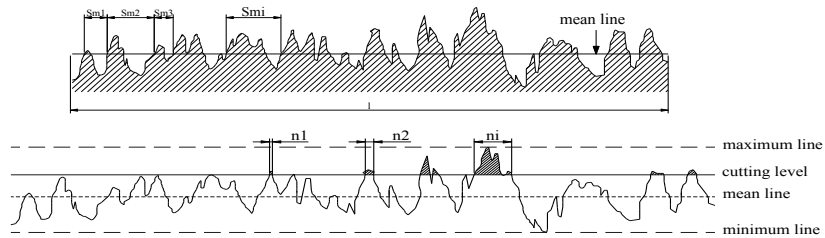
Symbol	Parameters	Definition
m_x	Mean value and line	Line whose height (mean value) is determined by minimal sum square deviation of the profile defined as follows: $X = \min \sum y^2(x)$
X_p	Maximum peak height	Distance between the highest point of the profile and the mean line
X_m	Minimum valley depth	Distance between the lowest point of the profile and the mean line
X_t	Maximum height	Maximum distance between the lowest and the highest point of the profile and its equal: $X_t = \max(X_p + X_m)$
X_a X_a'	Arithmetic mean deviation	Mean departure of the profile from the reference mean line as follows: $X_a = \frac{1}{l} \int_0^l y(x) dx$, approximated by $X_a' \approx \frac{1}{n} \sum_{i=1}^n y_i $
X_q	Root mean square deviation	Statistical nature parameter defined in the limits of the cut-off length as follows: $X_q = \frac{1}{l} \int_0^l y^2(x) dx$



R = roughness, W = waviness, P = total profile (instead of index "X")

Table 2-4: Horizontal amplitude parameters of surface profile as per EN ISO 4287

Symbol	Parameters	Definition
S_k	Skewness of surface height distribution	A measure of asymmetry of profile deviations about the mean line, as follows: $S_k = \frac{1}{R_q^3} \frac{1}{n} \sum_{i=1}^n Y_i^3$
S_m	Mean period of profile roughness	Mean value of mean line consecutively including a peak and a valley S_{mi} , as follows: $S_m = \frac{1}{n} \sum_{i=1}^n S_{mi}$
n_p	Bearing length	Sum of partial lengths n_i corresponding to the profile cut by a line parallel to the mean one for a given cutting level
t_p	Bearing length ratio	Ratio between bearing length and cut-off length, expressed as a percentage: $t_p = n_p/l$.



2.5 Laser profilometry

The laser profilometry method essentially consists in laser travel measurement with an optical displacement sensor [10], as shown in Figure 2-4. The most recently developed laser profilometers are fast and accurate and allow the measurement of surface topography down to the sub-micrometer level over an area of 500 × 500 mm, in both 3D and 2D outputs. The technique is based on the principle of optical triangulation and requires a light source (commonly a diode laser), imaging optics and a photodetector. A diode laser is used for generating a collimated beam of light, which is then projected onto a target surface. A lens is focused on the spot of the laser light reflected onto a photodetector, which generates a signal that is proportional to the spot's position on the detector. As the target surface height changes (z), the image spot may shift due to the parallax. The sensor scans in two directions (x,y) to generate a 3D image of the surface of the element being characterized. Examples of concrete surface profiles generated through laser profilometry are presented in Figure 2-5.

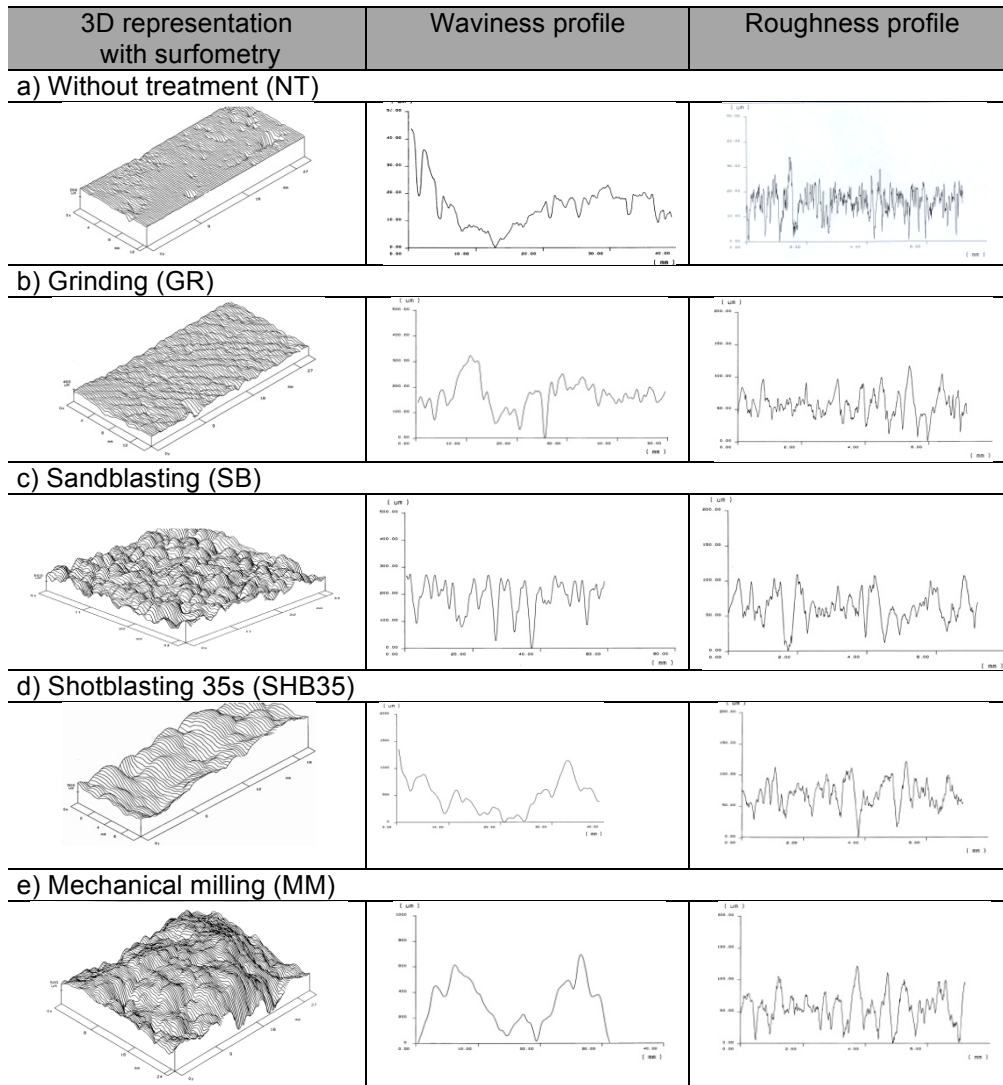


Figure 2-3: Examples of 3D representation with surfometry, waviness and roughness profiles after different surface treatments, as determined through mechanical profilometry (University of Liège)

The first applications of commercial laser profilometry were used to characterize surface geometry for tribology [11]. The technique has also been used to characterize concrete surfaces [8-11].

The recently developed circular track meter (CTM), in which a CCD laser displacement sensor is used, belongs to the same group of profilometers. Eight individual segments are analyzed to investigate profile at different angles (0° , 45° and 90°) with respect to the traveling

direction. The CCD is mounted on an arm which is driven by a DC motor and rotates at 80 mm above the surface with a 142 mm radius. The data are segmented into eight 111.5 mm arcs of 128 samples each. The profile characterization data generated with CTM are the average profile depth and the root mean square (RMS). More details can be found in the ASTM E2157-01 standard.

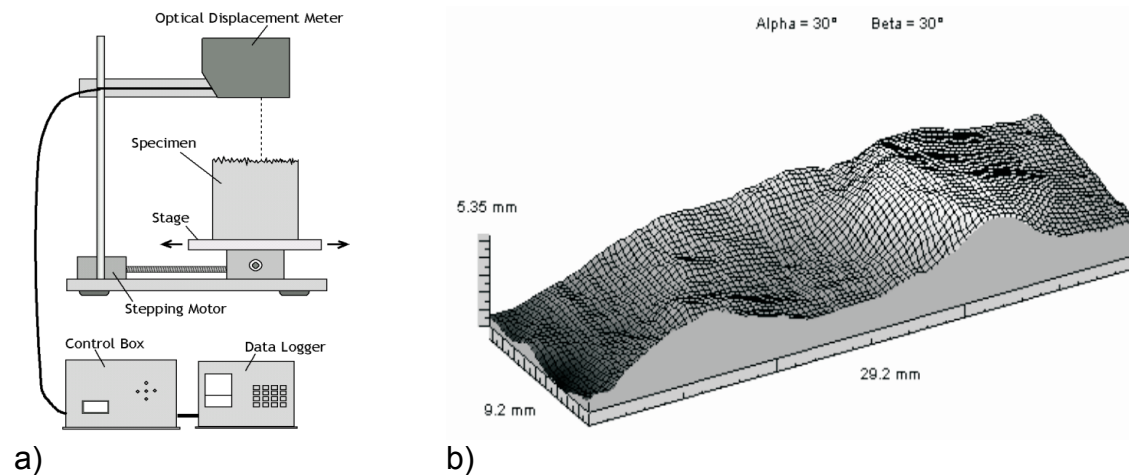


Figure 2-4: Laser profilometry with optical displacement meter – a) experimental setup; b) 3D representation of a shotblasted concrete substrate (Warsaw University of Technology)

2.6 Interferometric surfometry

The various types of profilometers described before are mainly used in laboratory conditions. Recent studies have been devoted to the development and experimentation of optical devices (Figure 2-6a) which can be used in the field for civil engineering applications [6, 7, 14, 16]. Systems based on the moiré projection technique are exhibiting very interesting potential for that purpose. The moiré phenomenon appears when two networks of light rays, made of equidistant lines (alternately opaque and transparent) are superimposed. The technique of surface profile characterization is based on the measurement of a parallel fringe pattern from a deformed

pattern projected on a non-plane surface (Figure 2-6b). The moiré fringes are similar to level lines representing the height variations of the object's surface. When a network of parallel fringes is projected onto a plane surface, it will not be deformed, but when projected onto an unspecified shape, this same network will be deformed. The main principle of the test is to compare two images with different moiré networks. The first image is the reference: it corresponds to the network of non-deformed parallel fringes. The second image contains the projected network deformed with respect to the non-plane shape. An algorithm analyzes the image and compares the grid of calibration and the deformed grid.

Maerz et al. [8] developed a portable concrete roughness testing device consisting of an optical laser-based imaging system that operates in accordance with the principles of the Schmalz microscope and the shadow profilometry method. It uses a laser profiling line ("laser striping") that produces a non-Gaussian (i.e., uniform) distribution of light intensity along the line. The investigated concrete surface is illuminated with thin slits of red laser light at an angle of 45° while the observations are performed at 90° (Figure 2-1). A high-resolution (tiny) board CCD camera with a 7.5 mm lens is fixed vertically on the protection housing.

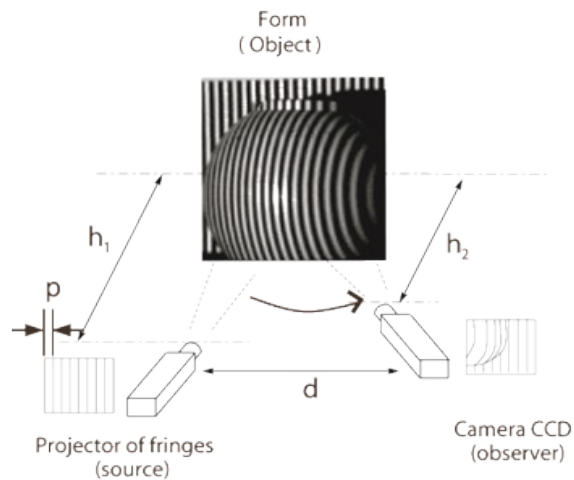
2.7 Profile description

After treatment, concrete surfaces present fractal topography. As with any fractal object, it is possible to break up this surface or this profile into a series of sub-profiles. Each sub-profile can be differentiated in terms of wavelength: there are, however, no limits or precise criteria involved in validating the choice of decomposition method (Figure 2-8). It is also possible to filter the results mathematically [5]. Since the two surfometry methods (mechanical and interferometry) have different resolution levels, it is possible to obtain complementary scales of topography. The method using a mechanical stylus at high resolution yields roughness (R) and waviness (W)

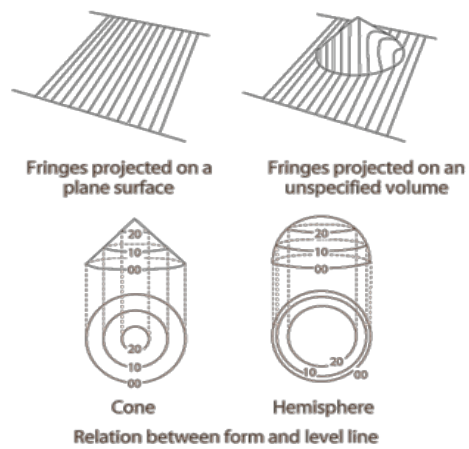
(Table 2-5: Surface profile) [4]. With the interferometry method at a resolution of 0.200- μm , it is possible to obtain two higher scales named meso-waviness (M) and shape (F). In mechanical profilometry, filtering is often carried out through the use of stylus with different diameters.

Treatment	Waviness	Roughness
As received, no treatment NT		
Grinding GR		
Sandblasting SB		
Shot-blasting 35s SHB35		
Hand milling HMIL		
Mechanical milling MMIL		

Figure 2-5: Examples of 3D representation of specimen surfaces obtained by laser profilometry after waviness and roughness filtering



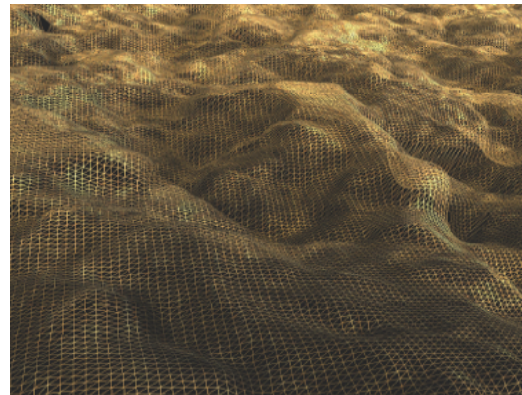
a)



b)



c)



d)

Figure 2-6: Optomorphological profilometry – a) principle of measurement; b) relationship between form and level line; c) testing equipment; d) example of 3D representation of concrete surface (University of Liège)

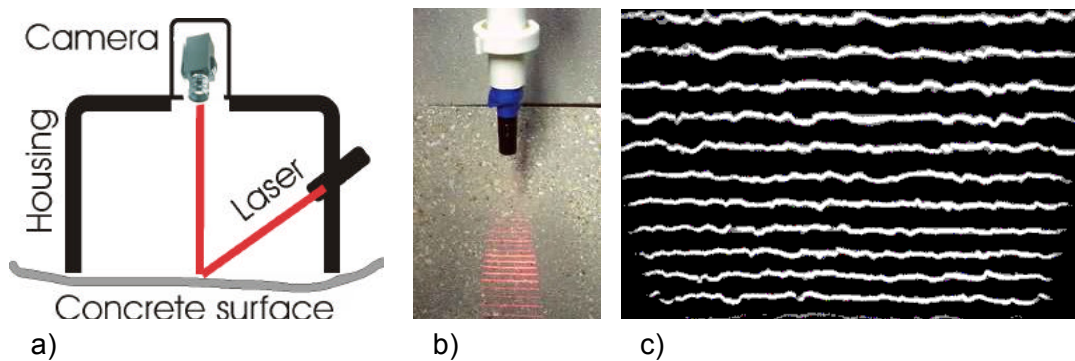


Figure 2-7: Laser profilometry – a) schematic representation of the laser profiling testing device; b) line laser; c) laser image of a concrete surface

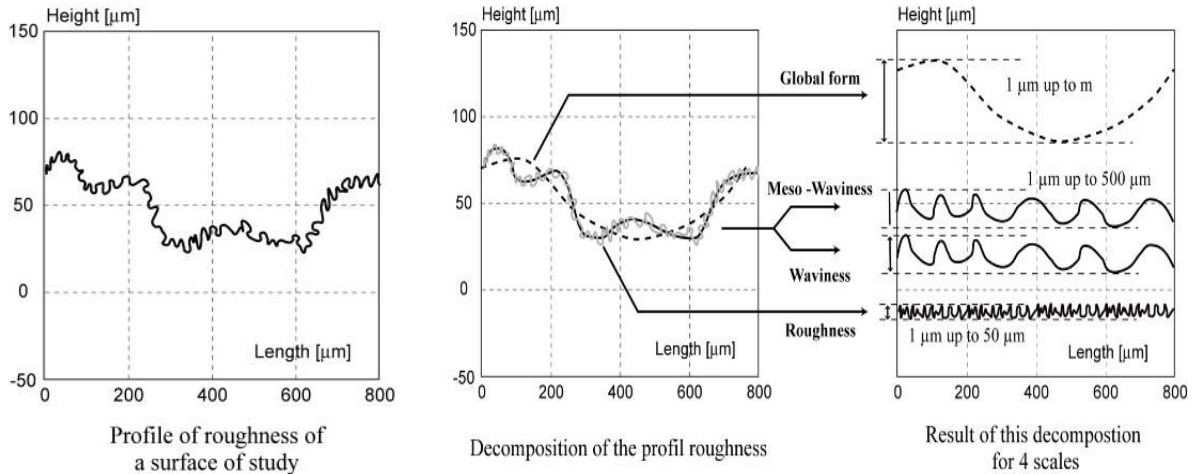
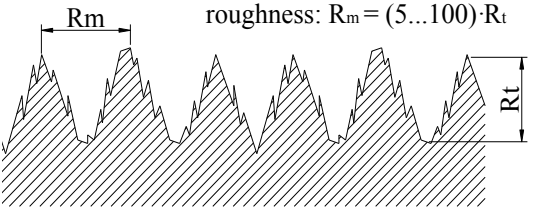
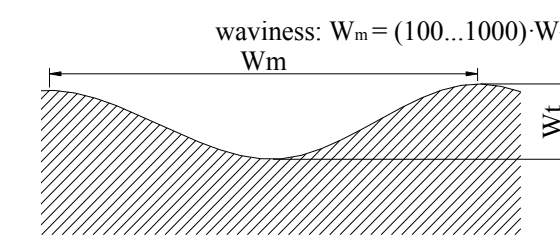


Figure 2-8: Effect of scale on profile decomposition

Table 2-5: Surface profile make up

Roughness	High frequencies gap between grooves (amplitude) R_m is 5–100 times the depth R_t	 <p>roughness: $R_m = (5 \dots 100) \cdot R_t$</p>
Waviness	Mean frequencies amplitude W_m is 100–1000 times the depth of holes W_t	 <p>waviness: $W_m = (100 \dots 1000) \cdot W_t$</p>

In accordance with EN ISO 4287, the total (primary) profile, the waviness and roughness profiles can be characterized by several vertical (Table 2-3) and horizontal (Table 2-4) amplitude parameters. Surface parameters are determined on the basis of the mean line as a reference line: this reference is usually defined in such a way that, in the limits of the profile length, the sum of the squared values of the altitudes of the profile measured versus this reference line is minimal.

Using horizontal profile parameters, the Abbott curve, also referred to as the bearing curve [4], can be determined. This provides information about the surface profile: a gradual decrease in the curve suggests a surface with few holes, while a more steeply decreasing curve is characteristic of a surface with a lot of holes. Important parameters for analyzing the distribution of holes and peaks, as well as the shape of the profile can be graphically calculated from the Abbott curve (Table 2-6). These parameters are crucial when it comes to evaluating of the quantity of slurry, mortar, etc., needed for the interface area between the concrete substrate and the new layer (Figure 2-9).

Table 2-6: Abbott curve parameters

Symbol	Parameters	Definition
C_R	Relative height of the peaks	Gives an idea of significance of the volume of very high peaks above the reference line
C_F	Depth of the profile	Excluding high peaks and deep holes gives information on surface flatness; a lower value of C_F indicates great surface flatness
C_L	Relative depth of the holes	Gives an idea of the significance of the volume of voids under the reference line

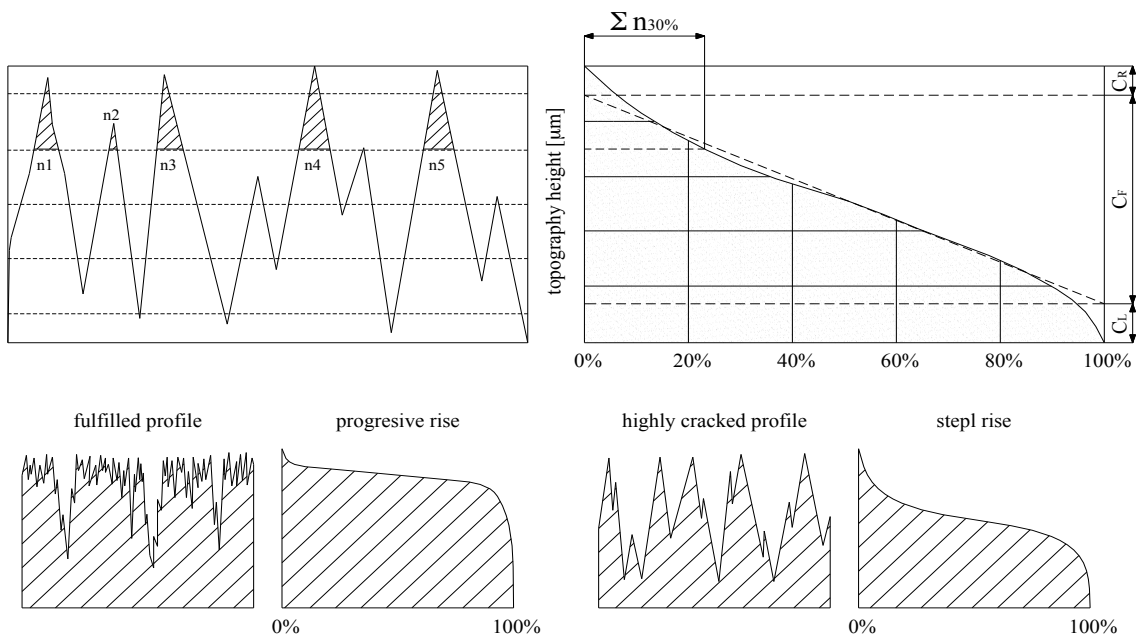


Figure 2-9: The Abbott curve and its interpretation

2.8 Profile description with advanced methods

Concrete surface geometry can be characterized using a scientific approach called quantitative fractography, which is based on image analysis [15, 17]. This approach is well developed in the case of metals and ceramics in comparison with the situation prevailing for concrete-like composites [15–18]. However, geometrical and stereological parameters are also of significant importance in concrete-like composites [19–23]. Besides the profile parameters determined as per EN ISO 4287, three additional stereological parameters could be considered for characterization of concrete surfaces after surface treatment [15, 20]: the profile (linear) roughness ratio R_L , the surface roughness ratio R_S , and the fractal dimension D . The first two parameters are obtained with the following equations:

$$R_L = L/L_o \quad (2-3)$$

where: L = length of the profile line

L_o = projected length of the profile line

$$R_S = S/S_o \quad (2-4)$$

where: S = true fracture surface area

S_o = apparent projected area

The fractal dimension D was introduced in materials science by Mandelbrot as a characteristic allowing to define the irregularity of an object boundaries [22]. The basic requirement for the fractal boundary is that some structural feature(s) or unit(s) is (are) sequentially repeated at different levels. This implies that, from a statistical point of view, similar morphology can be observed in a wide fracture surface magnification range: a measure of this self-similarity is a fractal dimension.

These stereological parameters can either be determined from the image of the profile recorded on the specimen cross-section or the profile obtained by profilometry. The geometry of the fracture surface of concrete-like composites is related to the scale of observation. This implies that the self-similarity of the fracture surface may not extend over all magnification ranges.

Due to the inherent technical difficulties in evaluating R_S , examination of cross-section profiles is frequently opted for, and the profile roughness ratio R_L is calculated using Equation 2-3. Determination of R_L from the profile image is easy with automated profilometry and image analysis (Figure 2-11a). Recent developments in stereological methods allow to estimate R_S from fracture profile studies without simplifying assumptions concerning the relationship between R_L and R_S . The surface roughness ratio R_S can be effectively evaluated using a vertical sectioning method [15]. In this method, an arbitrary axis is chosen, and the specimen is saw cut parallel to this axis (Figure 2-10). It has been shown that sections sampled on three saw cut planes forming an angle of 120° around the axis are sufficient to characterize the surface profile and evaluate satisfactorily R_S [24]. Wojnar [17] proposed a procedure to evaluate R_S which consists in counting the intersection points of the fracture profile with a so-called grid of cycloids (Figure 2-11b). The cycloids allow to relate the fracture area directly to the fracture profile, and the estimation of R_S is independent of the magnification.

2.9 Experimental comparison and analysis of the techniques

2.9.1 Concrete substrates and surface treatments

Several concrete substrates with different compressive strengths and prepared with a variety of surface treatment were characterized at Laval University, the University of Liège and the

Warsaw University of Technology. The series of experiments may be divided into three groups covering altogether a wide range of concrete strength values and types of surface preparation. The basic mixture design characteristics and average compressive strengths of the tested concretes are summarized in Table 2-7.

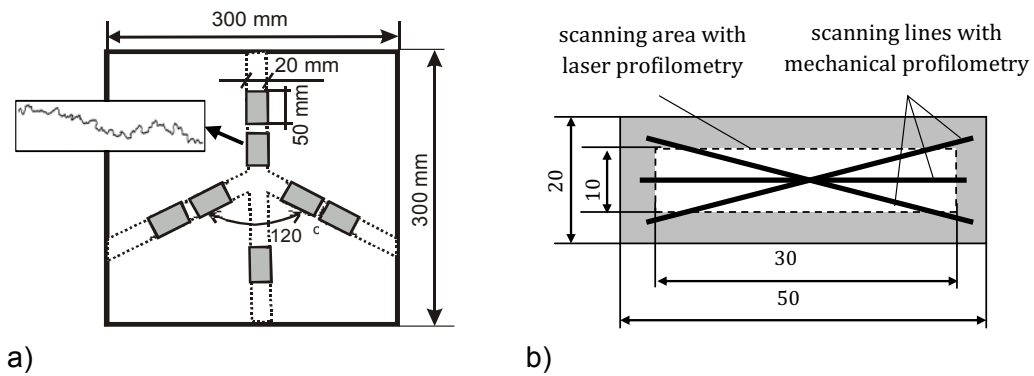


Figure 2-10: Illustration of a) sampling for microscopic observation; and b) surface geometry characterization with laser and mechanical profilometry

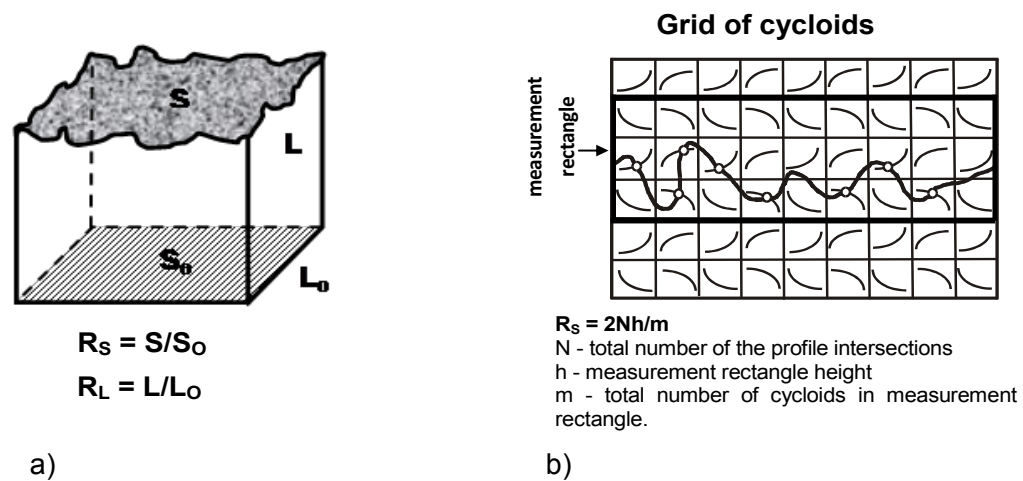


Figure 2-11: a) Significance of the R_S and R_L parameters; b) evaluation of the R_S value using grid of cycloids

Table 2-7: Composition and compressive strength of tested concrete substrates

Constituent / comp. strength	Group A	Group B			Group C		
	C20A	C25B	C35B	C50B	C30C	C40C	C45C
Cement	CEM I 32.5 R	CEM I 32.5 R			CEM I 52.5 N		
Sand	River sand (0/2)	River sand (0/2)			S-RRWSC-7 (0/2)		
Aggregate	Gravel 2/8	Gravel 2/8, 8/16			Crushed limestone 2/8, 8/14, 14/20		
W/C	0.60	0.54	0.42	0.31	0.72	0.59	0.50
Plasticizer	no	yes			no		
$f_{c,28-d}$ (MPa)	n/a	31.5	45.7	62.1	35.0	41.3	48.8

For each series of concrete slabs, four different surface preparation methods were used. In order to yield differences in profile roughness and the level of microcracking in the near-to-surface layer, the following surface treatment methods were selected in each group:

- Group A: Grinding (GR), sandblasting (SB), shotblasting (SHB20, SHB35 and SHB45, with treatment times of 20, 35, and 45 seconds, respectively), hand milling (HMIL) and mechanical milling (MMIL); untreated concrete samples (NT) were also tested as a control;
- Group B: Polishing (PL), dry sandblasting (SB-D), jack hammering (JH) and water jetting at 250 MPa pressure (HD);
- Group C: Gentle surface preparation methods were used to obtain profiles of similar amplitude and low-level microcracking: brushing (NT), wet sandblasting (SB-W), scarifying (SC) and water jetting at 12 MPa pressure (LC).

2.9.2 Evaluation of concrete surface texture with sand patch test

European standards EN 1766:2000 and EN 13036-2010 state that the validity of this measurement ranges from 0.25 to 5.0 mm. The results for the three groups are presented in Table 2-8.

The results for Group A clearly show the significant effect of treatment aggressiveness on surface roughness of the concrete substrate [27]. The SEM images and qualitative descriptions are presented in In general, it is found that a given treatment induces lower roughness as the

strength of the substrate concrete increases. Besides, the results for the polished slabs C40-P and C50-P are beyond the range of validity of the SPT, while the results for slabs C30-P and C40-HD (water jetting) fall just within. The surface obtained with water jetting is also very irregular, and the results are characterized by high coefficients of variation. Overall, water jetting yielded the roughest profiles, followed by scabbling, sandblasting and polishing. In Group C, it can be noticed that the test specimen surfaces exhibit smaller differences in profile roughness, essentially because treatments were overall less aggressive than in the two other groups.

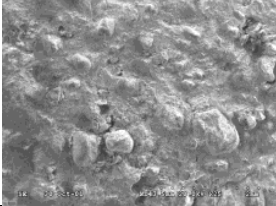
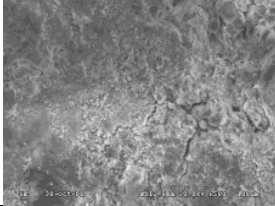
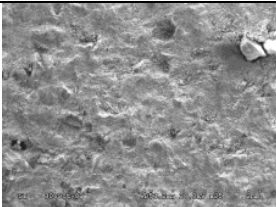
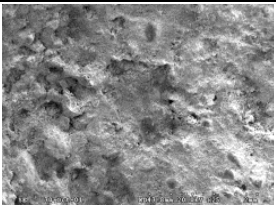
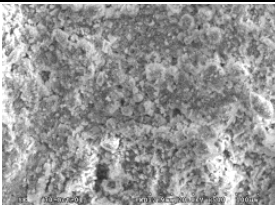
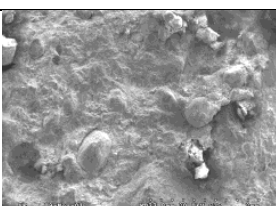
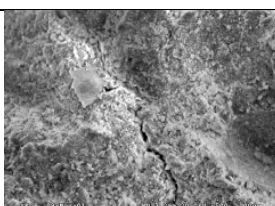
Table 2-9. The roughest surface treatments are shotblasting and sandblasting. Aggressiveness of the treatment strongly influences the quality of the near-to surface layer, as it governs the extent of induced microcracking [28].

Table 2-8: Results of the sand patch test for the various surface treatment techniques

Group A						
ID	Surface treatment	SRI (mm)		ID	Surface treatment	SRI (mm)
C20-NT	No treatment	0.55		C20-SHB35	Shotblasting 35 s	1.59
C20-GR	Grinding	0.72		C20-SHB45	Shotblasting 45 s	1.85
C20-SB	Sandblasting	1.40		C20-HMIL	Hand milling	0.79
C20-SHB20	Shotblasting 20 s	1.01		C20-MMIL	Mechanical milling	1.05
Group B			Group C			
ID	Surface treatment	SRI (mm)	ID	Surface treatment	SRI (mm)	
C30-PL	Grinding	0.25	C25-LC	Water jetting 12 MPa	0.37	
C40-PL		0.20	C35-LC		0.39	
C45-PL		0.14	C50-LC		0.16	
C30-SB-D	Dry sandblasting	0.29	C25-BR		Brushing	0.39
C40-SB-D		0.28	C35-BR	0.39		
C45-SB-D		0.31	C50-BR	0.41		
C30-SCA	Scabbling	0.89	C25-SB-W	Wet sandblasting	0.50	
C40-SCA		0.89	C35-SB-W		0.61	
C45-SCA		0.80	C50-SB-W		0.41	
C30-HD	Water jetting 250 MPa	2.22	C25-SC	Scarifying	0.66	
C40-HD		5.00	C35-SC		0.88	
C45-HD		3.20	C50-SC		0.50	

In general, it is found that a given treatment induces lower roughness as the strength of the substrate concrete increases. Besides, the results for the polished slabs C40-P and C50-P are beyond the range of validity of the SPT, while the results for slabs C30-P and C40-HD (water jetting) fall just within. The surface obtained with water jetting is also very irregular, and the results are characterized by high coefficients of variation. Overall, water jetting yielded the roughest profiles, followed by scabbling, sandblasting and polishing. In Group C, it can be noticed that the test specimen surfaces exhibit smaller differences in profile roughness, essentially because treatments were overall less aggressive than in the two other groups.

Table 2-9: SEM observations of concrete surfaces after various treatments

Example of surface view SEM: magnification 25× (left) and 500× (right)		Description
Grinding		
		Surface without sharp edges with few and non-uniformly located valleys at the surface; narrow cracks observed at higher magnifications.
Sandblasting		
		Surface similar to that after grinding; shallow irregularities of surface (peak-to-valley height did not exceed 1 mm); sharp edges of aggregate particles and microcracks observed at higher magnifications, very often forming non-uniform networks.
Shotblasting		
		Highest roughness of surface increasing with the treatment time; high irregularities of surface (peak-to-valley height increased locally to 7 mm for 45 seconds); formation of a dense network of microcracks and cracks, often along aggregate particles, as well as presence of deteriorated or removed particles were observed with increased treatment time.
Milling		
		Surfaces after milling similar and close to the concrete surface after shotblasting; very high irregularity of the surface, but lower than that after shotblasting; at higher magnifications deep and wide cracks, signs of particle removal and loosed concrete fragments were observed.

Further, the repeatability of the sand patch test and the effect of the volume of sand were analyzed. The tests were performed on four specimens of each concrete mixture from Group C. Comparison of the SRI values yielded when using 10 and 25 mL of sand, respectively, shows a very strong correlation ($r = 0.95$). However, the SRI values determined with a volume of sand of 25 mL were systematically 6% higher (Figure 2-12).

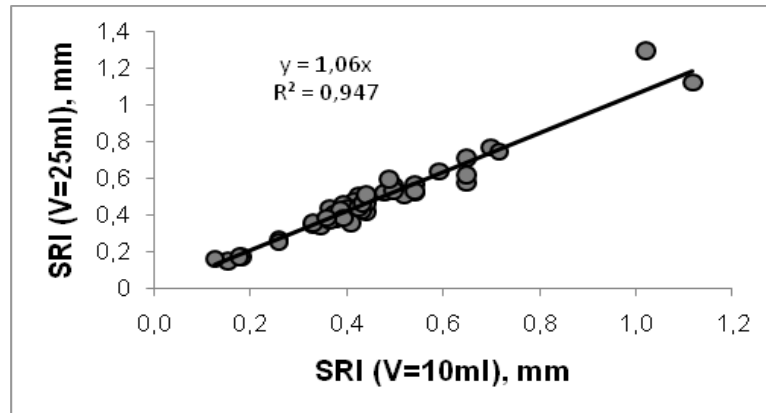


Figure 2-12: Influence of the sand volume used in the sand patch test

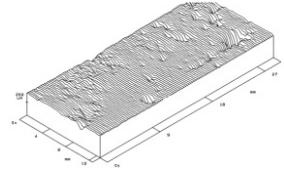
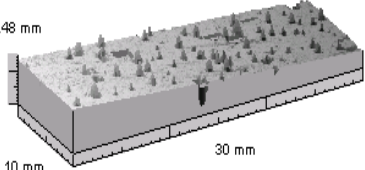
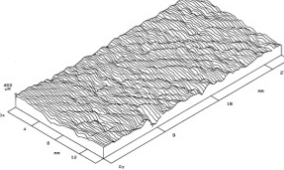
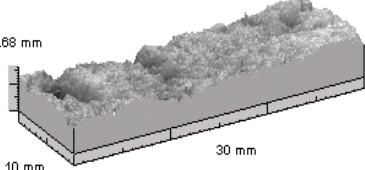
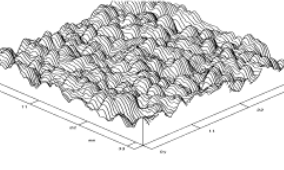
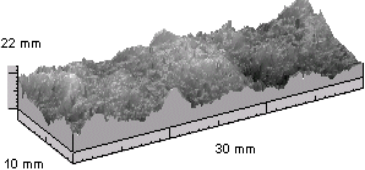
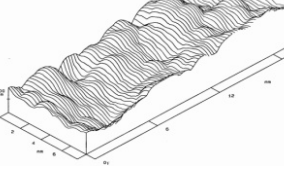
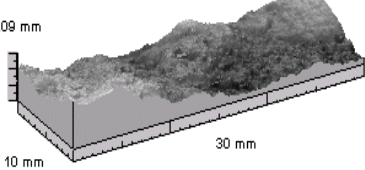
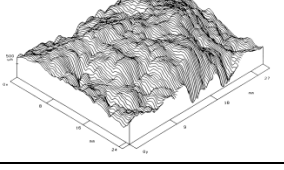
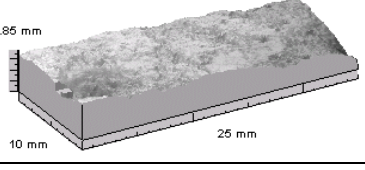
2.9.3 Mechanical vs. laser profilometry

A comparative study of surface roughness characterization with laser and mechanical profilometers was conducted using concrete specimens from the Group A series. Sampling was performed in accordance with the aforementioned vertical sectioning method (Figure 2-10). In the case of mechanical profilometry, the surface was scanned along three lines with a length of 30–40 mm; for laser profilometry, an area of 10 × 30 mm was scanned along parallel lines with a distance of 50 μm between the subsequent lines [12, 14]. Examples of surface roughness profiles are presented in Table 2-10.

The recorded profile was first transformed to remove the effect of the profile orientation (“shape” filtering) [6]. The total profile obtained was then filtered and decomposed into low and high frequencies to separate parameters of waviness and roughness, respectively. The filter used to separate waviness from the total profile was selected to be 0.8 mm for both methods. The total height of the profile X_t , the arithmetic mean of the deviations of the profile from the mean line X_a , and the maximum depth of valleys X_v , were selected for the surface geometry characterization for all levels of filtering [6], i.e., for the total ($X = P$), waviness ($X = W$) and roughness ($X = R$) profiles. The Abbott curve parameters were also calculated. Further in the

text, indexes p and s denote parameters measured by mechanical and laser profilometry respectively.

Table 2-10: The examples for concrete surface roughness representation with mechanical (left) and laser (right) profilometry

Treatment	Waviness	Roughness
As received, no treatment NT		
Grinding GR		
Sandblasting SB		
Shotblasting 35 s SHB35		
Mechanical milling MMIL		

The results of surface geometry characterization with the four methods can be summarized as illustrated in Figure 2-13. The geometrical parameters determined for the microscopic level (profile amplitude parameters) generally indicate that the highest roughness was obtained for shotblasting after 45 seconds and the lowest for grinding (Figure 2-13). With respect to profilometry methods, the waviness parameters are lower than those of the total profile by about

5% for mechanical profilometry and by 9% for laser profilometry. This confirms that the overall shape of the profile has been preserved through the waviness filtering process.

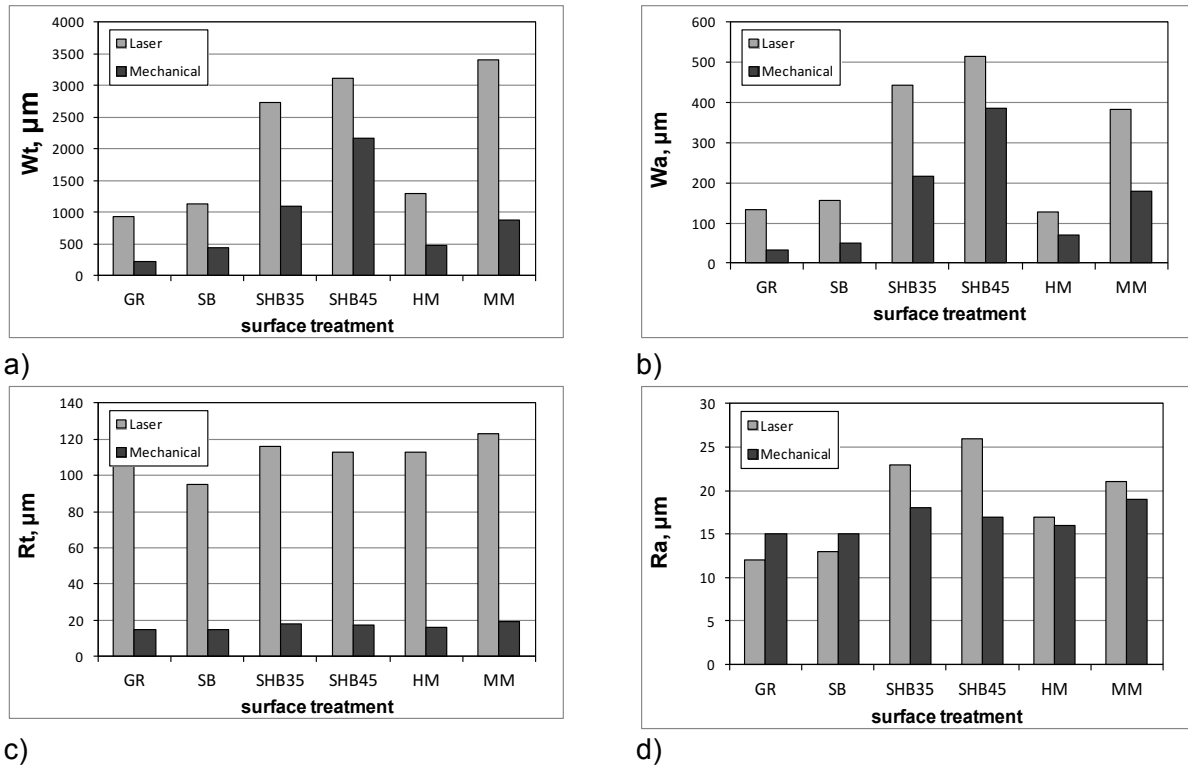


Figure 2-13: Waviness parameters a) W_t and b) W_a ; microroughness parameters c) R_t and d) R_a ; as determined through laser and mechanical profilometry

The mean roughness values are relatively close to each other, irrespective of the treatment type and the profilometry method being used ($R_{ap} = 17 \pm 2$ and $R_{as} = 19 \pm 7$). However, with the same filtering technique, the total height of the roughness profile determined through laser profilometry was 2.8–5.5 times higher than that obtained with mechanical profilometry. Hence, roughness parameters cannot strictly be used as surface quality indicators after treatment (Figure 2-13c, d).

Both the total height and the mean value of the waviness profile measured with laser profilometry are of the order of 1.3 to 4.3 times higher than those calculated through the mechanical method and 7 times higher in terms of Abbott parameters.

The relationships between parameters determined with laser and mechanical profilometry show different levels of statistical significance. Nevertheless, the results indicate that the surface profile characteristics determined with both methods are comparable, irrespective of the observation level. This observation is confirmed by the high correlation coefficient ($r > 0.94$) of the relationship between the corresponding mean values of waviness profile W_a (Figure 2-14a), and Abbott parameters C_R and C_F (Figure 2-14c). A higher scatter in the results for both profilometry methods was observed for other amplitude parameters. Lower statistical significance (Figure 2-14b) was obtained for the total heights of the waviness profile (W_{ts} vs. W_{tp}) and the maximum depth of the valleys (W_{vs} vs. W_{vp}) as well as the relative depth of holes, C_L (Figure 2-14c). This could be because of differences in the surface area scanned with laser and mechanical profilometry. However, Figure 2-14b and c indicate that the low correlation is due to the low values of amplitude parameters obtained through mechanical profilometry for the surface obtained with mechanical milling. This surface was too irregular and a significant number of deep and wide cracks (In general, it is found that a given treatment induces lower roughness as the strength of the substrate concrete increases. Besides, the results for the polished slabs C40-P and C50-P are beyond the range of validity of the SPT, while the results for slabs C30-P and C40-HD (water jetting) fall just within. The surface obtained with water jetting is also very irregular, and the results are characterized by high coefficients of variation. Overall, water jetting yielded the roughest profiles, followed by scabbling, sandblasting and polishing. In Group C, it can be noticed that the test specimen surfaces exhibit smaller differences in profile roughness, essentially because treatments were overall less aggressive than in the two other groups.

Table 2-9), which are better detected by the laser profilometer than by the stylus.

The relationship between W_a and SRI exhibits relatively high correlation coefficients (r), with values of 0.77 and 0.94 for laser and mechanical profilometry, respectively (Figure 2-14d). This confirms that SRI provides a satisfactory estimate of the mean deviation of a concrete surface profile and that it can be used for field evaluation of surface roughness.

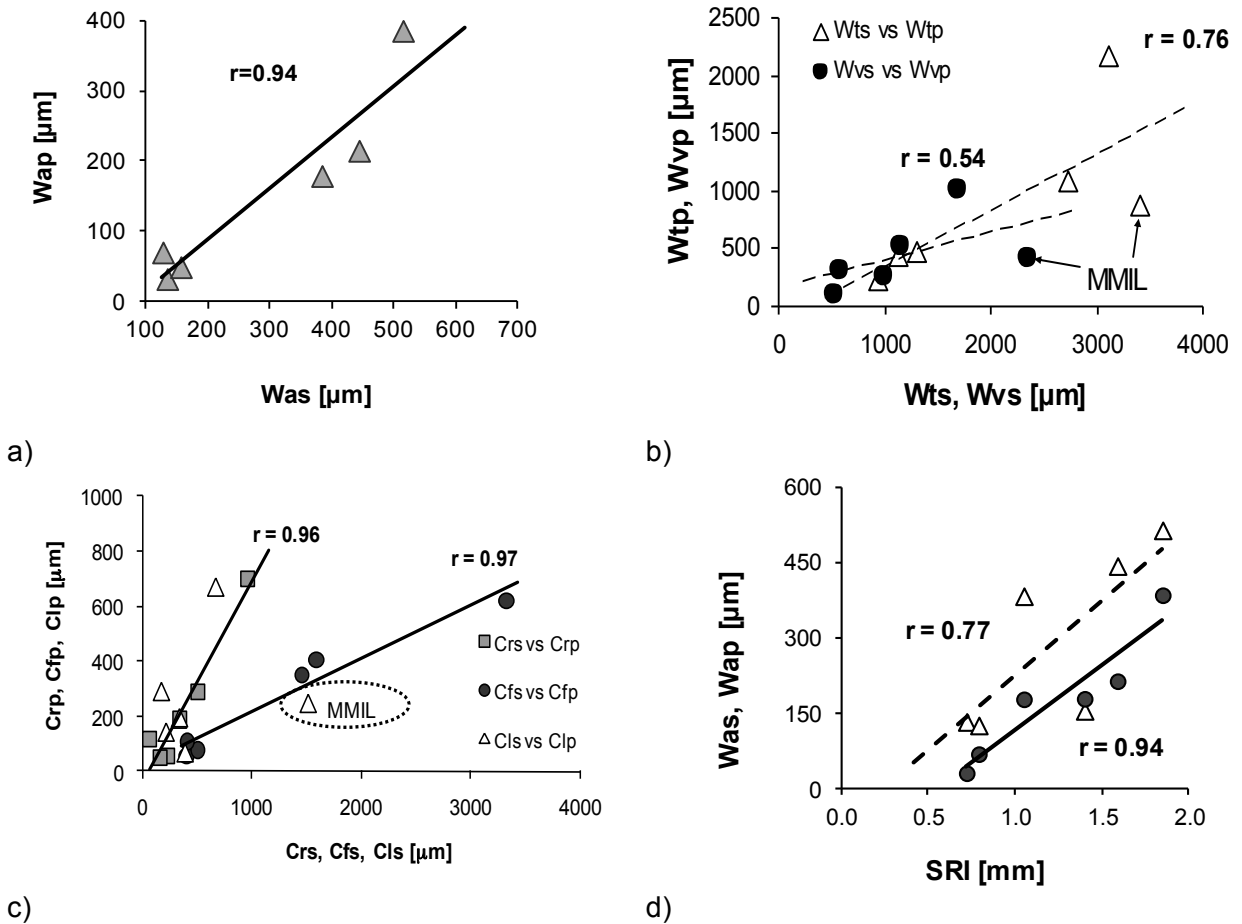


Figure 2-14: Relationships between waviness parameters a) W_a , b) W_t and W_v and c) Abbott parameters, determined through laser (Δ) and mechanical (\bullet) profilometry; d) relationship of W_{as} and W_{ap} vs. SRI

2.9.4 Surface roughness characterization with the microscopic observation method

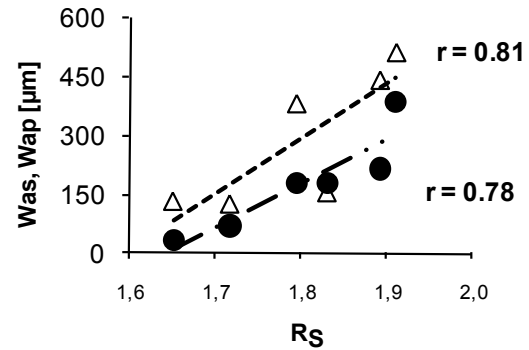
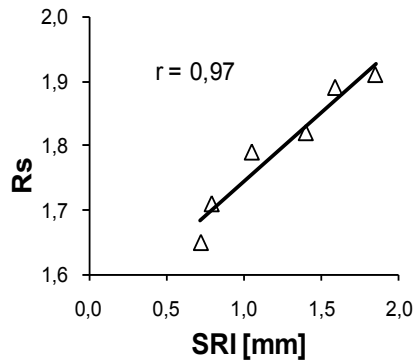
Microscopic observations were performed on 20 × 50 mm samples that were sawn from 300 × 300 mm Group A test specimens (Figure 2-10a). The geometric length of the profile was 350 mm for each substrate type. The values of the stereological parameters R_L and R_S were calculated using the computer program *Profile 1.1* [24] for the profile images recorded with a light microscope at 10× magnification. The fractal dimension D_b was calculated with the same program using the box-counting method [25]. The results are summarized in Table 2-11: Stereological parameters evaluated with the microscopic method for various types of surface preparation. It can be seen that among the different types of surface preparation investigated, hand milling resulted in the highest profile variability. Besides, the values of D_b are not found vary significantly from one method to the other and are comparable to those reported elsewhere for a wide range of concrete surfaces ($D_b = 1.03\text{--}1.25$) [20–22, 26, 27]. Unfortunately, it means that the fractal dimension is not sensitive enough for evaluating concrete surface profile characteristics in a discriminating fashion.

Table 2-11: Stereological parameters evaluated with the microscopic method for various types of surface preparation

Surface preparation	Statistical parameter	Stereological parameters		
		R_L	R_S	D_b
NT	Mean (mm)	1.477	1.739	1.089
	STD (mm)	0.077	0.116	0.038
	CV (%)	0.052	0.067	0.035
GR	Mean (mm)	1.451	1.703	1.110
	STD (mm)	0.082	0.125	0.071
	CV (%)	0.057	0.073	0.064
SB	Mean (mm)	1.554	1.837	1.139
	STD (mm)	0.127	0.262	0.041
	CV (%)	0.082	0.142	0.036
SHB20	Mean (mm)	1.563	1.870	1.104
	STD (mm)	0.116	0.171	0.035
	CV (%)	0.074	0.091	0.032
SHB45	Mean (mm)	1.578	1.892	1.084
	STD (mm)	0.180	0.262	0.038
	CV (%)	0.114	0.138	0.035
HMIL	Mean (mm)	1.475	1.682	1.085
	STD (mm)	0.099	0.345	0.043
	CV (%)	0.067	0.205	0.040
MMIL	Mean (mm)	1.503	1.779	1.094
	STD (mm)	0.099	0.148	0.042
	CV (%)	0.066	0.083	0.039

(all data in the table represents the average results for three specimens)

The analysis of the relationship between R_s and other parameters of profile characterization showed that R_s correlates strongly with SRI (high correlation coefficient $r = 0.97$; Figure 2-15a). The relationships between R_s and W_{as} and W_{ap} exhibit a weaker correlation ($r \sim 0.8$; Figure 2-15b).



a)

b)

Figure 2-15: Relationships a) R_s vs. SRI and b) R_s vs. arithmetic mean deviation of waviness profile, as determined through laser (W_{as}) and mechanical (W_{ap}) profilometry

2.9.5 Concrete surface texture evaluated with mechanical and interferometric methods

In a test comparison between mechanical and interferometric surface characterization approaches, three types of surface preparation techniques were investigated (Table 2-12): scarifying, high pressure water jetting (18,000 psi pressure and 6 gal./h water flow) and polishing. The latter was carried out using two abrasive rotating plates until the surface became smooth to the touch.

Figure 2-16 shows photographs of the respective profiles obtained with the surface preparation techniques investigated. A careful visual examination of all prepared surfaces leads to the following observations with respect to their macroscopic and visible effects:

- polishing produces a very smooth surface with brightness close to that of a mirror;
- the high-pressure water jetting technique induces a particular texture characterized by large waves mostly parallel to the water flow;
- scarifying generally induces some oriented macroroughness (grooved surface); in this study it was, however, intentionally eliminated by the operator by means of successive transverse and perpendicular operations.

Table 2-12: Surface preparation of specimens tested through interferometric and mechanical profilometry

Reference	Specimen size (batch)	Type of preparation
PTW	150 L (no. 4)	Polished troweled surface
HPW	150 L (no. 5)	High pressure water jetting
SC2	150 L (no. 6)	Scarifying



a) polishing



b) water jetting



c) scarifying

Figure 2-16: Concrete surface profiles obtained with selected surface preparation methods

A first series of mechanical profilometry measurements was performed using a stylus with a diamond sphere radius of 6 μm (Figure 2-2). The length of measurement was 8 mm and the filter used to separate roughness from the profile was set at 0.8 mm. Three profiles were recorded on one sample of each type of preparation, in different directions. A second series was carried out using this time a stylus with a length of 79 mm and a diamond with a radius of 1.5 mm in order to evaluate the waviness. The length of the measurement was increased to 30 mm or more. The filter was again set at 0.8 mm, and a 16-mm filter (twice the nominal size of the aggregates) was used to extract the shape from the profile. The data summarized in Table 2-13 show that the R_a , R_q and R_t values are 1.5–3 times smaller for the polished concrete profile than those obtained with water jetting and scarifying, while the amplitude and statistical roughness value are relatively close for water jetting and scarifying.

These findings confirm that the surface treatment technique (Figure 2-17: 3D representation of surfaces and corresponding roughness and waviness profiles for three different types of treatment) has no major influence on the microroughness (“high-frequency waves”) of the profile. Furthermore, it demonstrates once again that waviness parameters are sufficient to define concrete surface roughness.

As described previously, the optical method based on the moiré pattern is an interferometric technique used to obtain 3D profile information based on the interference of light and shade stripes [5]. The measurement accuracy is directly related to the density of the fringe network and the capacity of differentiation of the network by image analysis. Theoretically, with a light beam projection angle of 45° and a 512 × 512 pixel CCD camera, a resolution of approximately 1/5,000 of the size of the object can be obtained. In the present application, for a 350 × 350 mm surface area, the 3D resolution reached 200 µm, with a measurable maximum vertical amplitude of the order of 100 mm.

Three interferometric topography evaluations were carried out. Figure 2-18 shows the equipment used for optical measurement, which can be performed the actual surface of the specimen or member, irrespective of its size, without the need for sampling. At this scale, water jetting seems to induce the roughest profile, while polishing and scarifying yielded smoother and rather similar profiles. This is due to the bubble effect at the surface, which increases roughness. It can be seen in Table 2-14 that the roughness amplitude value (M_a) yielded with water jetting is 20 times that for scarifying and polishing. At this scale, the other treatments left rather smooth surfaces, polishing generating the flattest profile. Most of the apparent roughness of polished surfaces comes from the bubble holes.

Table 2-13: Surface profile characteristics determined through mechanical profilometry – waviness (W), roughness (R) and Abbot parameters (C)

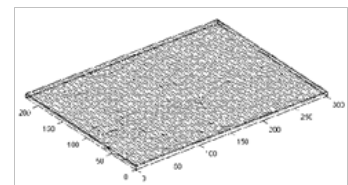
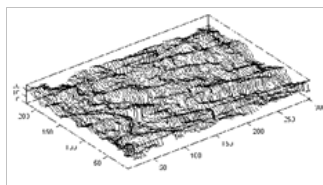
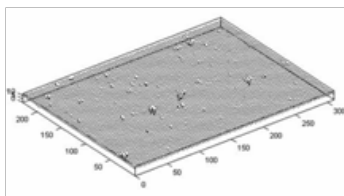
Surface profile parameter		Polishing	Water jetting	Scarifying
W_a	(mm)	6	420	127
W_p	(mm)	13	1003	346
W_q	(mm)	9	501	158
W_v	(mm)	47	923	445
W_t	(mm)	60	1926	791
R_a	(mm)	5	14	15
R_q	(mm)	7	17	19
R_t	(mm)	70	96	102
C_R	(mm)	4	152	412
C_F	(mm)	10	228	827
C_L	(mm)	14	231	537

a) Polishing

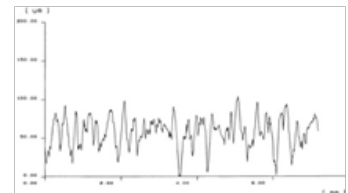
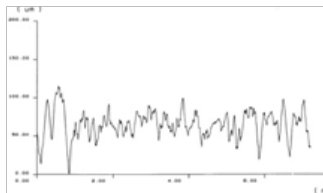
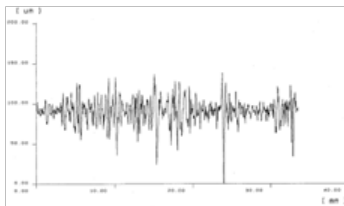
b) Water jetting

c) Grinding

Surface scan



Roughness profile



Waviness profile

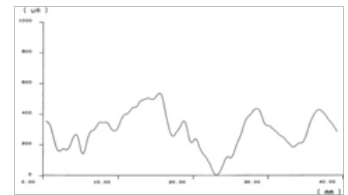
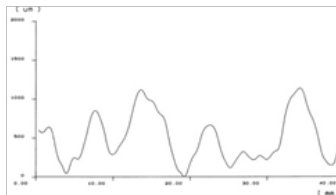
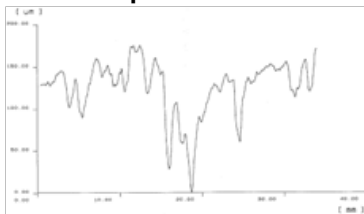


Figure 2-17: 3D representation of surfaces and corresponding roughness and waviness profiles for three different types of treatment



Figure 2-18: Use of an interferometric measuring device for concrete surface characterization

Table 2-14: Surface profile characteristics determined through interferometric profilometry – overall shape (F), meso-waviness (M) and Abbot parameters (C)

Surface profile parameter		Polishing	Water jetting	Scarifying
F_a	(mm)	0.137	0.358	0.326
F_t	(mm)	4.1	10.8	12.6
$F S_m$	(mm)	129	85.3	102.3
M_a	(mm)	0.169	2.85	0.315
M_t	(mm)	19.7	27.8	10.2
$M S_m$	(mm)	15.3	36.5	22.5
C_R	(mm)	0.30	4.65	0.41
C_F	(mm)	0.29	5.76	0.55
C_L	(mm)	0.35	5.71	0.81

2.9.6 CSP profiles vs. interferometric measurements

The aim of this part of the the investigation was to compare the surface geometry characteristics obtained with optical profilometry and visual method (CSP profiles). The nine CSP plates (Figure 2-19a) have been characterized at Laval University with the optometric method [5] using a 512×512 pixel CCD camera, a vertical resolution of $200 \mu\text{m}$ and a surface area of $350 \times 350 \text{ mm}$. The measurement length was approximately $500 \mu\text{m}$. Because of the vertical resolution of the test device, it is impossible to separate roughness from waviness in this case. A profile obtained through this approach consequently yields a description of the meso-waviness and overall shape. Figure 2-19b shows that the optometric device does not allow to detect any significant variations in terms of roughness level under a threshold CSP value (no. 5)

corresponding to the vertical resolution of the optometric device. Nevertheless, above this value, the optometric method accurately reproduces the surface roughness level in accordance with the CSP scale. Similar investigations were performed by Maerz et al. [7].

It can be concluded that it is possible to significantly improve the CSP replicate system through a real quantitative approach. The actual CSP plates are rather narrow with respect to the spectrum of CSPs obtained with actual surface preparation techniques. The identification of reference curves, similar to those presented by Perez et al. but on a wider scale of surface roughness, will help broaden the range of application of this method to much coarser profiles such as those obtained with jack hammering and water jetting, for example.

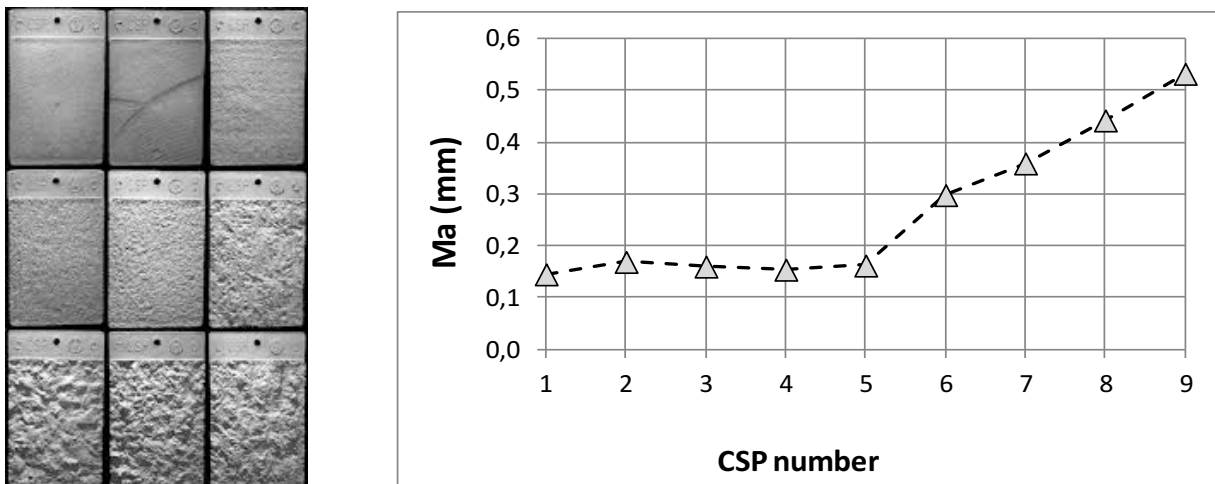


Figure 2-19: ICRI CSP evaluation (Guideline No. 310.2R–2013) – a) photographs of the nine replicates ordered from 1 to 9; b) characterization of the CSP replicates performed by Perez et al. using an interferometric method [5]

2.10 Conclusions

Characterization of surface roughness is an important aspect in assessing a concrete substrate prior to repair. Various techniques have recently been available for CSP characterization. The combination of different methods can yield a very accurate description of

roughness at various scale levels, depending on the roughness range to be analyzed. For instance, mechanical and laser (laboratory-type) profilometers allow for a more accurate microroughness characterization, while the interferometric (optical) method provides a better description of the shape of the profile. Nevertheless, investigations of a range of concrete surface treatments with very precise laser and mechanical profilometers clearly indicated that the surface treatment technique does not have much influence on microroughness (high-frequency waves). This indicates that only the waviness parameters actually need to be determined in order to assess surface roughness prior to repair.

Among the techniques available today, the best suited method for field assessment appears to be the CSP developed by ICRI: it is quick and easy to use and yields reliable information, irrespective of the surface orientation. However, its use is limited at present to surfaces of up to 6 mm in profile height, for which it was actually designed; it is clearly not suitable for water jetting or jack hammering evaluations.

The advantages of the sand patch test method are its speed and applicability in situ on a surface that must be protected from wind and rain. Its main limitations are the range of validity (0.25–5 mm), which usually excludes surfaces with high holes and peaks, and the ability to apply it only on horizontal surfaces. It does, however, have good correlations with statistical parameters such as W_a .

Since the operation of surface preparation essentially influences waviness, the optical method based on the moiré pattern, which offers significant advantages in terms of production rate and surface area treatment capability, could in fact be used alone to perform the whole surface roughness characterization. This method directly yields a handful of reliable quantitative data, but the equipment available today is not adapted to daily field applications. Nevertheless, with

the rapid technological development in that field, the availability of suitable optical devices may be in the near future. This would allow for even more rapid and objective assessments.

2.11 References

1. Silfwerbrand, J. (1990) Improving concrete bond in repaired bridge decks, *Concrete International*, 12: 61–66.
2. American Society of Mechanical Engineers (1978), American National Standard, Surface Texture, Waviness and Lay, ASME, New York.
3. Sherrington, I., Smith, E.H. (1988) Modern measurement techniques in surface metrology – Part I: Stylus instruments, electron microscopy and non-optical comparators, *Wear*, 125: 271–288.
4. Courard, L., Nélis, M. (2003) Surface analysis of mineral substrates for repair works: roughness evaluation by profilometry and surfometry analysis, *Magazine of Concrete Research*, 55: 355–366.
5. Perez, F., Bissonnette, B., Courard, L. (2009) Combination of mechanical and optical profilometry techniques for concrete surface roughness characterization, *Magazine of Concrete Research*, 61(6): 389–400.
6. Courard, L., Schwall, D., Piotrowski, T. (2007) Concrete surface roughness characterization by means of opto-morphology technique, Adhesion in Interfaces of Building Materials: a Multi-scale Approach (ed. L. Czarnecki and A. Garbacz), *Advances in Materials Science and Restoration*, No. 2, Aedificatio Publishers, 107–115.
7. Maerz, H., Chepur, P., Myers, J., Linz, J. (2001) Concrete Roughness Characterization Using Laser Profilometry for Fiber-Reinforced Polymer Sheet Application, *Transportation Research Board*, 80th Annual Meeting, Washington, D.C., Paper No. 01–0139.

8. Santos, P. and Júlio, E. (2008) Development of a Laser Roughness Analyzer to Predict In-Situ the Bond Strength of Concrete-to-Concrete Interfaces, *Magazine of Concrete Research*, 60 (5): 329–337.
9. Fukuzawa, K., Mitsui, M. and Numao, T. (2001) Surface roughness indexes for evaluation of bond strengths between CRFP sheet and concrete, *10th International Congress on Polymers in Concrete* (ICPIC 01, Ed. D. Fowler), Honolulu, Hawaii, no. 12.
10. Garbacz, A., Kostana, K. (2007) Characterization of concrete surface geometry by laser profilometry, *Adhesion in Interfaces of Building Materials: a Multi-scale Approach* (L. Czarnecki and A. Garbacz eds.), *Advances in Materials Science and Restoration, No. 2*, Aedificatio Publishers, 147–157.
11. Santos, M.D.S., Júlio, E.N.B.S. (2010) Comparison of Methods for Texture Assessment of Concrete Surfaces, *ACI Materials Journal*, 107 (5): 434–440.
12. Garbacz, A., Courard, L., Gorka, M. (2005) Effect of concrete surface treatment on adhesion in repair systems, *Magazine of Concrete Research*, 57: 49–60.
13. Courard, L., Garbacz, A., Schwall D., Piotrowski, T. (2006) Effect of concrete substrate texture on the adhesion properties of PCC repair mortar, *ISPIC, Symposium on Polymers in Concrete* (Eds. J. Barroso de Aguiar, S. Jalali, A. Camoes and R. M. Ferreira), Guimaraès, Portugal (2–4 April 2006): 99–110.
14. Garbacz A, Courard L., Kostana, K. (2006) Characterization of concrete surface roughness and its relation to adhesion in repair systems, *Materials Characterization*, 56: 281–289.
15. Kurzydłowski, K.J., Ralph, B. (1996) Quantitative description of microstructure, CRC, New York.
16. Siewczyńska, M. (2008) Effect of selected properties of concrete on adhesion of protective coating, Ph.D. Thesis, Poznań University of Technology.
17. Wojnar, L. (1995) Image Analysis: Applications in Materials Engineering, CRC, New York.

18. Underwood, E.E. (1987) Stereological analysis of fracture roughness parameters. *Acta Stereologica*, 6: 170–178.
19. Wang, Y., Diamond, S. (2001) A fractal study of the fracture surfaces of cement pastes and mortars using a stereoscopic SEM method, *Cement Concrete Research*, 31: 1385–1392.
20. Czarnecki, L., Garbacz, A., Kurach, J. (2001) On the characterization of polymer concrete fracture surface, *Cement and Concrete Composites*, 32: 399–409.
21. Brandt, A.M., Prokopski, G. (1993) On the fractal dimension of fracture surfaces of concrete elements, *Journal of Materials Science*, 28: 4762–4766.
22. Saouma, V.E., Barton, C.C. (1994) Fractals, fractures, and size effects in concrete, *Journal of Engineering Mechanics*, ASCE, 120: 835–854.
23. Yan, A., Wu, K.R., Zhang, D., Yao, W. (2003) Influence of concrete composition on the characterization of fracture surface, *Cement and Concrete Composites*, 25: 153–157.
24. Gokhale., A.M., Drury, W.J. (1990) A general method of estimation of fracture surface roughness – Part II: Practical considerations, *Metallurgical and Materials Transactions*, 21A: 1201–1207.
25. Issa, M.A., Hammad, A.M. (1994) Assessment and evaluation of fractal dimension of concrete fracture surface digitized image, *Cement and Concrete Research*, 24: 325–334.
26. Stroeven, P. (2000) A stereological approach to roughness of fracture surface and tortuosity of transport paths in concrete, *Cement and Concrete Composites*, 22: 331–341.
27. Courard, L., Garbacz, A., Gorka, M. (2004) Concrete surface treatments quantification by means of mechanical profilometry, ICPIIC, XIth International Congress on Polymers in Concrete (M. Maultzsch ed., Federal Institute for Materials Research and Testing), Berlin, Germany (June 2-4, 2004): 125–132.
28. Bissonnette, B., Courard, L., Vaysburd, A., Bélair, N. (2006) Concrete removal techniques: influence on residual cracking and bond strength, *Concrete International*, 28(12): 49–55.

2.12 Standards and test methods

ASTM E965-15, Standard Test Method for Measuring Pavement Macrotexture Depth Using a Volumetric Technique, ASTM International, West Conshohocken, (PA), USA, www.astm.org

ASTM E2157-09, Standard Test Method for Measuring Pavement Macrotexture Properties Using the Circular Track Meter, ASTM International, West Conshohocken, PA, 2009, www.astm.org

EN 1766: 2000, Products and systems for the protection and repair of concrete structures. Test methods. Reference concrete for testing, European Standard, Brussels, Belgium, 2000, <http://www.cen.eu>

EN ISO 4287:2009, Geometrical product specifications (GPS) — Surface texture: Profile method — Terms, definitions and surface texture parameters, European Standard, Brussels, Belgium, 2009, <http://www.cen.eu>

EN 13036-1:2010, Road and airfield surface characteristics – Test methods – Part 1: Measurement of pavement surface macrotexture depth using a volumetric patch technique, European Standard, Brussels, Belgium, 2010, <http://www.cen.eu>

ICRI Guideline No. 310.2R-2013 Selecting and Specifying Concrete Surface Preparation for Sealers, Coatings, Polymer Overlays, and Concrete Repair International Concrete Repair Institute, St. Paul (MN), USA, 2013, www.icri.org

Table of contents

Table of contents	i
List of tables	iii
List of figures	iv

Section 3 – Establish relationships between tensile bond, shear bond and substrate roughness parameters (CRC Proposal Task 2) 1

3.1 Introduction	1
3.2 Methodology	3
3.2.1 Test program conducted at USBR.....	3
3.2.1.1 Investigated variables and specimen preparation	3
3.2.1.2 Surface roughness characterization	5
3.2.1.3 Evaluation of surface integrity.....	6
3.2.1.4 Bond strength evaluation	7
3.2.2 Test program conducted at Laval University	9
3.2.2.1 Investigated variables and specimen preparation	10
3.2.2.2 Surface roughness characterization	12
3.2.2.3 Evaluation of surface integrity.....	13
3.2.2.4 Bond strength evaluation	14
3.3 Results and analysis	15
3.3.1 Test program conducted at USBR.....	15
3.3.1.1 Surface roughness.....	15
3.3.1.2 Mechanical integrity of the substrate	18
3.3.1.3 Bond strength	19

3.3.2	Test program conducted at Laval University	26
3.3.2.1	Surface roughness.....	26
3.3.2.2	Mechanical integrity of the substrate	30
3.3.2.3	Bond strength	31
3.4	Conclusions	42
3.5	References	45
3.6	Standards and test methods.....	46

List of tables

Table 3-1:	Test program conducted at USBR.....	4
Table 3-2:	Concrete mixture characteristics and mechanical properties (USBR).....	5
Table 3-3:	Test program conducted at UL	9
Table 3-4:	Concrete mixture characteristics and mechanical properties (UL program).....	10
Table 3-5:	Summary of surface roughness test results (USBR program).....	15
Table 3-6:	Summary of pull-off test results for the 40-MPa concrete substrate series (USBR program).....	20
Table 3-7:	Summary of torque test results for the 40-MPa concrete substrate series (USBR program).....	20
Table 3-8:	Summary of surface roughness test results (UL program).....	28
Table 3-9:	Summary of pull-off test results for the 20-MPa substrate series (UL program).....	32
Table 3-10:	Summary of pull-off test results for the 30-MPa substrate series (UL program).....	33
Table 3-11:	Summary of torque test results for the 20-MPa substrate series (UL program)	33
Table 3-12:	Summary of torque test results for the 30-MPa substrate series (UL program)	34

List of figures

Figure 3-1:	Preparation of test slabs at USBR.....	5
Figure 3-2:	Surface preparation of the test slabs at USBR.....	6
Figure 3-3:	Core-drilling template for mechanical bond testing (USBR program)	8
Figure 3-4:	Test slabs prepared at UL	10
Figure 3-5:	Scarification and shotblasting surface preparation at CRIB (UL program).....	11
Figure 3-6:	V-shape rippled acrylic dies and resulting profiled slabs (UL program)	12
Figure 3-7:	Core-drilling template for mechanical bond testing (UL program).....	14
Figure 3-8:	Computer interface for optical profilometry data treatment	17
Figure 3-9:	Correlation between macrottexture depth (ASTM E965-06) and optical profilometry characterization (USBR program)	17
Figure 3-10:	Results of Schmidt hammer soundings (ASTM C805) performed after surface preparation to evaluate the mechanical integrity of the exposed concrete surface (USBR program).....	18
Figure 3-11:	Results of pull-off tests performed on 40-MPa substrates after repair (USBR program) (<i>note</i> : SA – sandblasting; WJ – water jetting; JH – jackhammering).....	21
Figure 3-12:	Distribution of failure location in pull-off tests performed on 40-MPa substrates after repair (USBR program)	22
Figure 3-13:	Results of torque tests performed on 40-MPa substrates after repair (USBR program) (<i>note</i> : SA – sandblasting; WJ – water jetting; JH – jackhammering).....	22
Figure 3-14:	Distribution of failure location in torque tests performed on 40-MPa substrates after repair (USBR program)	23
Figure 3-15:	Results of pull-off tests (ASTM C1583) performed after repair as a function of the substrate CSP index (ICRI No. 310.2R-2013) generated by various preparation techniques (USBR program)	23
Figure 3-16:	Results of pull-off tests (ASTM C1583) performed after repair as a function of the substrate Macrottexture depth (ASTM E965) generated by various preparation techniques (USBR program).....	24
Figure 3-17:	Results of pull-off tests (ASTM C1583) performed after repair as a function of the substrate R_a value generated by various preparation techniques (USBR program).....	24

Figure 3-18: Results of pull-off tests (ASTM C1583) performed after repair as a function of the variability of the Schmidt hammer data (ASTM C805) yielded for different surface preparations (USBR program).....	25
Figure 3-19: Results of torque tests performed after repair as a function of the substrate roughness generated by various preparation techniques (USBR program).....	27
Figure 3-20: Shear bond to tensile bond strength ratio after repair as a function of the substrate R_a value generated by various preparation techniques (USBR program).....	28
Figure 3-21: Results of roughness evaluation performed after surface preparation by optical profilometry on both 20-MPa and 30-MPa substrates (UL program)	29
Figure 3-22: Results of pull-off experiments (CSA A23.2-6B modified) performed after surface preparation to evaluate the mechanical integrity of the exposed concrete surface and comparison with average the splitting tensile strength (f_{st}) value determined for each base mixture (UL program)	30
Figure 3-23: Results of pull-off tests performed on 20-MPa substrates after repair (UL program)	34
Figure 3-24: Distribution of failure location in pull-off tests performed on 20-MPa substrates after repair (UL program).....	35
Figure 3-25: Results of pull-off tests performed on 30-MPa substrates after repair (UL program)	35
Figure 3-26: Distribution of failure location in pull-off tests performed on 30-MPa substrates after repair (UL program).....	36
Figure 3-27: Results of torque tests performed on 20-MPa substrates after repair (UL program)	36
Figure 3-28: Distribution of failure location in torque tests performed on 20-MPa substrates after repair	37
Figure 3-29: Results of torque tests performed on 30-MPa substrates after repair (UL program)	37
Figure 3-30: Distribution of failure location in torque tests performed on 30-MPa substrates after repair (UL program).....	38
Figure 3-31: Results of pull-off tests (ASTM C1583) performed after repair as a function of the substrate roughness generated by various preparation techniques (UL program)	38
Figure 3-32: Results of direct tensile tests (CRD-C 164) performed after repair on cores extracted from the slabs as a function of the substrate roughness generated by various preparation techniques (UL program)	40

Figure 3-33: Results of direct tensile tests performed after repair on cores extracted from the artificially profiled 20-MPa test slab (UL program) 41

Figure 3-34: Results of torsional bond experiments performed after repair as a function of the substrate roughness generated by various preparation techniques (UL program) 41

Figure 3-35: Shear bond to tensile bond strength ratio after repair as a function of the substrate R_a value generated by various preparation techniques (UL program) 42

Section 3 – Establish relationships between tensile bond, shear bond and substrate roughness parameters (CRC Proposal Task 2)

In Task 2, experimental work was carried out both at the US Bureau of Reclamation in Denver (CO), USA, and the Research Center on Concrete Infrastructure (CRIB), Laval University, Quebec city (QC), Canada.

3.1 Introduction

In addition to adhesion and cohesion, another parameter often considered to be affecting the tensile bond between a repair material and existing concrete is the substrate roughness. In fact, this subject has been controversial for years.

In some studies, the reported bond test results have shown that surface roughness has only a minor influence on the tensile bond. For instance, in the tests performed by Silfwerbrand [1], bond to rough water jetted surface was compared with bond to smooth sandblasted surface. It was concluded that there could be a roughness “threshold value” beyond which further improvement on the roughness would not enhance bond strength. According to these test results, the “threshold value” ought to be close to the surface roughness of the typical sandblasted surfaces.

Still, it remains the opinion of a number of other specialists in the industry that a rougher surface is beneficial to bond strength. Talbot et al. [2] investigated the influence of surface preparation and concluded that concrete substrates with smoother surface profiles, produced for instance by grinding or simple sandblasting, experienced significant loss of bond strength with time. On the contrary, surfaces that were roughened mechanically and subsequently

sandblasted exhibited good bond durability. The reason for this may lie in the fact that high interface roughness, as it is commonly achieved in field repairs in practice, improves the resistance against interface shear stress resulting from repair material drying shrinkage.

Besides, as raised in the previous explanation for the potentially beneficial influence of roughness upon bond strength, the differential volume changes between the repair material and the substrate can induce potentially critical shear stresses in some areas of the interface [3]. However, in practice, bond strength of concrete repairs and overlays is generally defined as the tensile strength in the direction perpendicular to the interface plane and measured essentially in direct tension through pull-off testing.

It is necessary to realize that adhesion mechanisms in tension and in shear may differ significantly. For example, a high interface roughness may improve shear bond strength, whereas tensile mechanical bond strength primarily depends on vertical anchorage in pores and voids. Under service conditions, the repair interface is subjected to both tensile and shear stresses. When specifying and/or evaluating bond strength values, it might thus be important to address explicitly the dominant interface stress condition encountered in the actual structure.

To this day, relatively little data have been reported in relation with shear bond strength. Most published studies are in agreement that shear bond strength is higher than tensile bond strength. However, there is no agreement on the magnitude of the correlation. In the studies that were reviewed, the reported average shear bond strength to tensile bond strength ratio varies from 1.2 to 2.0. That range is obviously too wide for converting satisfactorily the pull-off test results to shear bond strength. However, it is easier to measure the tensile bond strength, and it can be used reliably as a definition of bond if a decent relationship between the two bond strength parameters is established.

Hence, the main objectives of this task were to establish the relationship between both tensile and shear bond strengths and the substrate roughness. Since roughness directly depends on the surface preparation method, this task is intended to shed new light on the subject and help resolving the controversy regarding the extent of its influence.

3.2 Methodology

Two experimental programs were conducted complementarily at the U.S. Bureau of Reclamation (USBR), Denver (CO), USA and at Laval University (CRIB), Quebec City (QC), Canada.

3.2.1 Test program conducted at USBR

The test program conducted at USBR is summarized in Table 3-1. Details pertaining to the test variables, the test specimens, the surface preparation techniques and the test methods are provided in the following subsections.

3.2.1.1 Investigated variables and specimen preparation

A series of 12 concrete slabs (1170×560×150 mm) was manufactured for the test program (Figure 3-1). The slabs were cast using a 40-MPa ready-mix concrete. The basic properties of both mixtures are displayed in Table 3-2. The slabs were exposed to drying at least six months to achieve relative dimensional stability, after what surface preparation was performed.

Three of the most common surface preparation techniques were selected for investigation: sandblasting (SA), water jetting (WJ), and jackhammering (JH), with the characteristics provided

in Table 3-1. Sets of four base slabs were prepared with each of these techniques, as shown in Figure 3-2.

Table 3-1: Test program conducted at USBR

Item	Details
<p>Test specimens</p> <ul style="list-style-type: none"> • Base slabs • Repaired test slabs 	<ul style="list-style-type: none"> - 1170×560×150 mm base concrete slabs - 1 slab series: 12 slabs prepared with 40-MPa OPC concrete - base slabs moist cured for 3 days after casting and exposed to drying for more than 6 months prior to repair - repairs performed on the slab series submitted to 3 different surface preparation methods and pre-wetted to <i>SSD</i>: 75-mm thick overlays with a 40-MPa OPC concrete mixture
<p>Investigated surface preparation techniques (surface prep. prior to repair)</p>	<ul style="list-style-type: none"> - sandblasting (SA) (4 slab per series) - 15-ksi handheld water jetting (WJ) (4 slab per series) - 15-lb handheld jackhammering (JH) (4 slab per series)
<p>Characterization test methods for:</p> <ul style="list-style-type: none"> • Surface roughness • Surface integrity • Bond strength (28-d) 	<ul style="list-style-type: none"> - ICRI <i>Concrete Surface Profile (CSP)</i> index - ASTM <i>Macrotexture Depth</i> test (<i>Sand Patch</i> test) - Optical profilometry - Schmidt hammer - Pull-off test - Torque test

After surface preparation, evaluation of surface integrity and characterization of surface roughness were performed. The slabs were then repaired (75-mm overlay) with the same 40-MPa concrete mixture. The repair concrete mixtures properties are also summarized in Table 3-2. The repaired specimens were moist-cured for 3 days, after what they were air-dried for at least 28 days, until the bond strength tests were carried out.



Figure 3-1: Preparation of test slabs at USBR

Table 3-2: Concrete mixture characteristics and mechanical properties (USBR)

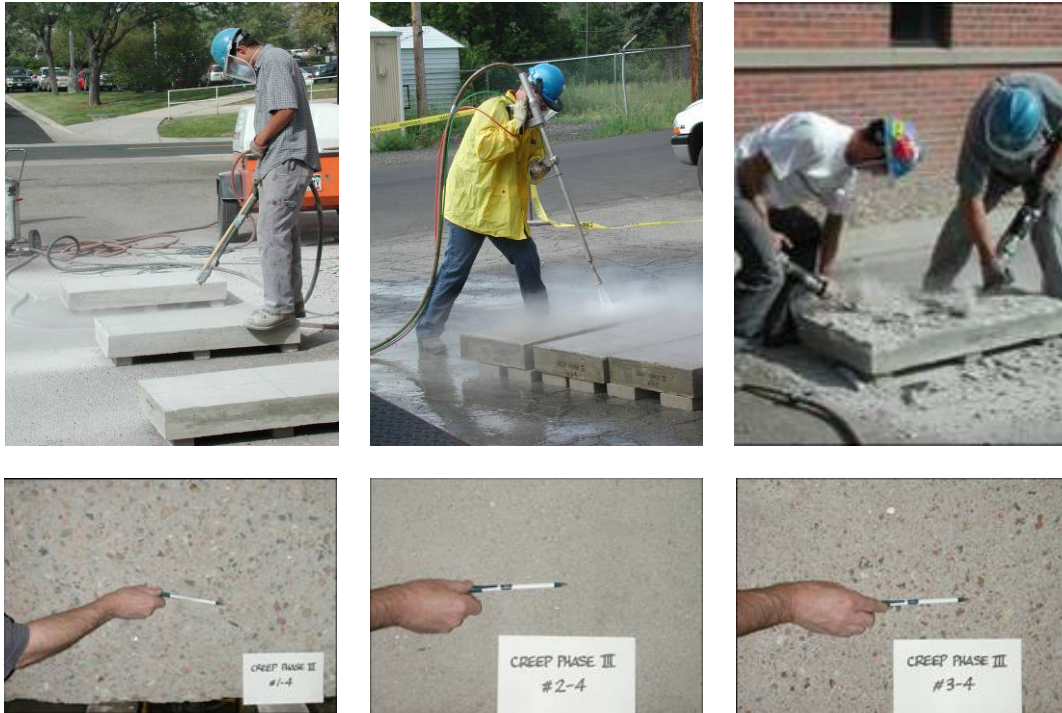
Material	Test slab concrete mixtures	Repair concrete mixture
Nominal strength	40 MPa (6000 psi)	40 MPa (6000 psi)
Mixture characteristics	ASTM Type I cement 14-mm coarse aggregates	ASTM Type I cement 14-mm coarse aggregates
Fresh concrete properties Slump (mm) Air content (%)	75 3.2	75 4.5
Compressive strength ¹ (MPa) 7 d 28 d	- 38.7	34.1 39.2
Splitting-tensile strength ² (MPa) 7 d 28 d	- 3.1	3.8 4.4
Elastic modulus ³ (GPa) 7 d 28 d	- -	24.2 26.1

¹ASTM C39; ²ASTM C496; ³ASTM C469.

3.2.1.2 Surface roughness characterization

The roughness of the surface profiles achieved with the various investigated surface preparation techniques was evaluated with three different methods. All slab profiles were characterized in accordance with ICRI *Concrete Surface Preparation* index (CSP; ICRI No.

310.2R-2013), with the *Macrotexture depth* method (EN 13036-1 / ASTM E965-06) – often referred to as the sand patch test method – and a *Moiré*-type optical profilometry method to evaluate the average half-amplitude parameter (R_a).



a) Sandblasting

b) Water jetting (15 ksi)

c) Jackhammering (15 lb)

Figure 3-2: Surface preparation of the test slabs at USBR

3.2.1.3 Evaluation of surface integrity

Surface integrity of the prepared test slab was evaluated on an exploratory basis through Schmidt hammer soundings. It was reported by Courard et al. [4] to be a potentially interesting mean for detecting the presence of surface damage, provided that the number of tests is sufficient. Seeking a simple and field-friendly way to assess surface integrity prior to repair, Schmidt hammer soundings were thus performed in a systematic fashion on all prepared test

slabs, using a template grid with regularly-spaced data points collected along the X- and Y- directions over the whole surface.

3.2.1.4 Bond strength evaluation

All 12 repaired test slabs were characterized for bond strength with a combination of pull-off tests and torsional shear tests.

For the evaluation of tensile bond strength, the most widely used method is the pull-off test (ASTM C1583; CAN/CSA A23.2-6B; EN 1542; BS 1881). This test method consists of drilling a core through the repair material down to a minimum depth within the substrate, gluing a steel dolly onto the top of the core with epoxy, and to pull on the steel dolly using a special loading rig. The tensile bond strength is equal to the maximum recorded stress when failure occurs in the interfacial zone, whereas a lower boundary value of bond strength is obtained when failure occurs elsewhere. In this part of the study, the pull-off strength tests were performed in accordance with the CAN/CSA A23.2-6B procedure.

Torsional shear tests have been included on the experimental program to evaluate the bond shear response and sensitivity with respect to the tensile behavior. In this test procedure, a ring glued to the surface is twisted off using a torque housing with eccentric loading. The housing is anchored to the surface and the loading is performed with the same pulling unit as in the pull-off test procedure (different adapters). There is no standard procedure for this test. More information can be found on the manufacturer's website (germann.org) and in a paper by Petersen and Poulsen [5].

The pull-off and shear tests were performed at least 28 days after pouring of the overlays. All 12 repaired test slabs were characterized for bond strength with a combination of nine pull-off tests and nine torsional shear tests on each of them, resulting in a total 36 pull-off tests and 36 shear bond strength tests per slab series. The template for the different tests is presented in Figure 3-3: Core-drilling template for mechanical bond testing (USBR program) (note: the pull-off tests with an inclination are addressed in the next section of the report). The pull-off and shear bond tests were performed at specific locations from one test slab to the other to assure better reproducibility of the results.

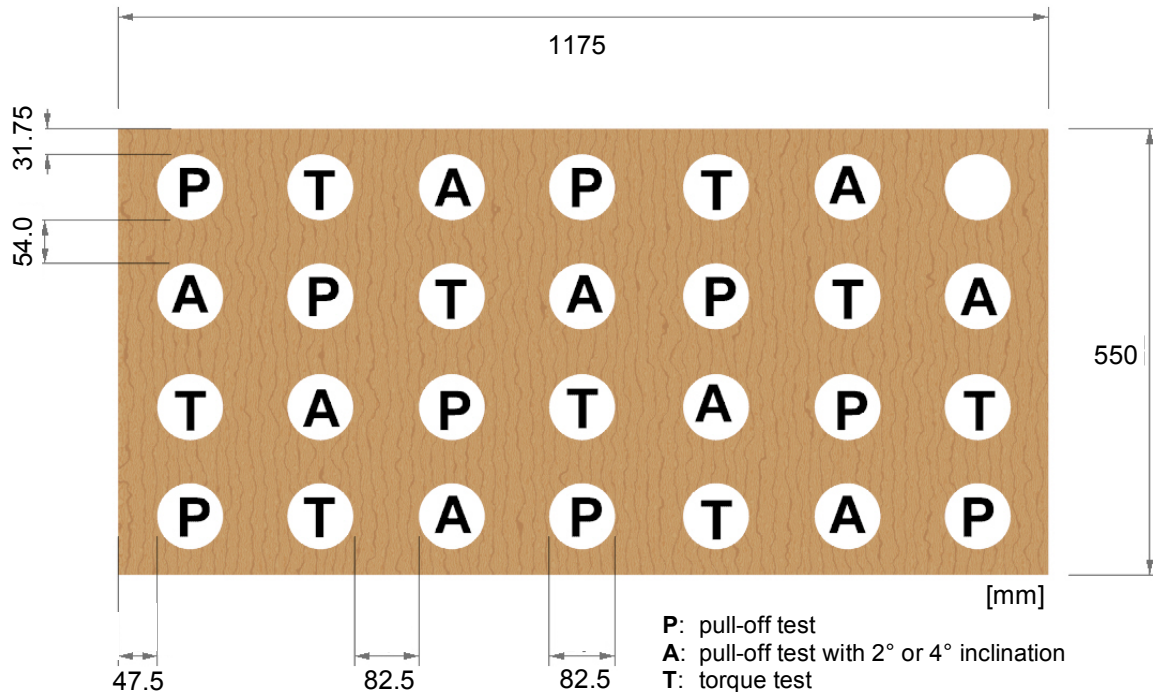


Figure 3-3: Core-drilling template for mechanical bond testing (USBR program)
(note: the pull-off tests with an inclination are addressed in the next section of the report)

3.2.2 Test program conducted at Laval University

The test program conducted at Laval University (UL) is summarized in Table 3-3. Details pertaining to the test variables, the test specimens, the surface preparation techniques and the test methods are provided in the following subsections.

Table 3-3: Test program conducted at UL

Item	Details
<p>Test specimens</p> <ul style="list-style-type: none"> • Base slabs • Repaired test slabs 	<ul style="list-style-type: none"> - 1250×625×150 mm base concrete slabs - 2 slab series: 16 slabs prepared with 20-MPa OPC concrete 15 slabs prepared with 30-MPa OPC concrete - base slabs moist cured for 3 days after casting and exposed to drying for more than 3 months prior to repair - repairs performed on the two slab series submitted to various surface preparation methods and pre-wetted to SSD: 75-mm thick overlays with a 40-MPa OPC concrete mixture
<p>Investigated surface preparation techniques (surface prep. prior to repair)</p>	<ul style="list-style-type: none"> - scarifying (SC) (3 slabs per series) - shotblasting (SH) (3 slabs per series) - sandblasting (SA) (3 slabs per series) - water jetting (WJ) (3 slabs per series) - jackhammering (JH) (3 slabs per series) - artificially cast roughness profiles (1 slab / 20-MPa series)
<p>Characterization test methods for:</p> <ul style="list-style-type: none"> • Surface roughness • Surface integrity • Bond strength (28-d) 	<ul style="list-style-type: none"> - ICRI <i>Concrete Surface Profile</i> (CSP) index - Optical profilometry - Schmidt hammer - Pull-off test - Pull-off test - Torque test

3.2.2.1 Investigated variables and specimen preparation

Two series of 16 concrete slabs (625×1250×150 mm) were manufactured for the test program (Figure 3-4). The first series was made with a 30-MPa ready-mix concrete, while the second series was prepared using a 20-MPa concrete. The basic properties of both mixtures are displayed in Table 3-4. The slabs were exposed to drying for at least three months to achieve relative dimensional stability, after what surface preparation was performed.



Figure 3-4: Test slabs prepared at UL

Table 3-4: Concrete mixture characteristics and mechanical properties (UL program)

Material	Test slab concrete mixtures		Repair concrete mixture
Nominal strength	20 MPa (3000 psi)	30 MPa (4500 psi)	40 MPa (6000 psi)
Mixture characteristics	$w/cm = 0.65$	$w/cm = 0.57$	$w/cm = 0.40$
	CSA Type 10 cement 20-mm coarse aggregates		CSA Type 10 cement 14-mm coarse aggregates Black pigments (6% wgt of C)
Fresh concrete properties ¹			
Slump (mm)	80	80	80
Air content (%)	6	6	6
Compressive strength ² (MPa)			
7 d	17.1	27.4	37.8
28 d	20.8	33.1	43.6
56 d	21.5	35.4	46.1
Splitting-tensile strength ³ (MPa)			
7 d	1.7	2.9	2.6

28 d	1.9	3.2	2.9
56 d	2.0	3.3	3.0
Elastic modulus ⁴ (GPa)			
7 d	18.2	24.2	25.3
28 d	19.7	27.1	27.5
56 d	-	29.5	-

¹Specified values; ²ASTM C39, ³ASTM C496, ⁴ASTM C469.

In order to cover a sufficiently large spectrum in terms of roughness and, at the same time, to address most usual surface preparation techniques, the following methods were selected for investigation: sandblasting (SA), shotblasting (SH), scarifying (SC), 15,000-psi handheld water jetting (WJ), and 15-lb handheld jackhammering (JH) (Figure 3-5). In both test slab series, sets of three base slabs were prepared with each of these techniques. In addition, to prevent the potential influence of any induced damage and isolate the effect of roughness upon bond strength, one artificially profiled test specimen was cast in each slab series. V-shape rippled acrylic dies were installed at the bottom of the test slab forms to obtain wave amplitude values of 2, 4, 6 and 8 mm respectively in four adjacent areas along the specimen length, the wavelength being of 30 mm in all of them (Figure 3-6).



Figure 3-5: Scarification and shotblasting surface preparation at CRIB (UL program)

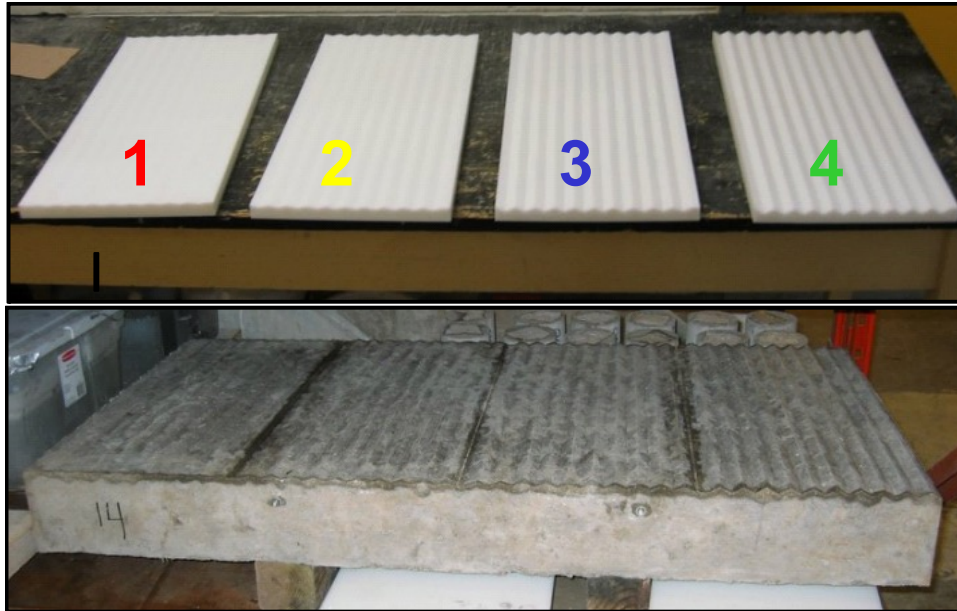


Figure 3-6: V-shape rippled acrylic dies and resulting profiled slabs (UL program)

After surface preparation, evaluation of surface integrity and characterization of surface roughness were performed. The slabs were then repaired (75-mm overlay) with a 40-MPa repair concrete. The artificially profiled slabs (one per slab series) were very lightly sandblasted to remove laitance. In order to easily locate the interface location on the cores and establish more precisely the failure mode and path, a black pigment was added to the repair material at the time of mixing (rate of addition: 6 % by weight of cement). The repair concrete mixtures properties are also summarized in Table 3-4. The repaired specimens were moist-cured for 7 days, after what they were air-dried for at least 28 days, until the bond strength tests were carried out.

3.2.2.2 Surface roughness characterization

The roughness of the surface profiles achieved with the various investigated surface preparation techniques was evaluated with two different methods. All slab profiles were first characterized in accordance with ICRI *Concrete Surface Preparation* index (CSP; ICRI No.

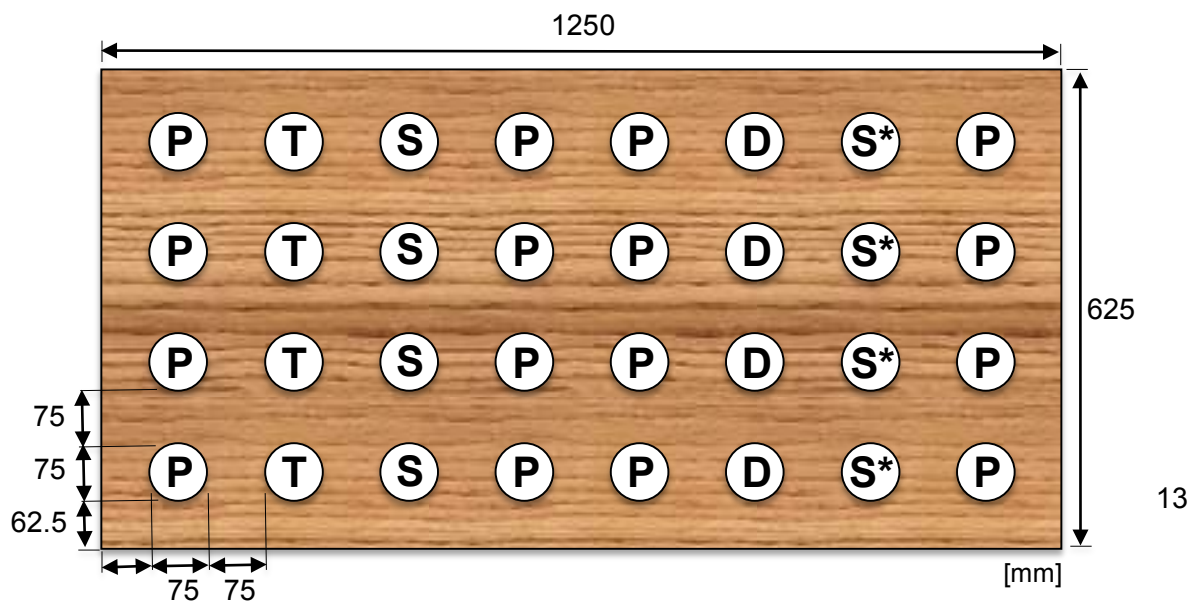
310.2R-2013), and then using *Moiré*-type optical profilometry to yield the average half-amplitude parameter (R_a).

3.2.2.3 Evaluation of surface integrity

Surface integrity of the prepared test slab was evaluated through pull-off experiments and, still on an exploratory basis, Schmidt hammer soundings.

Seeking a simple and field-friendly way to assess surface integrity prior to repair, Schmidt hammer soundings were performed in a systematic fashion on all prepared slabs, using a template grid with regularly-spaced data points collected in the X- and Y- directions over the whole surface.

Pull-off tests were performed immediately after the Schmidt soundings. Surface integrity of the prepared test slab was evaluated through pull-off experiments performed on the prepared slabs, in accordance with a procedure proposed by Courard and Bissonnette [6]. It has proven to be reliable for detecting the presence of surface damage, provided that the number of tests is sufficient. On each tested slab, eight substrate pull-off tests were performed (4 on 75-mm cores; 4 on 100-mm cores), in accordance with the pattern shown on Figure 3-7.



- 62.5 **P:** pull-off test (repair)
 T: torque test (repair)
 S: substrate pull-off test (**S***: 100-mm core)
 D: full-depth core extracted for direct tensile testing (repair)

Figure 3-7: Core-drilling template for mechanical bond testing (UL program)

3.2.2.4 Bond strength evaluation

All 32 repaired test slabs were characterized exhaustively for bond strength with a combination of pull-off tests, direct tensile tests and torsional shear tests.

For the evaluation of tensile bond strength, pull-off tests were performed in accordance with CAN/CSA A23.2-6B. In addition to the pull-off tests, direct tensile bond strength tests were performed on cores taken from the slabs. As part of the specimen preparation procedure, a five-millimeter deep circumferential saw cut was performed on the cores at the interface level in order to reduce their cross-sectional area and promote interfacial failure. Core preparation was completed by gluing steel dollies at both ends. The specimens were then tested in a universal testing frame in accordance with the U.S. Army Corps of Engineers test method for determining direct tensile strength (CRD-C 164).

Torsional shear tests have again been carried out to evaluate the bond shear response and sensitivity with respect to the tensile behavior, using the same test procedure used at USBR.

The pull-off, direct tension and shear bond tests were performed at least 28 days after pouring of the overlays. All 32 repaired test slabs were characterized for bond strength with a combination of 16 pull-off tests, four direct tensile tests and four torsional shear tests on each of

them, resulting in a total 48 pull-off tests, 12 direct tensile tests, and 12 shear bond strength tests per slab series. The template for the different tests is presented in Figure 3-7. The different tests were performed at specific locations from one test slab to the other to assure better reproducibility of the results.

3.3 Results and analysis

3.3.1 Test program conducted at USBR

3.3.1.1 Surface roughness

The surface roughness characteristics corresponding to the various surface preparation profiles, as obtained using the ICRI CSP index (ICRI No. 310.2R-2013), the ASTM E965-06 Macrotexture depth test method, and optical profilometry respectively, are summarized in Table 3-5.

Overall, the roughness parameters determined with the three different characterization methods are consistent: sandblasting and jackhammering yielded the lowest and highest roughness values respectively, while water jetting yielded an intermediate profile, somewhat on the low side.

Table 3-5: Summary of surface roughness test results (USBR program)

Test	Parameter	Surface preparation		
		Sandblasting	Water jetting	Jackhammering
ICRI CSP profiles (ICRI No. 310.2R-2013)	Avg. CSP index (1-9)	4.5	6	> 9
Macrotexture depth (ASTM E965-06)	Avg. depth (mm)	0.5	1.4	5.8
Optical profilometry	Half-amplitude R _a (mm)	0.4	0.5	2.6

It is interesting to compare the quantitative evaluations generated with the ASTM procedure and optical profilometry. The macrotexture depth test method allows to the average depth of the surface profile roughness, while the optical method yields a 3-D representation of the profile, which is treated to extract roughness parameters R_a , as shown in Figure 3-8. Since the R_a parameter corresponds to half of the surface profile wave amplitude, it should then be expected to amount approximately to half the macrotexture depth yielded in accordance with ASTM E965-06. On the graph of

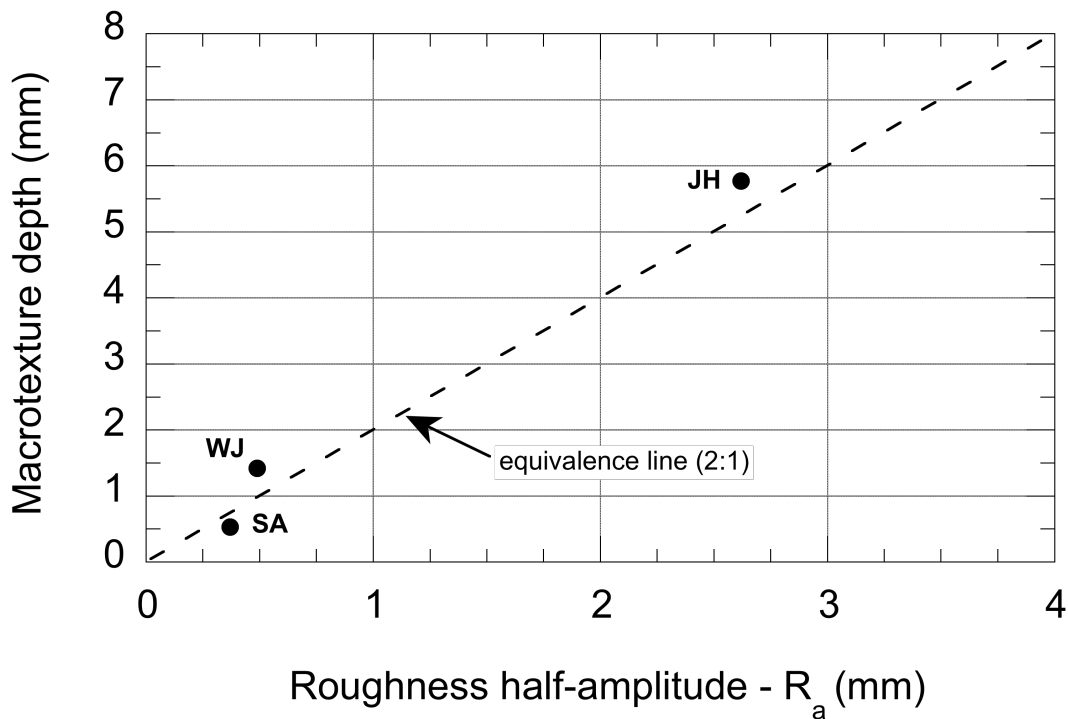


Figure 3-9, the experimental data actually show a satisfactory correlation.

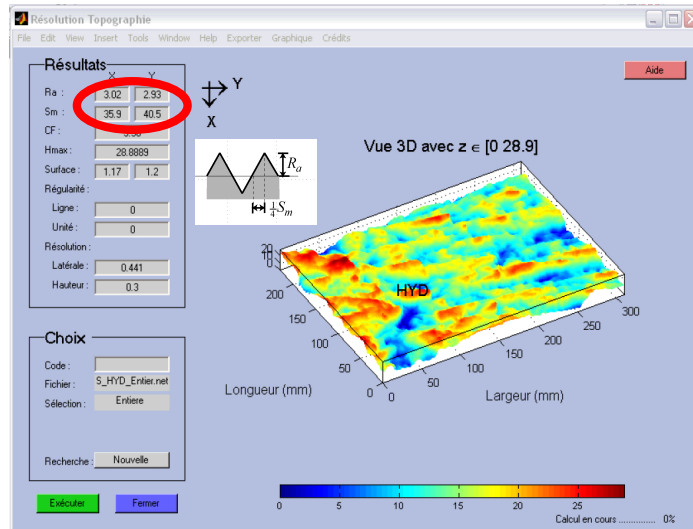


Figure 3-8: Computer interface for optical profilometry data treatment (example shown: test slab prepared with water jetting)

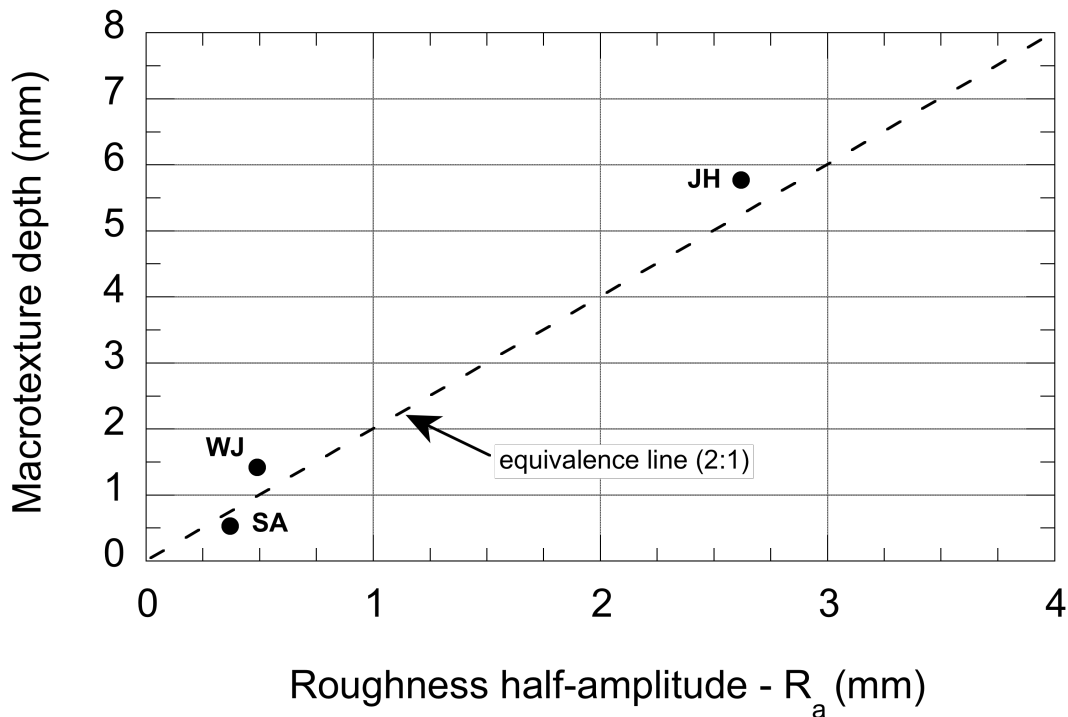


Figure 3-9: Correlation between macrotexture depth (ASTM E965-06) and optical profilometry characterization (USBR program) (note: SA – sandblasting; WJ – water jetting; JH – jackhammering)

3.3.1.2 Mechanical integrity of the substrate

Data recorded from the Schmidt hammer soundings performed on the substrate subjected to various types of surface preparation are summarized in Figure 3-10. According to Courard et al. [4], data variability, not in as much as the absolute values, would provide an indication of the presence and importance of defects in the substrate. As a matter of fact, on surfaces exhibiting significant waviness, the rebound recorded with the Schmidt hammer is affected negatively. The comparatively low estimated strength values for both water jetted and jackhammered are thus not surprising. Nevertheless, it can be observed in the figure that the latter are characterized by a significantly larger variability, which may potentially reflect the presence of surface defects induced by the hammer tip. Such damage induced into the substrate by jackhammers and the various types of impact breakers, generally referred to as bruising, was assessed in a previous study [7].

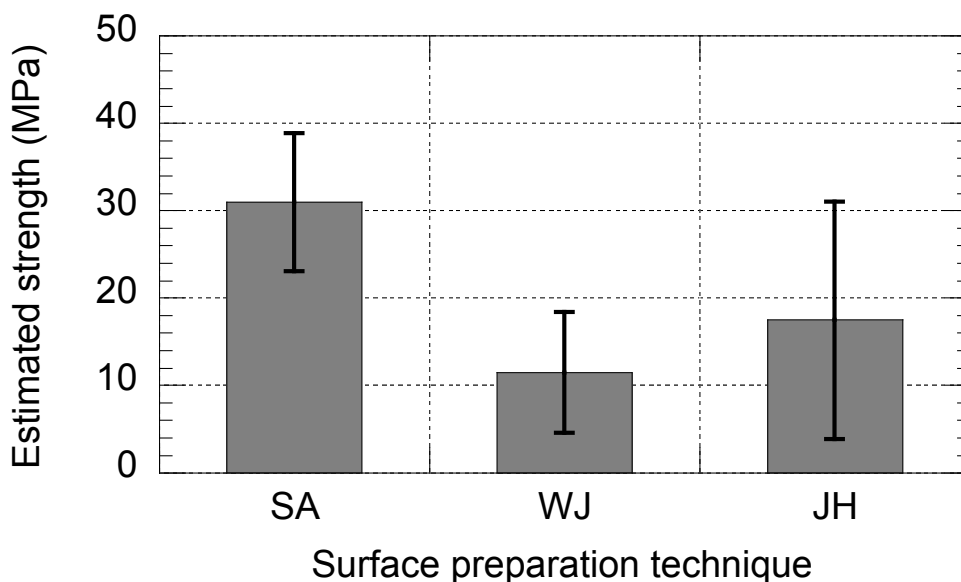


Figure 3-10: Results of Schmidt hammer soundings (ASTM C805) performed after surface preparation to evaluate the mechanical integrity of the exposed concrete surface (USBR program)

(note: SA – sandblasting; WJ – water jetting; JH – jackhammering)

3.3.1.3 Bond strength

The detailed results of the various bond strength tests performed on the experimental slabs are presented in Tables

Table 3-6 and Table 3-7, and in Figures Figure 3-11 to Figure 3-14.

Pull-off testing

When comparing the pull-off test results obtained on sandblasted and water jetted surfaces in Figures Figure 3-11 to Figure 3-14, the small increase in surface roughness generated with the latter method apparently resulted in a slightly stronger bond. However, even though jackhammering yielded a much coarser surface profiles than the two other investigated surface preparation methods, the pull-off strength values recorded for the corresponding repaired slabs rank as the lowest.

As far as the relationship observed between pull-off strength and substrate roughness is concerned, the graphs of Figures Figure 3-15 to Figure 3-17 hereafter all exhibit similar trends, irrespective of the method used for characterizing roughness.

It appears that bond strength slightly increase with the level of roughness of the substrate, provided that no or limited damage is induced. In fact, the failure location distributions (

Table 3-6 and Figure 3-12) tend to show that from sandblasting to water jetting, failure is somehow pushed away from the interfacial zone down into the substrate (75 %), while with jackhammering, the tendency is reversed and failure occurs preferentially in the interfacial area

(70 %). This is consistent with the respective levels variability found for the Schmidt hammer data on the different surface preparations (Figure 3-18).

The reversed tendency observed for the aggressive jackhammering technique has to be attributed to the presence of disseminated defects left on the surface after completion of the jackhammering operations, as confirmed by the microanalysis findings of a previous investigation [7]. Where the extent of the defects induced in the substrate becomes significant, the positive influence of increased roughness is found to be completely offset mechanically by the adverse effects of bruising.

Table 3-6: Summary of pull-off test results for the 40-MPa concrete substrate series (USBR program)

Surface preparation method	Test parameters	Location of failure					Overall
		Core end	Substrate	Interface	Repair	Dolly	
Sandblasting (SA)	Number of test results (%)	20 (57.1)	2 (5.7)	10 (28.6)	1 (2.9)	2 (5.7)	35 (100.0)
	Avg. strength [MPa] (std. dev.)	1.91 (0.24)	2.04 (0.16)	1.29 (0.45)	1.63 -	1.20 (1.02)	1.69 (0.46)
Water jetting (WJ)	Number of test results (%)	27 (75.0)	6 (16.7)	1 (2.8)	2 (5.6)	0 (0.0)	36 (100.0)
	Avg. strength [MPa] (std. dev.)	1.94 (0.32)	2.01 (0.30)	1.99 -	1.83 (0.13)	- (-)	1.96 (0.30)
Jackhammering (JH)	Number of test results (%)	4 (11.1)	7 (19.4)	25 (69.4)	0 (0.0)	0 (0.0)	36 (100.0)
	Avg. strength [MPa] (std. dev.)	1.57 (0.25)	1.03 (0.27)	1.35 (0.47)	- (-)	- (-)	1.31 (0.44)

Table 3-7: Summary of torque test results for the 40-MPa concrete substrate series (USBR program)

Surface preparation method	Test parameters	Location of failure					Overall
		Core end	Substrate	Interface	Repair	Dolly	
Sandblasting (SA)	Number of test results (%)	2 (5.7)	11 (31.4)	12 (34.3)	10 (28.6)	0 (0.0)	35 (35.0)
	Avg. strength [MPa] (std. dev.)	1.21 (0.00)	1.51 (0.64)	1.28 (0.65)	2.14 (0.46)	- (-)	1.60 (0.71)
Water jetting	Number of test results (%)	8 (22.2)	10 (27.8)	8 (22.2)	10 (27.8)	0 (0.0)	36 (100.0)

(WJ)	Avg. strength [MPa] (std. dev.)	1.80 (0.84)	1.93 (0.35)	2.34 (0.57)	2.28 (0.53)	0.00 (-)	2.05 (0.56)
Jackhammering (JH)	Number of test results (%)	8 (24.2)	6 (18.2)	10 (30.3)	7 (21.2)	1 (3.0)	33** (100.0)
	Avg. strength [MPa] (std. dev.)	1.57 (0.53)	1.89 (0.93)	1.46 (0.49)	2.66 (1.11)	6.30* (-)	1.84 (0.85)

* value discarded in calculating the overall average strength

** for one test core, the failure location was not reported

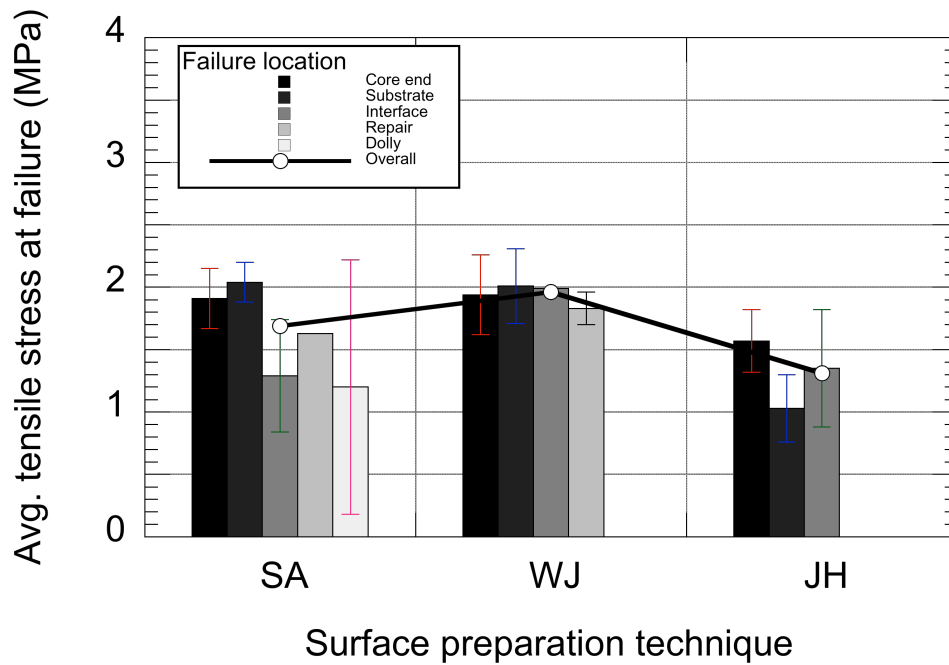


Figure 3-11: Results of pull-off tests performed on 40-MPa substrates after repair (USBR program)

(note: SA – sandblasting; WJ – water jetting; JH – jackhammering)

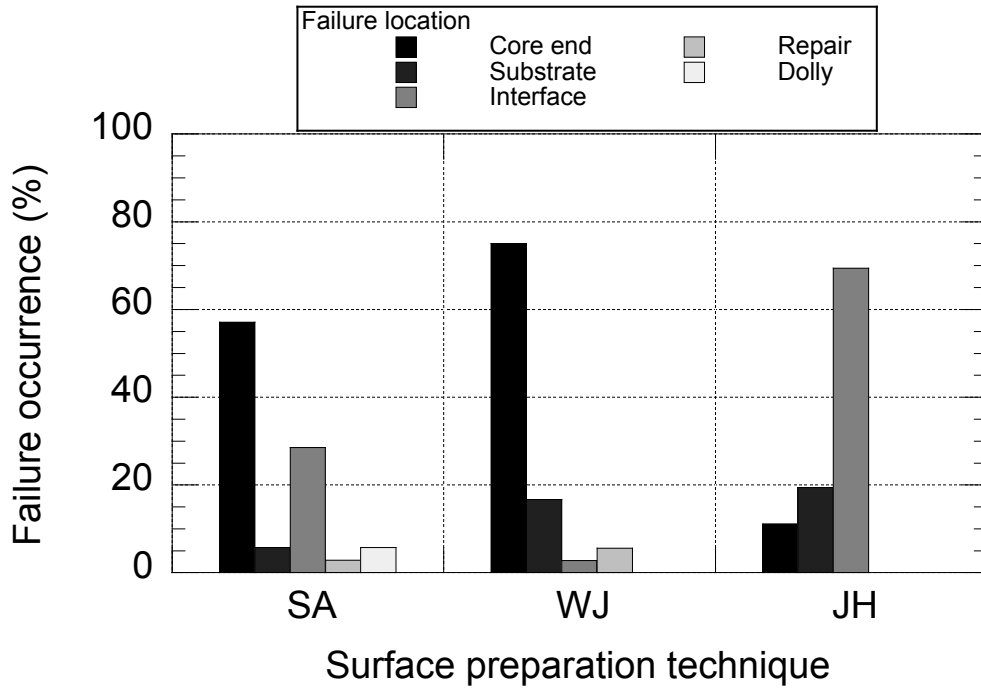


Figure 3-12: Distribution of failure location in pull-off tests performed on 40-MPa substrates after repair (USBR program)
 (note: SA – sandblasting; WJ – water jetting; JH – jackhammering)

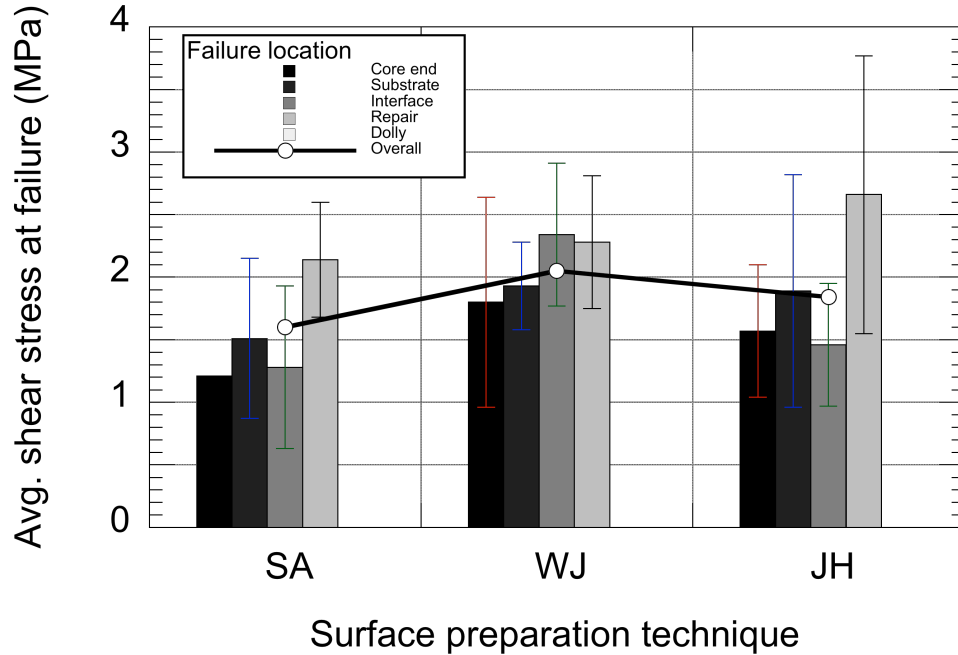


Figure 3-13: Results of torque tests performed on 40-MPa substrates after repair (USBR program)
 (note: SA – sandblasting; WJ – water jetting; JH – jackhammering)

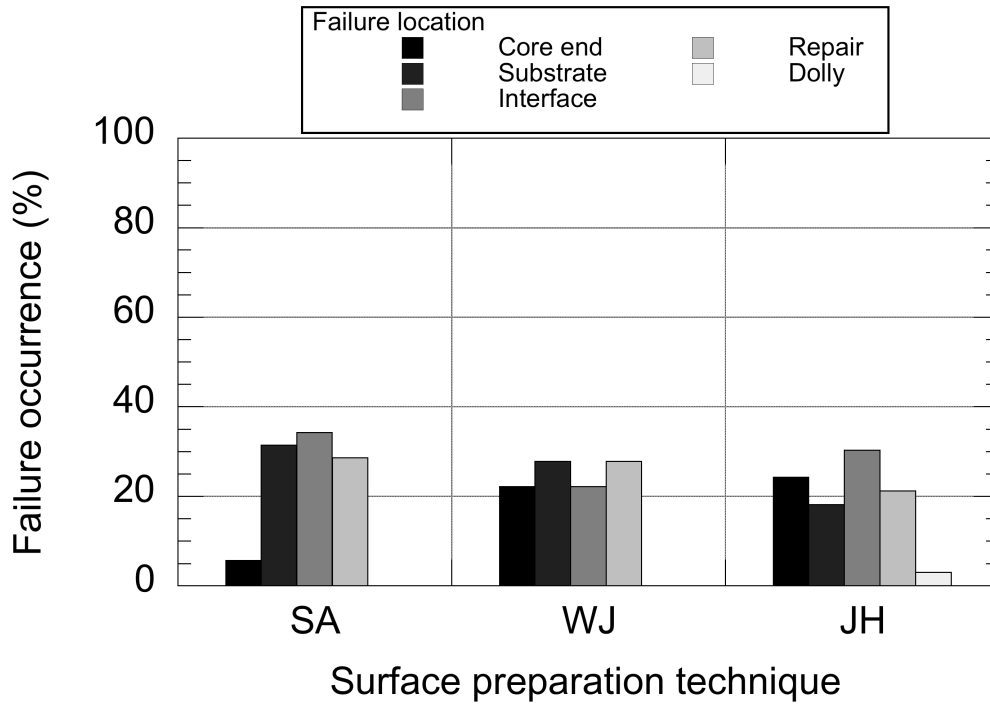


Figure 3-14: Distribution of failure location in torque tests performed on 40-MPa substrates after repair (USBR program)
 (note: SA – sandblasting; WJ – water jetting; JH – jackhammering)

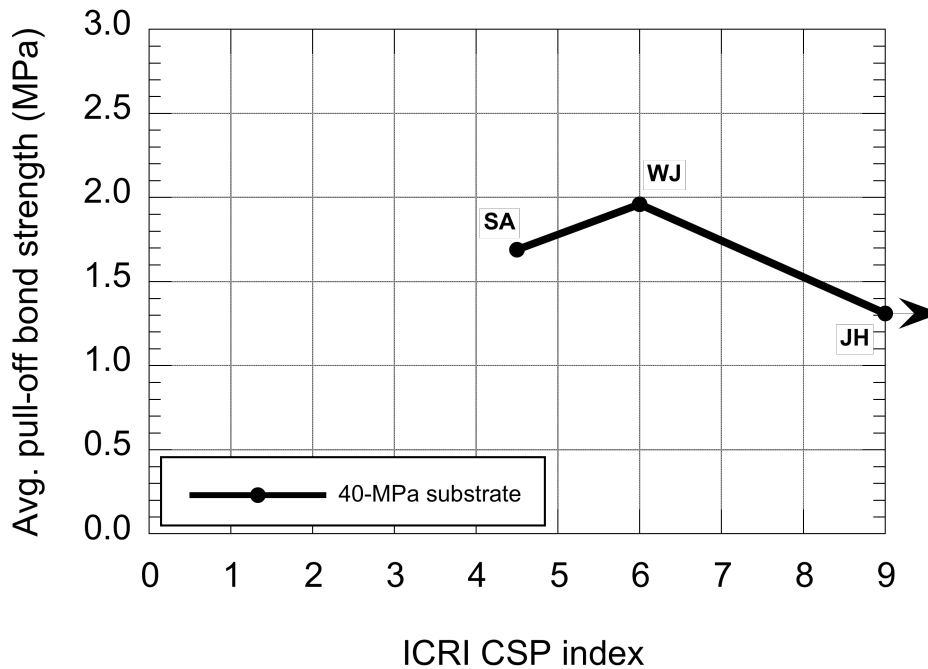


Figure 3-15: Results of pull-off tests (ASTM C1583) performed after repair as a function of the substrate CSP index (ICRI No. 310.2R-2013) generated by various preparation techniques (USBR program)
 (note: SA – sandblasting; WJ – water jetting; JH – jackhammering)

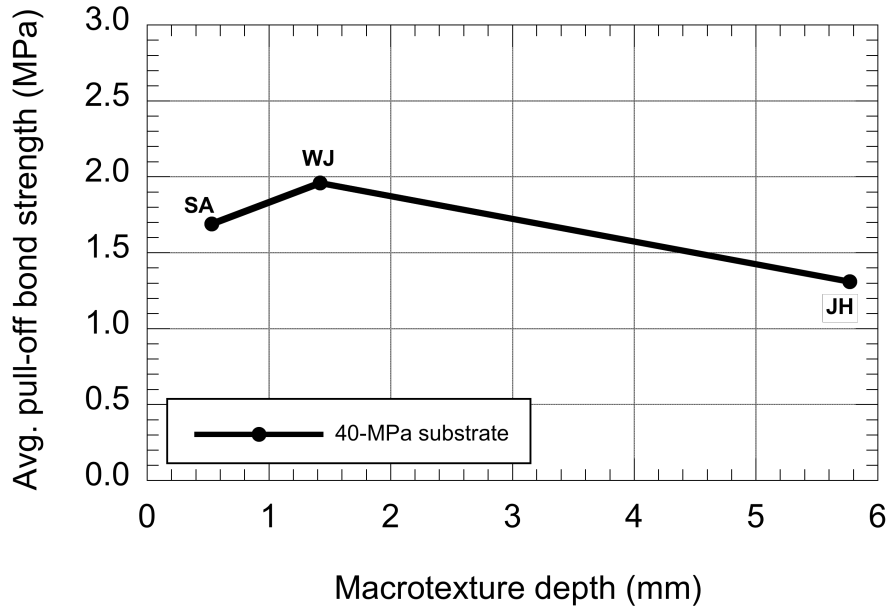


Figure 3-16: Results of pull-off tests (ASTM C1583) performed after repair as a function of the substrate Macrot texture depth (ASTM E965) generated by various preparation techniques (USBR program)
(note: SA – sandblasting; WJ – water jetting; JH – jackhammering)

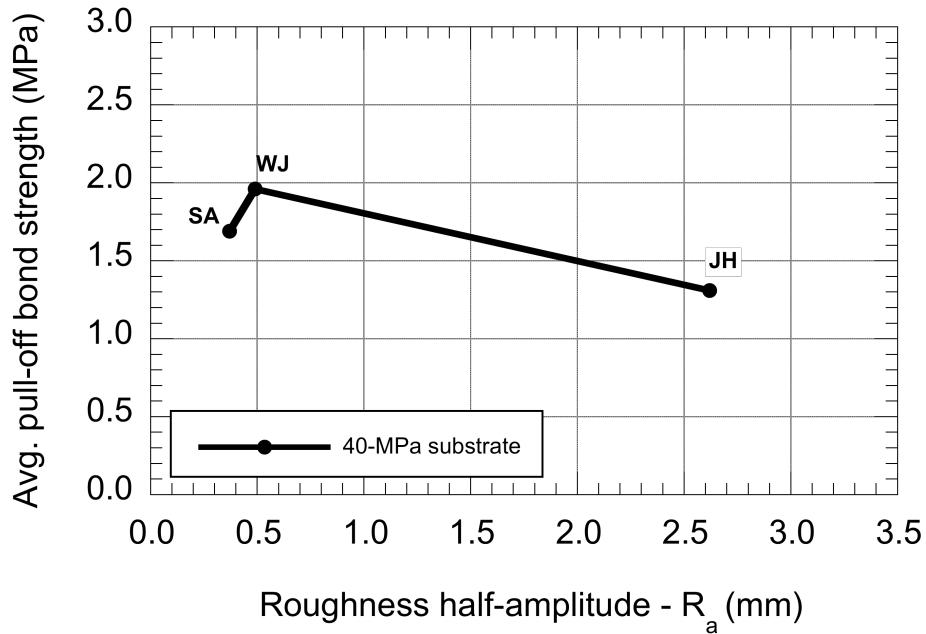


Figure 3-17: Results of pull-off tests (ASTM C1583) performed after repair as a function of the substrate R_a value generated by various preparation techniques (USBR program)
(note: SA – sandblasting; WJ – water jetting; JH – jackhammering)

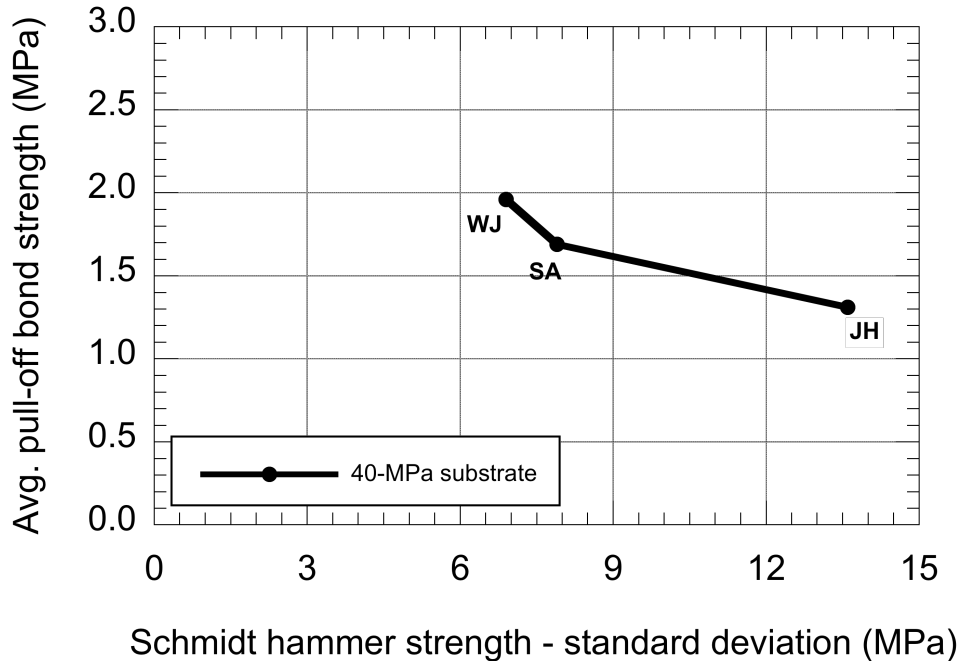


Figure 3-18: Results of pull-off tests (ASTM C1583) performed after repair as a function of the variability of the Schmidt hammer data (ASTM C805) yielded for different surface preparations (USBR program)

(note: SA – sandblasting; WJ – water jetting; JH – jackhammering)

Torque testing

The torsional shear bond test results presented in Table 3-7, Figures Figure 3-13 and Figure 3-14 exhibit trends that are similar to those observed for the pull-off results in terms of average bond strength, but not with regards to the failure location distribution. In fact, contrarily to the direction tension case, failure under a torsional load appears to be more or less uniformly distributed along the length of the test cores.

The relationship observed experimentally between shear bond strength and roughness is plotted on the graph of Figure 3-19. Based on this graph, roughness appears to play a more important role in shear bond than in tension bond, which is somewhat consistent with what could be intuitively expected. Nevertheless, when considering the shear bond to tensile bond strength ratio as a function of the R_a value (Figure 3-20), the sharp increase observed for the coarse

jackhammered substrates must thus be interpreted with caution. While a positive influence of increased roughness upon shear bond strength cannot here be dismissed, it appears that the damage induced in the vicinity of the surface is more detrimental to the bond in direct tension than in shear.

Besides, the shear bond to tensile bond strength ratios recorded experimentally are observed to be in the lower portion of the typical range (1.2 – 2.0) reported by Vaysburd et al. [9]. It should be stressed that in many instances, shear tests involve the use of a normal compressive force, which necessarily translates into a smaller corresponding tensile stress for a given imposed shear load, and ultimately, a larger shear-to-tension stress ratio. In addition, when approaching the ultimate shear loading, the presence of a normal force tends to stabilize the specimen and prevent premature failure. In the shear bond test procedure carried out as part of the present investigation, no normal force is applied against the testing surface. This may explain why the bond values recorded in torsional shear are close to the tensile bond values determined with the pull-off experiment, in particular for flatter bond interfaces. It may thus also explain, at least in part, the increased variability of the bond test data obtained in torsion as compared to those yielded with the pull-off test.

3.3.2 Test program conducted at Laval University

3.3.2.1 Surface roughness

The surface roughness characteristics corresponding to the five different surface preparation profiles, as obtained using the ICRI CSP index (ICRI No. 310.2R-2013) and optical profilometry respectively, are summarized in Table 3-8.

As can be seen in the table, the ICRI CSP plates merely cover the roughness values recorded for scarifying, all other techniques being out of range for the given concrete and experimental conditions. As convenient a tool these templates can be, with the existing scale, their use is limited to surface treatment applications where little of the existing concrete is actually removed (see Section 2). In fact, they are intended for surface treatments, not really for repair.

Overall, the comparative roughness data determined for the various surface preparation techniques are consistent with data from a previous study [8]. Comparatively, the recorded surface roughness half-amplitude values (R_a) obtained by optical profilometry shifted slightly towards the rougher side in comparison with what was obtained in the USBR program (for the corresponding preparation methods). The observed shift is likely associated with differences in the aggregates and characterization devices used in the two test programs.

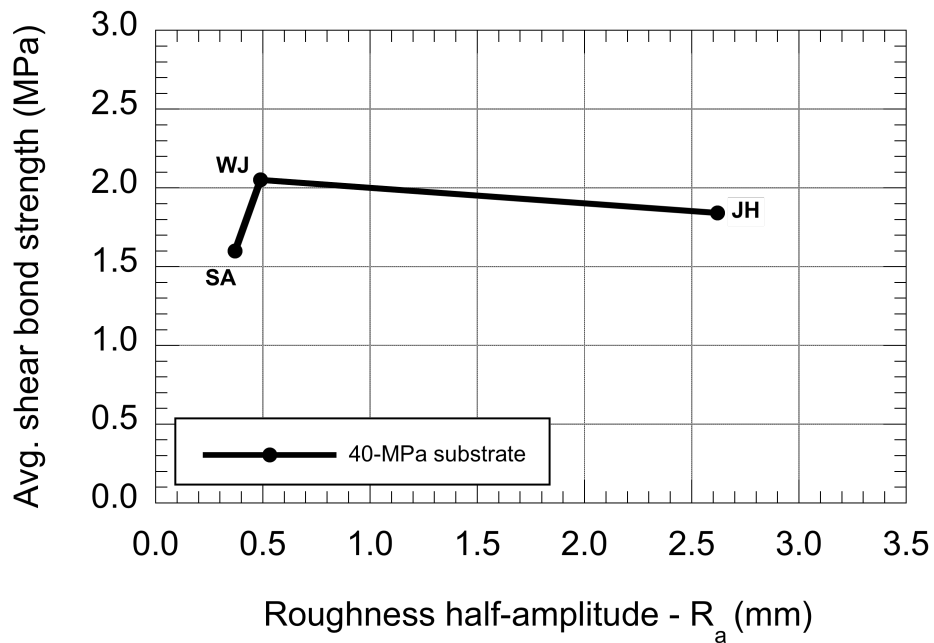


Figure 3-19: Results of torque tests performed after repair as a function of the substrate roughness generated by various preparation techniques (USBR program)
(note: SA – sandblasting; WJ – water jetting; JH – jackhammering)

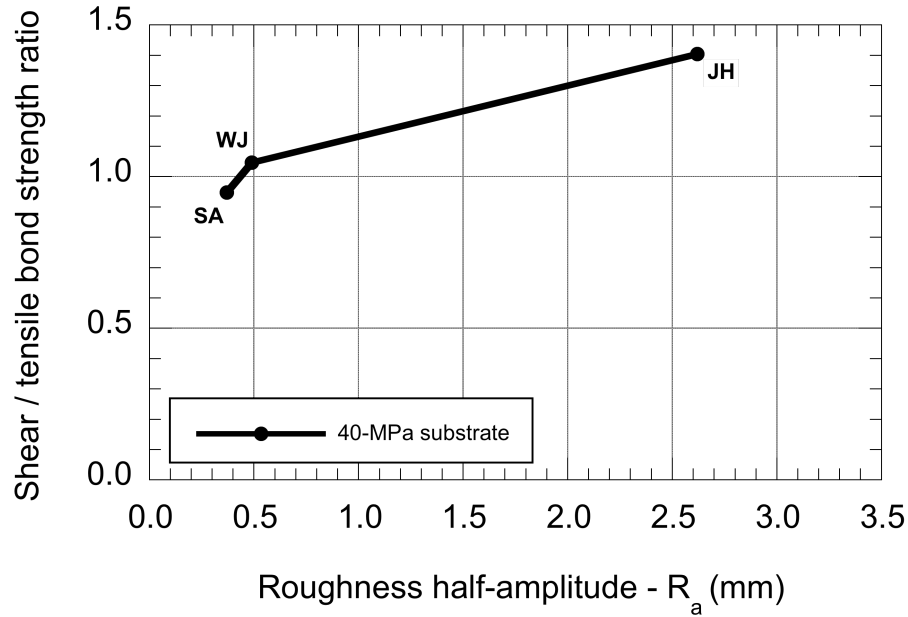


Figure 3-20: Shear bond to tensile bond strength ratio after repair as a function of the substrate R_a value generated by various preparation techniques (USBR program)
(note: SA – sandblasting; WJ – water jetting; JH – jackhammering)

Table 3-8: Summary of surface roughness test results (UL program)

Test	Parameter	Substrate nominal strength	Surface preparation				
			Scarifying	Shotblasting	Sandblasting	Water jetting	Jackhammering
ICRI CSP profiles (ICRI No. 310.2R-2013)	Avg. CSP index (1-9)	20-MPa	6.5	> 9	> 9	> 9	> 9
		30-MPa	6	> 9	> 9	> 9	> 9
Optical profilometry	Half-amplitude R _a (mm)	20-MPa	0.25	0.66	0.69	2.09	3.00
		30-MPa	0.22	0.62	0.66	1.54	2.22

The R_a values determined experimentally are plotted on the graph of Figure 3-21. For sake of comparison, the R_a values recorded for the ICRI CSP rubber templates are also displayed on this graph. The largest half-amplitude values (1.50 – 3.75 mm) were obtained with the jackhammer and water jetting, while the lowest values were recorded respectively for the

scarified, the shotblasted and the sandblasted surfaces (< 1 mm). It can also be observed that for all slabs and templates, surface roughness is uniform, with most data points sitting on or close to the equality line (where the values determined in the X-direction and the Y-direction are equal).

It must then be emphasized that the *meso*-roughness level, which is directly related to the aggregate size distribution of the substrate concrete, is being considered here. The large waviness observed for instance on both water jetted and jackhammered surfaces is extracted from the calculation by filtering. Nevertheless, the recorded R_a values suggest that water jetting and jackhammering both leave more and larger exposed aggregate particles than the other techniques.

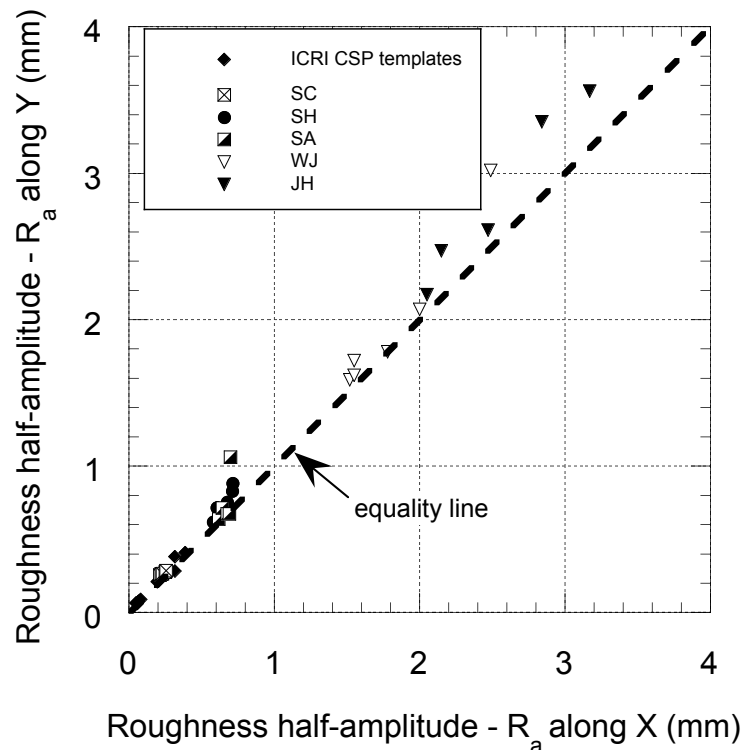


Figure 3-21: Results of roughness evaluation performed after surface preparation by optical profilometry on both 20-MPa and 30-MPa substrates (UL program)
 (note: SC – scarifying; SH – shotblasting; SA – sandblasting; WJ – water jetting; JH – jackhammering)

3.3.2.2 Mechanical integrity of the substrate

The average tensile strength values recorded in the substrate pull-off tests performed for the various types of preparation are summarized in Figure 3-22. Overall, the results obtained with the 20-MPa and 30-MPa substrates respectively are consistent with the standard characterization test results summarized. It can further be observed that for a given substrate quality, the average pull-off strength values obtained with sandblasting, shotblasting and scarifying are all close from the corresponding base concrete splitting-tensile strength. It can be asserted that the corresponding substrates were virtually undamaged by the surface preparation operations. Actually, in most of the tests, failure occurred at the bottom of the core, far from the surface.

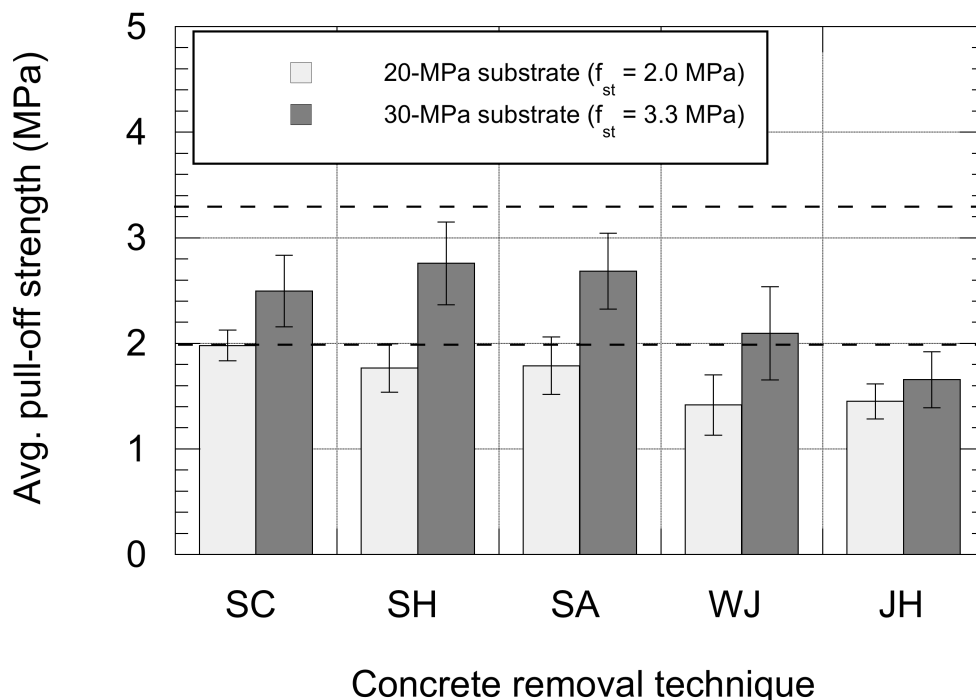


Figure 3-22: Results of pull-off experiments (CSA A23.2-6B modified) performed after surface preparation to evaluate the mechanical integrity of the exposed concrete surface and comparison with average the splitting tensile strength (f_{st}) value determined for each base mixture (UL program)
(note: SC – scarifying; SH – shotblasting; SA – sandblasting; WJ – water jetting; JH – jackhammering)

In the case of water jetting, the lower recorded strength values are most likely not due to damage, as the bond strength test results subsequently show, but rather to a pull-off test bias for that given type of surface profile. Indeed, the waviness created by water jetting was particularly important, and although special care was taken to glue the dolly adequately and to ensure proper alignment of the testing device, it could apparently not fully compensate.

In comparison, the average cohesion values recorded for the jackhammered slabs are significantly lower, especially in the 30-MPa series. Again, this is assumed to be a consequence of surface defects induced by the hammer tip, as reflected by the prevalent number of pull-off specimen failure occurrences near the surface.

3.3.2.3 Bond strength

The detailed results of the various bond strength tests performed on the experimental slabs are presented in Tables Table 3-9 to Table 3-12 and in Figures Figure 3-23 to Figure 3-30.

Pull-off testing

Except for the slabs prepared by jackhammering, the pull-off test results (Tables Table 3-9 and Table 3-10) are close to the corresponding substrate pull-off strength values (see Figure 3-22), for both slab series. In the 20-MPa slabs, where it is particularly close, failure of the pull-off specimens occurred systematically in the substrate (again, except for the jackhammered slabs). In the 30-MPa slabs, with the difference in strength between the repair material and substrate material being smaller, failures were drawn a little more towards the interfacial zone.

On jackhammered slabs, irrespective of the substrate concrete strength, the differences observed in terms of pull-off strength magnitude and failure location are manifest. Even though lightweight hammers (15-lb) were used, the recorded pull-off strength values are significantly lower and most of the time (> 83 %), failure occurred in the interface area. As for the correspondingly weaker superficial pull-off strength values, this clearly has to be attributed to the presence of disseminated defects left within the substrate surface layer after completion of the jackhammering operations.

Concerning the relationship between pull-off strength and substrate roughness, the recorded data tend again to show that pull-off strength increases with the value of R_a , provided that no or limited damage is induced (Figure 3-31). Where the extent of damage becomes significant, as in the case here of jackhammered slabs, the positive influence of increased roughness is erased by the detrimental effects of bruising.

Table 3-9: Summary of pull-off test results for the 20-MPa substrate series (UL program)

Surface preparation method	Test parameters	Location of failure				Overall
		Substrate	Interface	Repair	Dolly	
Scarifying (SC)	Number of test results (%)	45 (93.8)	1 (2.1)	0 (-)	2 (4.2)	48 (100.0)
	Avg. strength [MPa] (std. dev.)	1.69 (0.30)	1.81 (-)	- (-)	1.88 (0.35)	1.70 (0.29)
Shotblasting (SH)	Number of test results (%)	48 (100.0)	0 (-)	0 (-)	0 (-)	48 (100.0)
	Avg. strength [MPa] (std. dev.)	1.75 (0.21)	- (-)	- (-)	- (-)	1.75 (0.21)
Sandblasting (SA)	Number of test results (%)	47 (97.9)	0 (-)	0 (-)	1 (2.1)	48 (100.0)
	Avg. strength [MPa] (std. dev.)	1.75 (0.16)	- (-)	- (-)	1.13 (-)	1.74 (0.19)
Water jetting (WJ)	Number of test results (%)	46 (95.8)	2 (4.2)	0 (-)	0 (-)	48 (100.0)
	Avg. strength [MPa] (std. dev.)	1.82 (0.19)	1.78 (0.11)	- (-)	- (0.00)	1.81 (0.19)
Jackhammering (JH)	Number of test results (%)	4 (8.3)	44 (91.7)	0 (-)	0 (-)	48 (100.0)
	Avg. strength [MPa] (std. dev.)	1.39 (0.22)	1.18 (0.31)	- (-)	- (-)	1.20 (0.31)

Table 3-10: Summary of pull-off test results for the 30-MPa substrate series (UL program)

Surface preparation method	Test parameters	Location of failure				Overall
		Substrate	Interface	Repair	Dolly	
Scarifying (SC)	Number of test results (%)	12 (25.0)	36 (75.0)	0 (-)	0 (-)	48 (100.0)
	Avg. strength [MPa] (std. dev.)	2.48 (0.40)	2.38 (0.29)	- (-)	- (-)	2.40 (0.32)
Shotblasting (SH)	Number of test results (%)	22 (45.8)	20 (41.7)	4 (8.3)	2 (4.2)	48 (100.0)
	Avg. strength [MPa] (std. dev.)	2.53 (0.24)	2.57 (0.29)	2.62 (0.27)	2.21 (0.11)	2.54 (0.26)
Sandblasting (SA)	Number of test results (%)	39 (83.0)	3 (6.4)	5 (10.6)	0 (-)	47 (100.0)
	Avg. strength [MPa] (std. dev.)	2.64 (0.37)	2.49 (0.57)	2.95 (0.16)	- (-)	2.67 (0.37)
Water jetting (WJ)	Number of test results (%)	34 (70.8)	13 (27.1)	1 (2.1)	0 (-)	48 (100.0)
	Avg. strength [MPa] (std. dev.)	2.64 (0.26)	2.43 (0.38)	2.94 (-)	0.00 (-)	2.59 (0.31)
Jackhammering (JH)	Number of test results (%)	1 (2.1)	47 (97.9)	0 (-)	0 (-)	48 (100.0)
	Avg. strength [MPa] (std. dev.)	1.27 (-)	1.47 (0.47)	- (-)	- (-)	1.48 (0.47)

Table 3-11: Summary of torque test results for the 20-MPa substrate series (UL program)

Surface preparation method	Test parameters	Location of failure				Overall
		Substrate	Interface	Repair	Dolly	
Scarifying (SC)	Number of test results (%)	6 (50.0)	5 (41.7)	1 (8.3)	0 (0.0)	12 (100.0)
	Avg. strength [MPa] (std. dev.)	1.06 (0.35)	1.36 (0.46)	1.32 (-)	- (-)	1.24 (0.42)
Shotblasting (SH)	Number of test results (%)	5 (41.7)	6 (50.0)	0 (0.0)	1 (8.3)	12 (100.0)
	Avg. strength [MPa] (std. dev.)	0.87 (0.21)	1.11 (0.38)	- (-)	3.12 (-)	1.18 (0.68)
Sandblasting (SA)	Number of test results (%)	2 (16.7)	9 (75.0)	1 (8.3)	0 (0.0)	12 (100.0)
	Avg. strength [MPa] (std. dev.)	1.52 (0.10)	1.22 (0.34)	1.40 (-)	- (-)	1.32 (0.35)
Water jetting (WJ)	Number of test results (%)	4 (33.3)	6 (50.0)	1 (8.3)	1 (8.3)	12 (100.0)
	Avg. strength [MPa] (std. dev.)	1.98 (0.60)	1.20 (0.54)	2.25 (0.00)	1.01 (0.00)	1.53 (0.66)
Jackhammering (JH)	Number of test results (%)	0 (0.0)	12 (100.0)	0 (0.0)	0 (0.0)	12 (100.0)
	Avg. strength [MPa] (std. dev.)	- (-)	1.23 (0.41)	- (-)	- (-)	1.23 (0.41)

Table 3-12: Summary of torque test results for the 30-MPa substrate series (UL program)

Surface preparation method	Test parameters	Location of failure				Overall
		Substrate	Interface	Repair	Dolly	
Scarifying (SC)	Number of test results (%)	2 (16.7)	8 (66.7)	2 (16.7)	0 (0.0)	12 (100.0)
	Avg. strength [MPa] (std. dev.)	1.15 (0.25)	1.90 (0.75)	3.22 (0.71)	- (-)	2.00 (0.91)
Shotblasting (SH)	Number of test results (%)	1 (8.3)	8 (66.7)	0 (0.0)	3 (25.0)	12 (100.0)
	Avg. strength [MPa] (std. dev.)	1.56 (0.00)	1.63 (0.33)	- (-)	2.55 (0.71)	1.86 (0.58)
Sandblasting (SA)	Number of test results (%)	4 (33.3)	7 (58.3)	1 (8.3)	0 (0.0)	12 (100.0)
	Avg. strength [MPa] (std. dev.)	2.10 (1.46)	1.63 (0.25)	1.39 (-)	- (-)	1.77 (0.82)
Water jetting (WJ)	Number of test results (%)	2 (16.7)	5 (41.7)	2 (16.7)	3 (25.0)	12 (100.0)
	Avg. strength [MPa] (std. dev.)	1.41 (0.37)	1.70 (0.53)	2.25 (0.61)	2.48 (0.65)	1.89 (0.61)
Jackhammering (JH)	Number of test results (%)	2 (16.7)	10 (83.3)	0 (0.0)	0 (0.0)	12 (100.0)
	Avg. strength [MPa] (std. dev.)	1.15 (0.08)	1.39 (0.61)	- (-)	- (-)	1.35 (0.56)

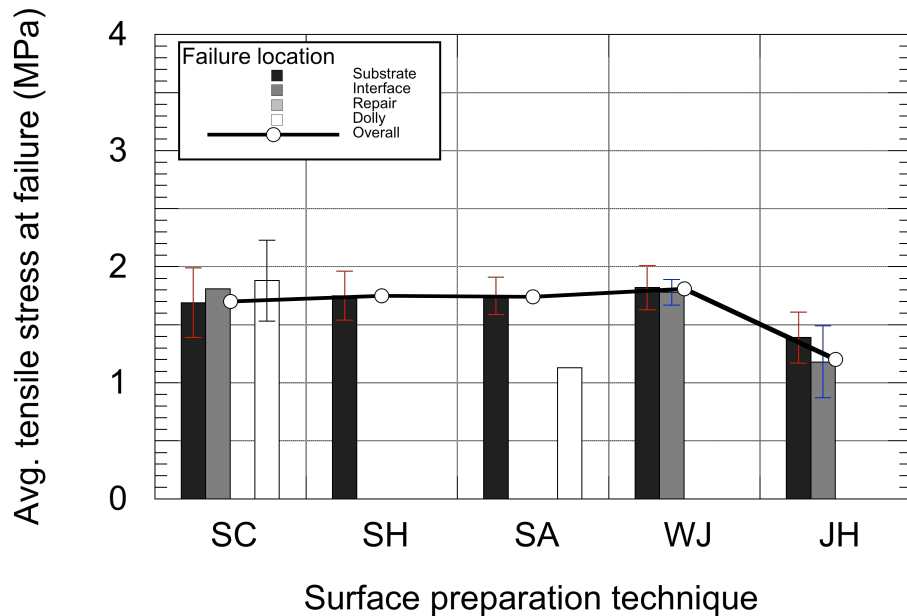


Figure 3-23: Results of pull-off tests performed on 20-MPa substrates after repair (UL program)

(note: SC – scarifying; SH – shotblasting; SA – sandblasting; WJ – water jetting; JH – jackhammering)

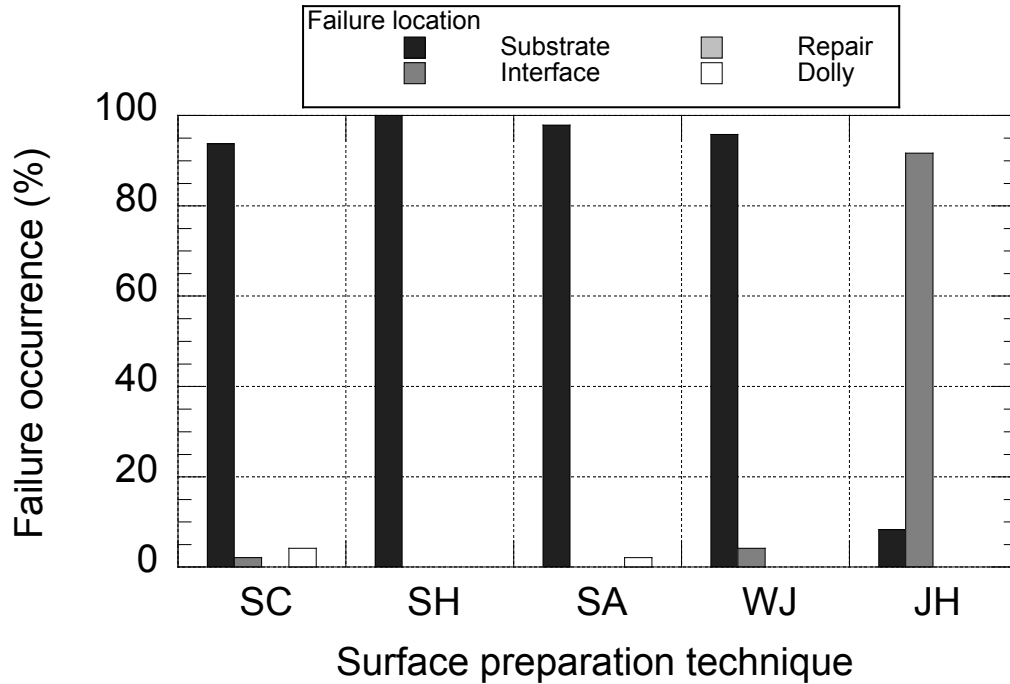


Figure 3-24: Distribution of failure location in pull-off tests performed on 20-MPa substrates after repair (UL program)
 (note: SC – scarifying; SH – shotblasting; SA – sandblasting; WJ – water jetting; JH – jackhammering)

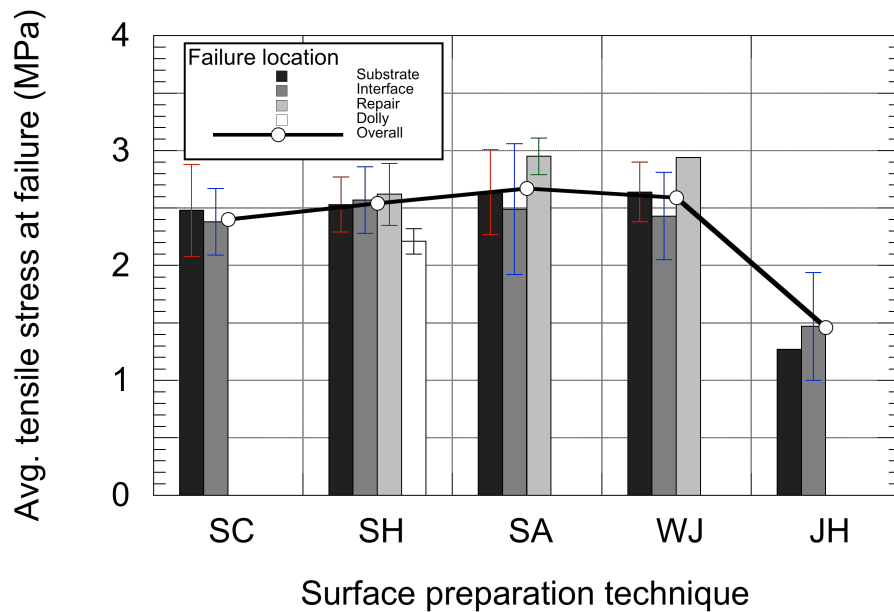


Figure 3-25: Results of pull-off tests performed on 30-MPa substrates after repair (UL program)
 (note: SC – scarifying; SH – shotblasting; SA – sandblasting; WJ – water jetting; JH – jackhammering)

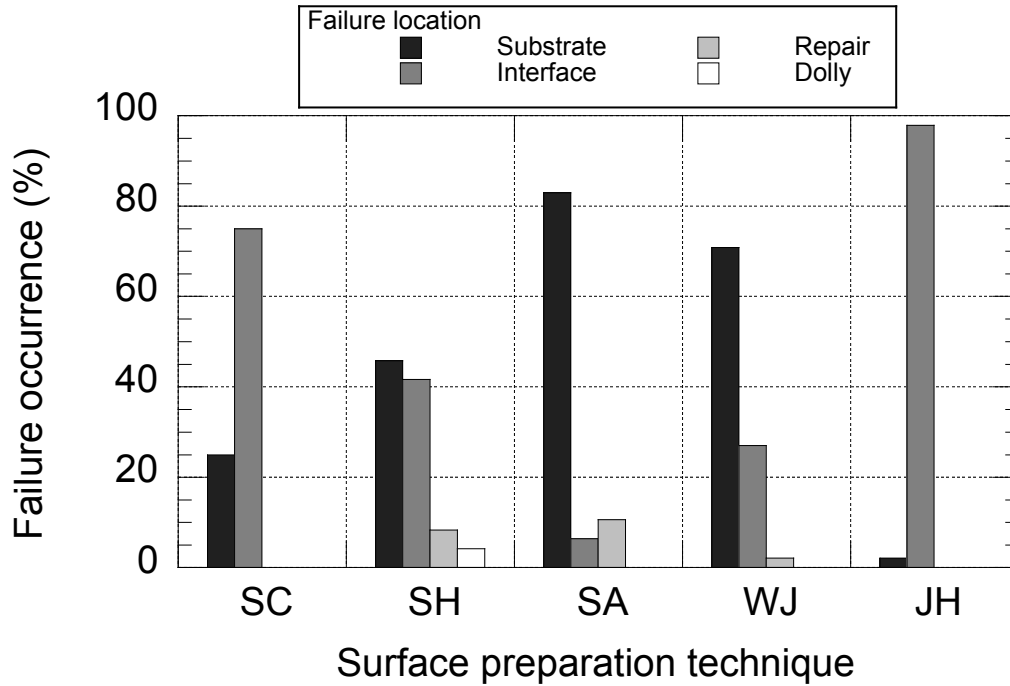


Figure 3-26: Distribution of failure location in pull-off tests performed on 30-MPa substrates after repair (UL program)
 (note: SC – scarifying; SH – shotblasting; SA – sandblasting; WJ – water jetting; JH – jackhammering)

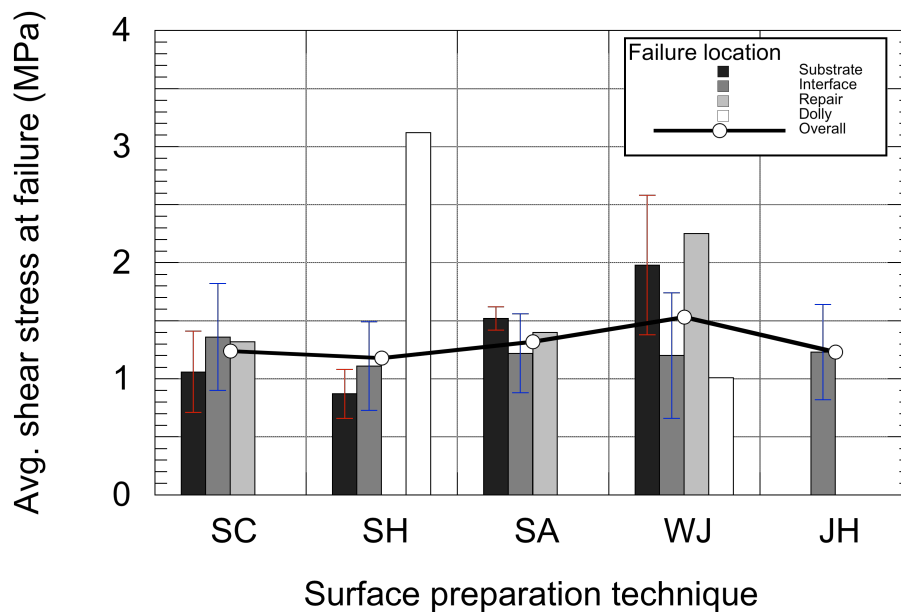


Figure 3-27: Results of torque tests performed on 20-MPa substrates after repair (UL program)
 (note: SC – scarifying; SH – shotblasting; SA – sandblasting; WJ – water jetting; JH – jackhammering)

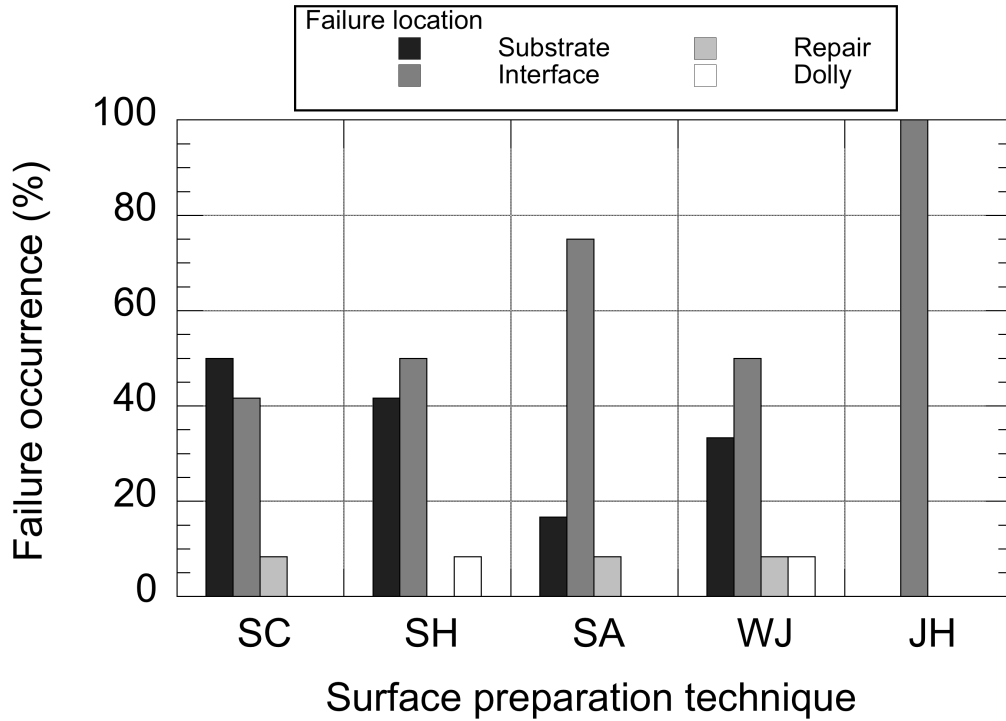


Figure 3-28: Distribution of failure location in torque tests performed on 20-MPa substrates after repair (UL program)
 (note: SC – scarifying; SH – shotblasting; SA – sandblasting; WJ – water jetting; JH – jackhammering)

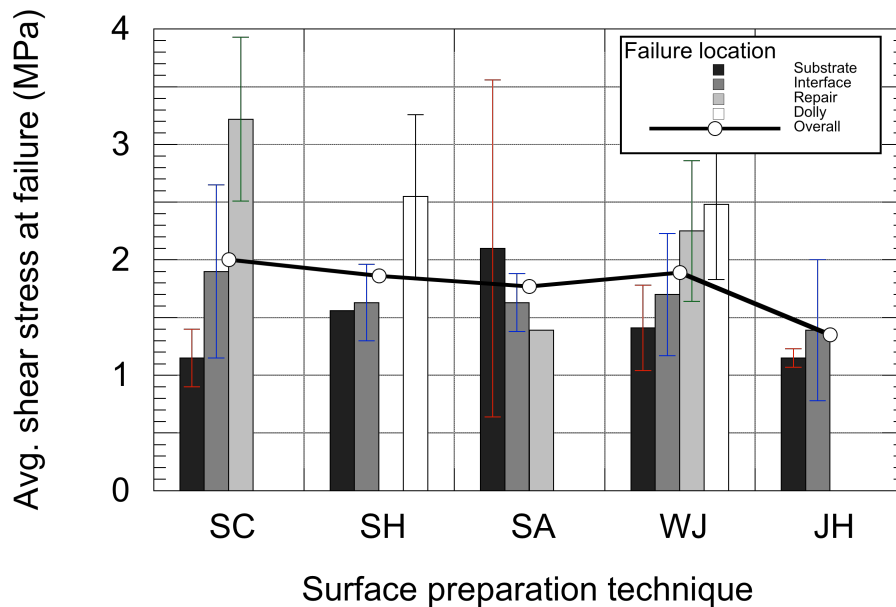


Figure 3-29: Results of torque tests performed on 30-MPa substrates after repair (UL program)
 (note: SC – scarifying; SH – shotblasting; SA – sandblasting; WJ – water jetting; JH – jackhammering)

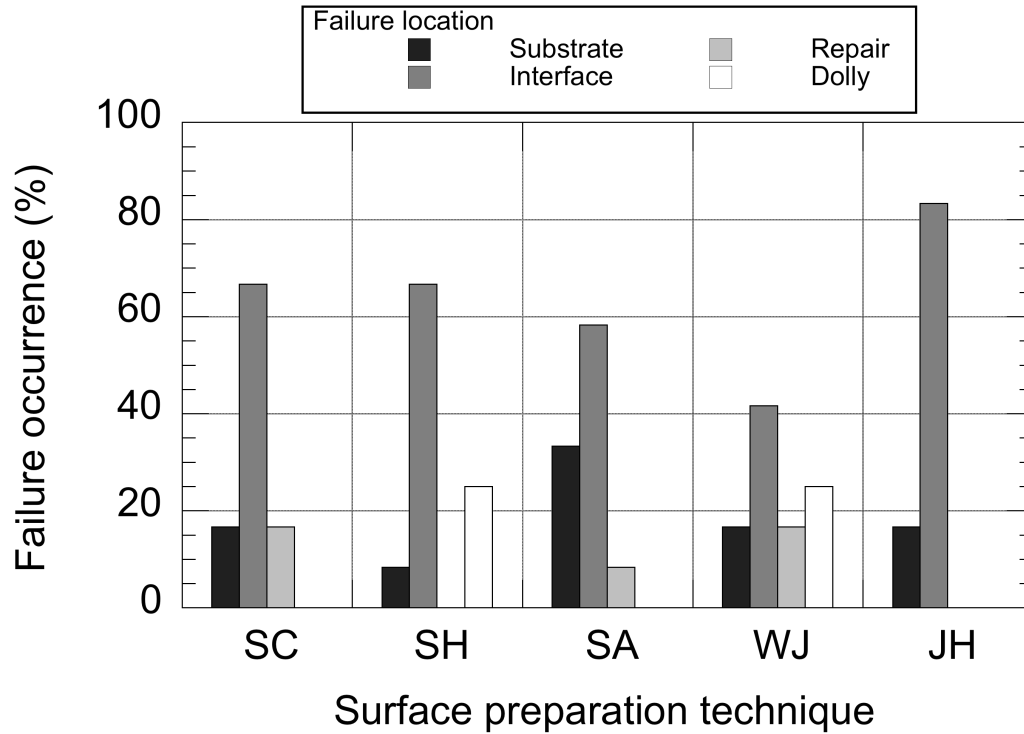


Figure 3-30: Distribution of failure location in torque tests performed on 30-MPa substrates after repair (UL program)
 (note: SC – scarifying; SH – shotblasting; SA – sandblasting; WJ – water jetting; JH – jackhammering)

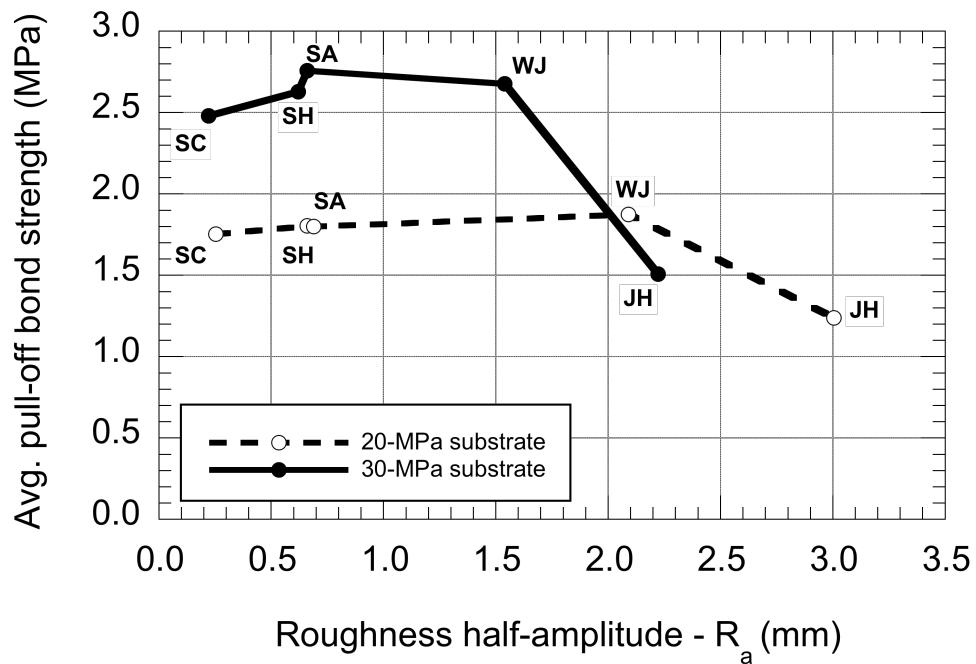


Figure 3-31: Results of pull-off tests (ASTM C1583) performed after repair as a function of the substrate roughness generated by various preparation techniques (UL program)
 (note: SC – scarifying; SH – shotblasting; SA – sandblasting; WJ – water jetting; JH – jackhammering)

Direct tensile testing

The average bond strength results in direct tension for both slab series prepared with the various investigated concrete removal techniques are displayed in Figure 3-32. The observed trends are similar to those exhibited by the pull-off tests, although the recorded values are different. In comparison with the pull-off results, the values recorded on the 20-MPa substrates shifted up, while those recorded on the 30-MPa substrates shifted down, such that the two direct tension curves are almost superimposed. Given the configuration of the tensile specimens, which promotes bond failure, the recorded values are likely more representative of the actual bond strength in tension. On that basis, the experimental results suggest that the substrate strength has little influence on the magnitude of the bonding forces developed at the interface.

As for the pull-off test results, the direct tensile test results in Figure 3-32 suggest that the average bond strength in tension is slightly increasing with the substrate roughness amplitude as far as no or little damage is induced by the surface treatment. This is actually confirmed by the results obtained with the artificially profiled slabs (20-MPa slab series), as illustrated in Figure 3-33. In absence of superficially induced damage, it clearly shows that increasing the surface of contact between the substrate and the repair material leads to a stronger bond, at least in tension.

Torque testing

The torsional shear bond test results presented in Tables Table 3-11 and Table 3-12, Figures Figure 3-27 to Figure 3-30 exhibit trends that are overall similar to those observed for the pull-off results in terms of average bond strength, but not with regards to the failure location distribution.

Failures in torsion were not recorded to be much distributed along the length of the test cores as it did in the USBR program, but it was again more dispersed than the pull off failures.

The torsional shear bond test results are presented as a function of the substrate roughness parameter R_a in Figure 3-34. Both in terms of magnitude and trends, they show similarity with the pull-off data, with the substrate strength, roughness and mechanical integrity appearing as influential parameters. Based on this figure, the influence of roughness appears to be somehow more subtle than in the case of pull off testing. Hence, the relationship between the shear bond to tensile bond ratio and the R_a value (Figure 3-35) does not exhibit any definite trend revealing for instance whether shear bond strength may be more or less favorably influenced by the substrate roughness than tensile bond strength. Again, in appraising such data, it must be kept in mind that the results obtained on the jackhammered surface are largely affected by the preparation-induced damage within the substrate.

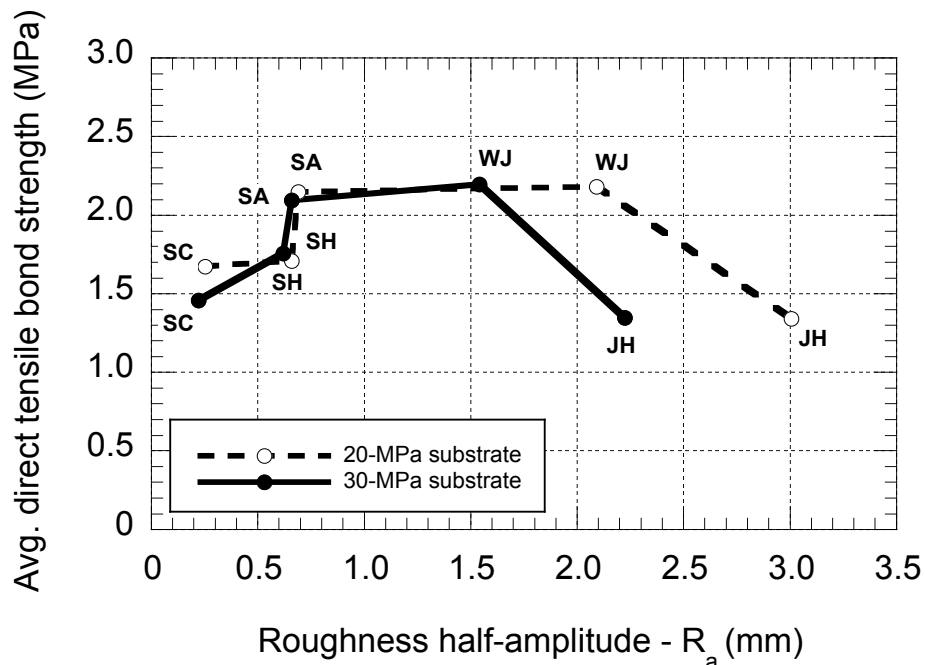


Figure 3-32: Results of direct tensile tests (CRD-C 164) performed after repair on cores extracted from the slabs as a function of the substrate roughness generated by various preparation techniques (UL program)
(note: SC – scarifying; SH – shotblasting; SA – sandblasting; WJ – water jetting; JH – jackhammering)

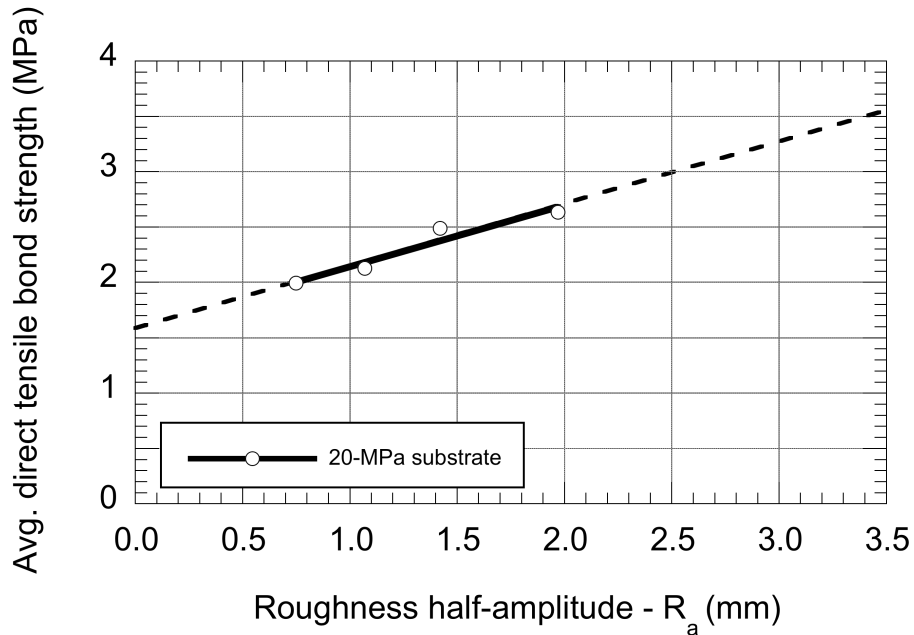


Figure 3-33: Results of direct tensile tests performed after repair on cores extracted from the artificially profiled 20-MPa test slab (UL program)

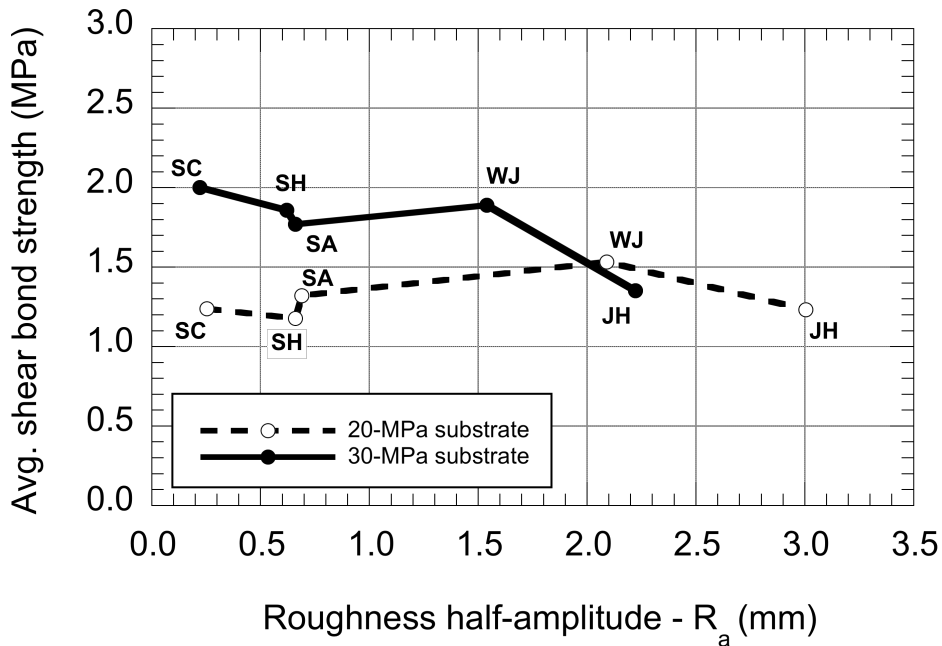


Figure 3-34: Results of torsional bond experiments performed after repair as a function of the substrate roughness generated by various preparation techniques (UL program)
(note: SC – scarifying; SH – shotblasting; SA – sandblasting; WJ – water jetting; JH – jackhammering)

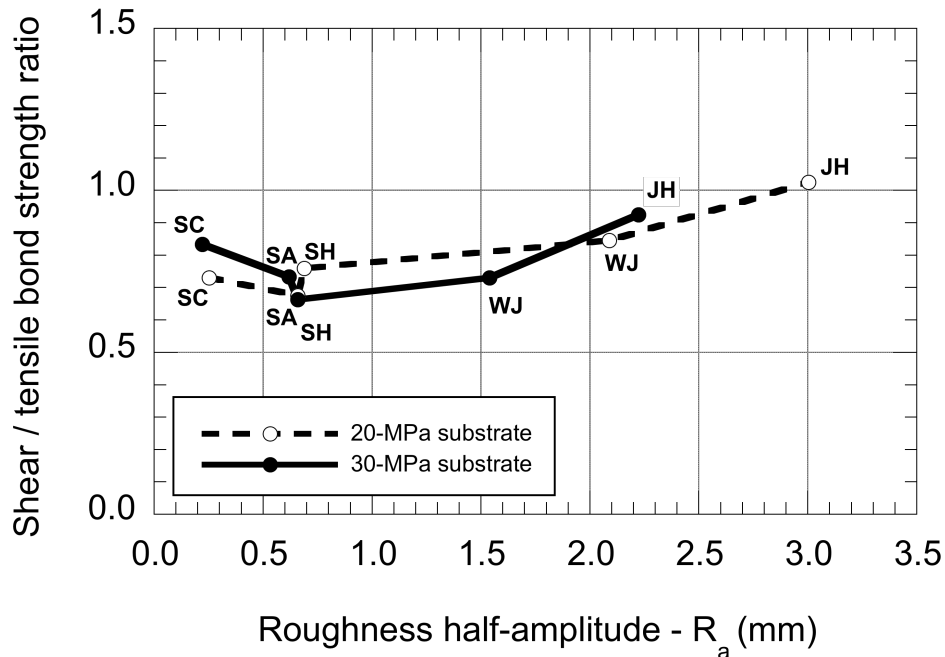


Figure 3-35: Shear bond to tensile bond strength ratio after repair as a function of the substrate R_a value generated by various preparation techniques (UL program)
(note: SC – scarifying; SH – shotblasting; SA – sandblasting; WJ – water jetting; JH – jackhammering)

Besides, it can be observed that the experimental shear bond to tensile bond strength ratios obtained in this program are even lower than those presented earlier in the test program conducted at USBR, with values ranging this time from 0.66 to barely 1.0. This finding further supports the statements made before related to the absence of a normal load in the torsional bond test procedure. Clearly, the experimental relationships generally reported between typical shear tests and direct tensile testing does not apply here, in the absence of a normal load.

3.4 Conclusions

Bond strength of concrete repairs depends on a number of parameters. It has been clearly shown that when substrate-induced damage is prevented or kept below a certain level, tensile bond strength increases with the substrate coarseness. Still, one of the most important parameters apparently remains the mechanical integrity of the substrate. In that regard, it must

be stressed that the use of impacting methods such as jackhammering leaves significant damage at the surface, which can easily outweigh the benefits of an increased roughness.

When considering the relationship between interfacial pull-off bond and shear bond strengths in composite repair overlay systems, the test results yielded during the experimental research and summarized herein do not exhibit the same trends as often reported or described in the scientific documentation (again, it must be stressed that reported hard data comparisons are extremely scarce). No general correlation between the two physical characteristics could be established due to the fact that the various surface preparation techniques result in different types of profiles and induced defects. The combination of these parameters influence pull-off bond and shear bond strength measurements in different ways.

Relating interface shear and tension test results in a highly heterogeneous medium such as a concrete composite system is in fact questionable, as both obey to different combinations of bond mechanisms, which are affected to varying degrees by the interface and substrate characteristics (adhesion, friction, interface roughness and geometry, mechanical integrity of the substrate, etc.). Besides, there are some considerations inherent to the experimental test methods for bond assessment, which strongly influence the actual state of stress building up inside the material and ultimately leading to failure. For instance, many of the shear test procedures developed for concrete involve a normal force acting in at least one direction. In the investigated torsional bond test procedure, no such normal force is acting, making difficult the comparison of the data with some previously published works.

Overall, it can be concluded it is a convenient and useful in-situ method for evaluating the mechanical integrity of the concrete surface prior to repair, as well and the repair bond strength.

A reliable evaluation of these properties can be obtained, provided that a minimum number of tests are performed, with adequate equipment and properly conducted test procedure.

Still, the tensile pull-off test has potential shortcomings, which must be considered in the analysis of any result. The first potential problem – addressed subsequently in this report – is misalignment of the pulling force, which leads to stress concentrations and can exert a significant influence on recorded bond strength values. Another problem that is commonly encountered with tensile pull-off tests is that failure often occurs outside the interfacial zone, either in the repair layer or within the existing substrate. When such a failure occurs, the recorded maximum stress merely represents a lower bound value for interface bond strength. A third problem is that the coring operation may damage the interface between the repair and the substrate, which is likely to affect bond and thereby reduce the measured pull-off strength.

Among the two bond test methods compared in the present investigation, the pull-off test is the only one commonly used in practice because the equipment is widely available and it is relatively easy to carry out in the field. Torsional tests may also be performed on site without too much difficulty, but they are very seldom used for a number of reasons, the most significant being probably the non-existence of specifications in that respect in repair guidelines and the lack of a standard test procedure.

Further work and analysis including bond ageing will allow more definite conclusions based upon which it will be possible to issue broader recommendations for concrete surface preparation prior to repair.

3.5 References

1. Silfwerbrand, J. (1990) Improving Concrete Bond in Repaired Bridge Decks, *Concrete International*, 12: 61-66.
2. Talbot, C., Pigeon, M., Beaupré, D., Morgan, D.R. (1994) Influence of Surface Preparation on long-term bonding of shotcrete, *ACI Materials Journal*, 91(6): 560-566.
3. Beushausen, H.D. (2005) Long-term Performance of Bonded Concrete Overlays Subjected to Differential Shrinkage, Ph.D. Thesis, University of Cape Town, South Africa, 265 pp.
4. Courard, L., Bissonnette, B., Vaysburd, A.M., Bélaïr N., Lebeau, F. (2012) Comparison of destructive methods to appraise the mechanical integrity of a concrete surface. *Concrete Repair Bulletin* 25(4): 22-30.
5. Petersen, C.G., Poulsen, E. (1997) *In-Situ Testing of Near-to-Surface Layer of Concrete and Epoxy-Bonded CFRP Strips*, US-Canada-Europe Workshop on Bridge Engineering, Zürich, Switzerland.
6. Courard, L., Bissonnette, B. (2004) Adaptation of the pull-off test for the evaluation of the superficial cohesion of concrete substrates in repair works: analysis of the test parameters. *Materials and Structures* 37(269): 342-350 (in French).
7. Bissonnette, B., Courard, L., Vaysburd, A.M., Bélaïr, N. (2006) Concrete removal techniques: influence on residual cracking and bond strength. *Concrete International* 28(12):49-55.
8. Bélaïr, N. (2005) *Contribution to the Development of a Quantitative Surface Characterization Protocol for Concrete in View of Repair (Contribution à la Mise au Point d'une Procédure de Caractérisation Quantitative des Surfaces en Béton en Vue de Travaux de Réfection)*, MSc dissertation, Université Laval, 199 p. (in French).
9. Bissonnette, B., Vaysburd, A.M., von Fay, K.F. (2012) *Best Practices for Preparing Concrete Surfaces prior to Repairs and Overlays* (Report No. MERL 12-17) US Bureau of Reclamation, Denver (CO), USA, 92 p.

3.6 Standards and test methods

ASTM C39 / C39M-16, Standard Test Method for Compressive Strength of Cylindrical Concrete Specimens, ASTM International, West Conshohocken, (PA), USA, 2016, www.astm.org

ASTM C469 / C469M-14, Standard Test Method for Static Modulus of Elasticity and Poisson's Ratio of Concrete in Compression, ASTM International, West Conshohocken, (PA), USA, 2014, www.astm.org

ASTM C805 / C805M-13a, Standard Test Method for Rebound Number of Hardened Concrete, ASTM International, West Conshohocken, (PA), USA, 2013, www.astm.org

ASTM C1583 / C1583M-13, Standard Test Method for Tensile Strength of Concrete Surfaces and the Bond Strength or Tensile Strength of Concrete Repair and Overlay Materials by Direct Tension (Pull-off Method), ASTM International, West Conshohocken (PA), USA, 2013, www.astm.org

ASTM E965-15, Standard Test Method for Measuring Pavement Macrotexture Depth Using a Volumetric Technique, ASTM International, West Conshohocken, (PA), USA, www.astm.org

BS 1881-207:1992, Testing Concrete. Recommendations for the Assessment of Concrete Strength by Near-to-Surface Tests, NBS, Newcastle upon Tyne, UK, 1992, www.thenbs.com

CRD-C 164-92, Standard Test Method for Direct Tensile Strength of Cylindrical Concrete or Mortar Specimens, U.S. Army Engineering Research and Development Center (ERDC), Vicksburg, Miss, USA, 1992, <http://www.publications.usace.army.mil>

CSA A23.2-6B, Determination of Bond Strength of Bonded Toppings and Overlays and of Direct Tensile Strength of Concrete, Mortar, and Grout, A23.1-14/A23.2-14 – Concrete Materials and Methods of Concrete Construction / Test Methods and Standard Practices for Concrete, CSA Group, Toronto, ON, Canada, 2014, <http://www.csagroup.org>

EN 1542:1999, Products and Systems for the Protection and Repair of Concrete Structures - Test Methods - Measurement of Bond Strength by Pull-Off, European Standard, Brussels, Belgium, 1999, <http://www.cen.eu>

ICRI Guideline No. 210.3R-2013, Guide for Using In-Situ Tensile Pulloff Tests to Evaluate Bond of Concrete Surface Materials, International Concrete Repair Institute, St. Paul (MN), USA, 2013, www.icri.org

ICRI Guideline No. 310.2R-2013 Selecting and Specifying Concrete Surface Preparation for Sealers, Coatings, Polymer Overlays, and Concrete Repair International Concrete Repair Institute, St. Paul (MN), USA, 2013, www.icri.org

Table of contents

Table of contents	i
List of tables.....	iii
List of figures	iv
Section 4 – Evaluate the effect of misalignment in a tensile pull-off test on bond strength	1
4.1 General introduction	1
4.2 Background information.....	2
4.3 Objectives and methodology	4
4.4 Theoretical study	5
4.4.1 Causes of misalignment.....	7
4.4.2 Core depth and angle	8
4.5 Experimental programs	11
4.5.1 Pull-off experiments on monolithical substrates (U. of Liège).....	11
4.5.2 Pull-off experiments on repaired substrates (USBR).....	14
4.6 Conclusions	18
4.7 References	19

List of tables

Table 4-1: Calculated pull-off test stress differentials induced by a 4° misalignment	7
Table 4-2: Direct tensile test and pull-off test results	12
Table 4-3: Compressive strength of concrete samples	15
Table 4-4: Average pull-off test results - repaired substrates	17

List of figures

Figure 4-1: Pull off testing misalignments	3
Figure 4-2: Effect of the angle, the core depth and diameter on ultimate load reduction coefficient.....	4
Figure 4-3: FEM mesh for Pull-off simulation (4° coring angle and 30 mm coring depth) ...	6
Figure 4-4: Pull-off geometry considered in the numerical analysis	7
Figure 4-5: Axial stress (σ_y) distribution for misalignment angles of 0°, 2° and 4° and coring depths of 15 and 30 mm.....	9
Figure 4-6: Theoretical axial stress (σ_y) amplification as a function of the misalignment angle of inclination and coring depth in a pull-off experiment.	10
Figure 4-7: Special device for controlling the coring axis inclination at U. of Liège	12
Figure 4-8: Average pull-off strength values for concrete slabs C30/37	14
Figure 4-9: Surface treatment of concrete prior to repair	15
Figure 4-10: Experimental setup for coring under controlled inclination at USBR	16
Figure 4-11: View of a 4°-inclined core after pull-off extraction	17
Figure 4-12: Average pull-off test results - repaired substrates	18

Chapter 4 – Evaluate the effect of misalignment in a tensile pull-off test on bond strength

This part of the report is related to Task 3, as described in the original research program. The experimental work has been carried out both at the University of Liège, ArGEnCo Dept, GeMME Building Materials, Belgium and at the U.S. Bureau of Reclamation, Denver (CO), U.S.A.

4.1 General introduction

The bond between concrete substrate and repair to a large degree depends on the quality of the substrate concrete prepared to receive a repair and adhesion between substrate and repair [1]. Bond strength is measured as the stress required for separating substrate and repair [2]. In general, bond tests are designed to apply tensile, shear, or torsional stress to interface of the repaired system [3, 4]. The most common test widely used is the tensile pull-off test on cores [5, 6]. The popularity of this test relates mainly to two circumstances: (1) it can evaluate the tensile strength of the substrate surface prior to repair, and tensile bond strength between repair and substrate, and (2) it can be carried out on-site on an existing structure as well as in the laboratory.

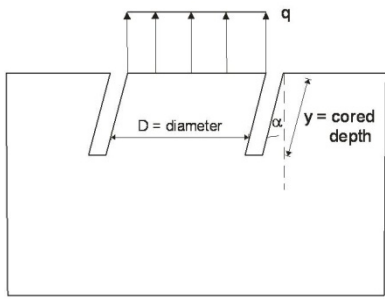
For the identification of tensile substrate concrete and bond strengths, a force must be applied perpendicular to the interface plane. Any misalignment of the pull-off force leads to stress peaks in the member, which might have an influence on measured strength values. Misalignments usually might be induced by the core drilling process, an uneven substrate surface, and by the dolly attachment process, and are for all practical purposes generally difficult to avoid. Each misalignment source or their combination may create a situation at which the measured stress at failure does not represent actual tensile strength at the interface of the repair or substrate. Some of the misalignment problems might be minimised or dominated in the limited

amount of laboratory tests this, however, is a cumbersome procedure if a large number of tests have to be conducted under in-situ conditions.

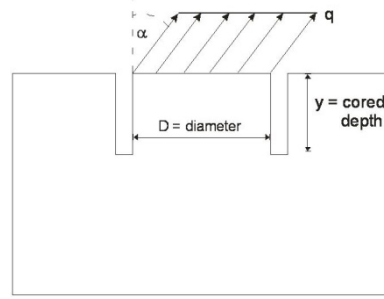
4.2 Background information

Concrete repair process usually involves the removal of deteriorated or contaminated material and surface preparation prior to application of a repair material. It is necessary therefore, to assess the quality of the residual concrete substrate since it can significantly affect the short term bond strength and long term performance of a repair system [1]. The pull-off test is a simple and effective test for evaluating the residual properties of the substrate [6] as well as the interface bond in the composite repair system [7]. In a previous research [8], the influence of different test parameters on the recorded strength was investigated, namely the dolly size (thickness and diameter), the core drilling depth, the loading rate, and the number of tests. The geometry of the dolly and the depth of core drilling into the substrate were also found as critical factors in testing bond in repair systems [8, 9].

Another potentially influential parameter of the pull-off test, namely the test alignment, has not received much attention. Still, the primary requirement in any direct tension test method is to ensure the pulling force is aligned with and parallel to the specimen axis at all times to avoid bending effects. Two main causes may induce misalignment in a pull-off experiment: inclination of the core axis caused by inaccurate core drilling (Figure 4-1(a)), and inclination of the pulling force caused by inaccurate positioning of the dolly (Figure 4-1(b)). Real-world, on-site conditions often limit the capability of the personnel performing the test to avoid the misalignment situations. Pull-off test misalignment very often arises from difficult on-site conditions, such as a highly irregular support that prevents a proper installation of the drilling system and thus leads to inaccurate coring.



a) Coring axis inclination (angle α ; dolly not shown)



b) Inclination of the pulling force caused by the dolly misplacement (dolly not shown)

Figure 0-1: Pull off testing misalignments

Austin et al. [5] investigated the effect of misalignment on measured pull-off bond strength. The average misalignment in the experiments he performed was 0.06 in. (1.5 mm) at a depth of 2 in. (50 mm), which translates to an angle of inclination of 1.7°. The study concluded that such a misalignment caused an increase in maximum stress of the order of 20% at the core periphery.

Cleland and Long [6] performed numerous tests on cores drilled to a depth up to 40 mm into the repair substrate and inclination to the vertical of up to 20° in order to evaluate what effect it has on the measured pull-off bond strength. The authors proposed a correction factor to be applied to the measured results based on the magnitude of the inclination angle (Equation 4-1).

$$\text{Correction factor} = \frac{1}{\left[1 - \left(\frac{8 \cdot \tan \alpha}{D}\right) \cdot y\right]} \quad (4-1)$$

where α , D , y are the angle of inclination of the coring axis (with respect to an axis normal to the surface), the core diameter and the coring depth respectively, as shown on Figures 4-1 and 4-2.

Misalignment in pull-off tests may have a substantial influence on pull-off test result for angles of inclination of more than 5° (**Erreur ! Nous n'avons pas trouvé la source du renvoi.**). The reduction in the core depth or increase of the dolly diameter will minimize the negative effects of misalignment. It should be stated, however, that the above conclusions are strictly theoretical in nature, as they do not take into account such factors as potential stress relaxation and the possibility that the core brittle zones are not necessarily corresponding to the stress concentration zones.

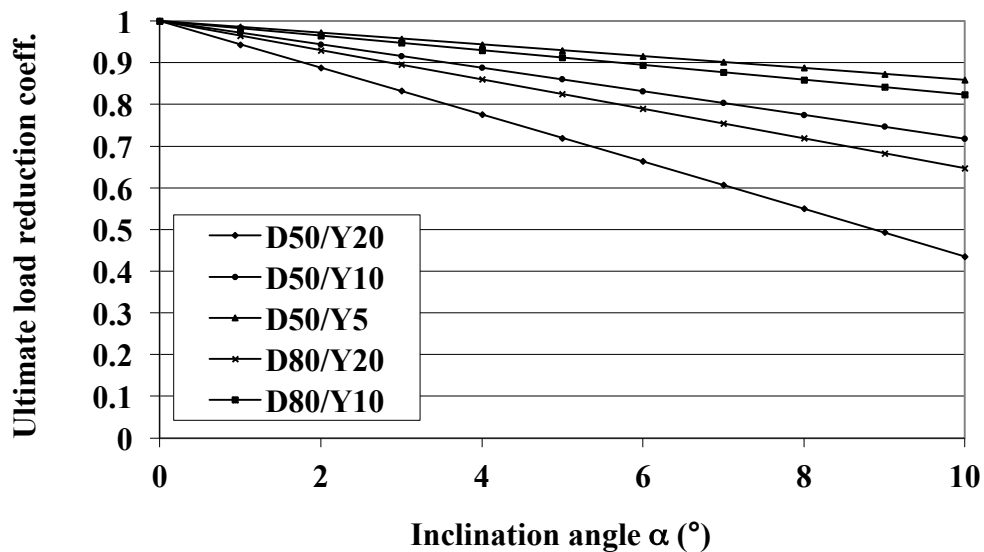


Figure 0-2: Effect of the angle, the core depth and diameter on ultimate load reduction coefficient

4.3 Objectives and methodology

To evaluate the pull-off test result sensitivity to these parameters, an experimental program to answer the following questions was undertaken:

- What is the influence of minor load misalignments - that is, within naked-eye detection capability - on pull-off strength test results?

- Do coring and pulling load misalignments influence the results differently?

A theoretical analysis was first carried out at the University of Liège to determine whether the core axis and load misalignment could influence the pull-off test results in a different fashion and what was the overall sensitivity of the results to these experimental biases. Two distinct experimental programs were then conducted in parallel: pull-off experiments were performed on monolithic concrete substrates at the University of Liège, Belgium, while similar experiments were performed on composite repair systems at the U.S. Bureau of Reclamation (USBR), Denver, Colorado, USA.

The following variables were selected for investigation in the theoretical analysis and test programs:

Theoretical and experimental pull-off study on monolithic substrates

- Coring axis inclination 0°, 2° & 4°
- Pulling force inclination in the quality/integrity test 0°, 2° & 4°
- Core depth in the substrate 15 mm (5/8 in.)
30 mm (1-¼ in.)

Experimental pull-off study on repaired (composite) substrates

- Coring axis inclination 0°, 2° & 4°
- Core depth in the composite repair system 100 mm (4 in.)
- Core depth into the substrate 25 mm (1 in.)

4.4 Theoretical study

Finite element (FEM) calculations were performed with the *Lagaprog*s software, developed at the University of Liege, Belgium, to predict the mechanical stresses within and around the partial

cores in the concrete substrates [10]. The numerical modeling is based upon a constitutive law for elastic solids. Using this model, a mechanical analysis of elastic isotropic solids was carried out, assuming isothermal conditions.

The following concrete characteristics were assumed in the analysis [11]:

- Elasticity modulus: 30 GPa (4,350 ksi)
- Poisson ratio: 0.20 (0.20)
- Density: 2500 kg/m³ (4,215 lb/yd³)
- Applied stress: 1 MPa (145 psi)

The pull-off testing experiment was addressed as a two-dimensional plane strain problem. Figure 4-3 presents the finite element mesh. The load was assumed to be uniformly applied over the specimen top surface, implying that the results were not influenced by the dolly material characteristics and thickness. The analysis was performed on the longitudinal cross section, with emphasis being given to the end of coring areas, corresponding to points A and B in Figure 0-4.

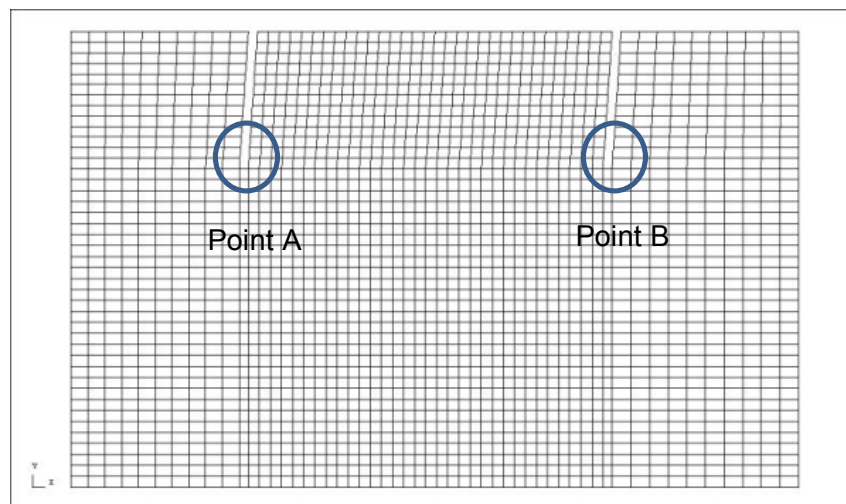


Figure 0-3: FEM mesh for Pull-off simulation (4° coring angle and 30 mm coring depth)

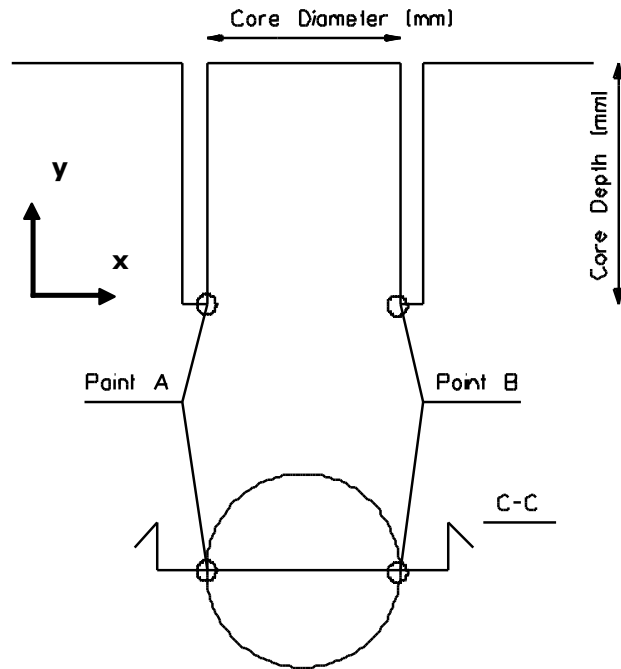


Figure 0-4: Pull-off geometry considered in the numerical analysis

4.4.1 Causes of misalignment

First, a sensitivity analysis was performed to establish whether the two possible sources of misalignment, that is, coring misalignment and pulling misalignment, exert the same influence on pull-off test results. Numerical simulations were carried out, assuming only core inclination load inclination angles of 4 degrees and a core depth of 30 mm (1.2 in.). Results are summarized in Table 0-1.

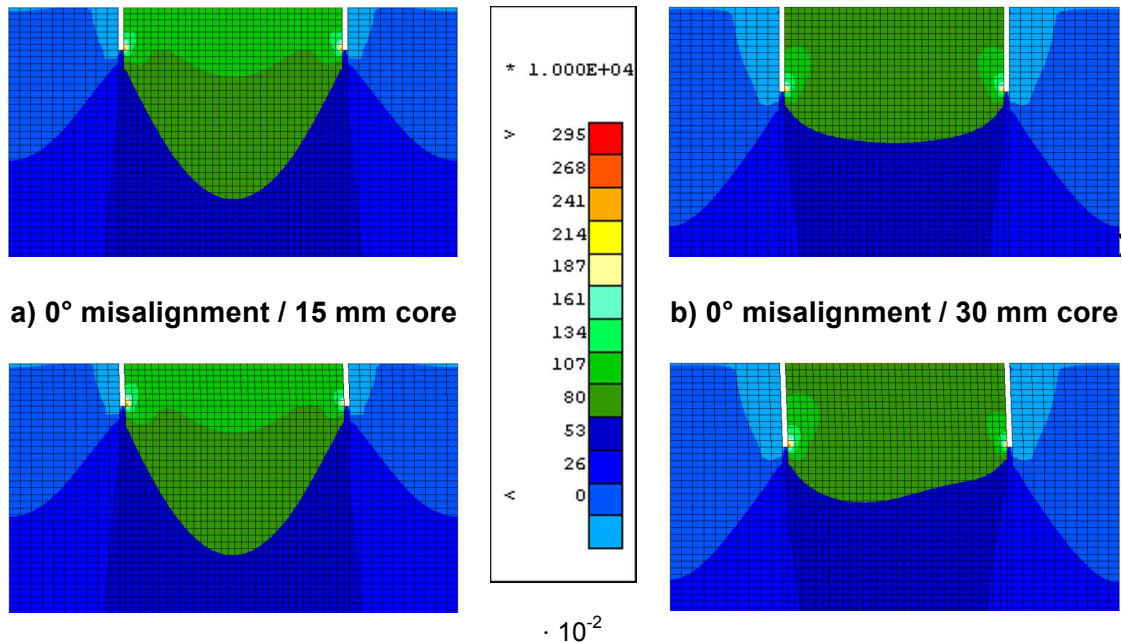
For a given shift angle, both types of misalignment yield very similar results, and it can be concluded that their influence on pull-off test results is comparable. A slight difference is found when comparing transverse stresses (σ_x), but it is sufficiently small to assume that it does not affect the pull-off strength data within its intrinsic range of variability.

Table 0-1: Calculated pull-off test stress differentials induced by a 4° misalignment

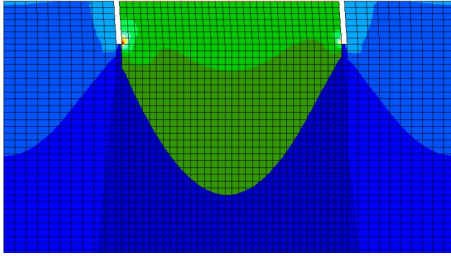
Testing conditions	Point A		Point B	
	σ_x [MPa]	σ_y [MPa]	σ_x [MPa]	σ_y [MPa]
4° – core misalignment 15 mm coring depth	1.1	3.2	0.8	2.2
4° – load misalignment 30 mm coring depth	1.4	3.2	0.6	2.2

4.4.2 Core depth and angle

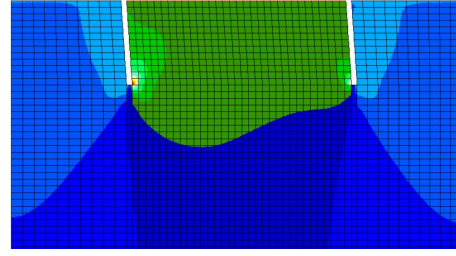
Initially axi-symmetrical with respect to the vertical axis under a perfectly vertical load, the stress field induced by the pulling effort in the cored area becomes increasingly asymmetrical as the load inclination shifts from 0° to 2°, and then to 4° (Figure 4-5). Under a load perfectly aligned with the coring axis (0°), in addition to the absence of stress asymmetry, transverse stresses (σ_x) at the bottom of the core cut are very small. These stresses also increase when the angle of inclination increases, especially at the bottom of the core. The largest stress imbalance, either for axial (σ_y) or transverse (σ_x) load, occurs A within the load plane between points located at the tip of each slit and identified as A and B (Figure 4-4), where the maximum and minimum stresses are found respectively.



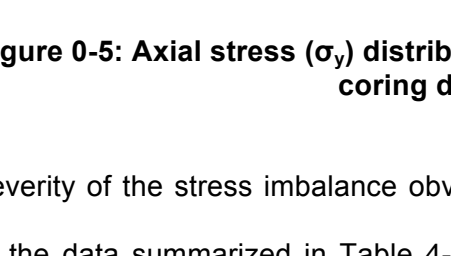
c) 2° misalignment / 15 mm core



d) 2° misalignment / 30 mm core



e) 4° misalignment / 15 mm core



f) 4° misalignment / 30 mm core

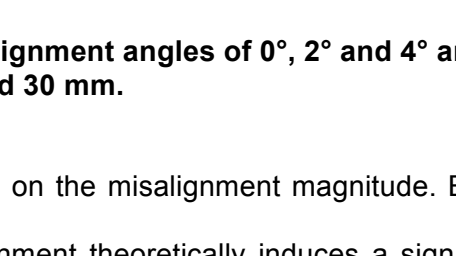


Figure 0-5: Axial stress (σ_y) distribution for misalignment angles of 0°, 2° and 4° and coring depths of 15 and 30 mm.

Severity of the stress imbalance obviously depends on the misalignment magnitude. Based upon the data summarized in Table 4-1, a 4° misalignment theoretically induces a significant axial stress (σ_y) differential at the bottom of the core. Stress distributions were calculated for different core depths and angles of inclination. As the value of the angle of inclination increases, the maximum axial stress increases at a progressively increasing rate (Figure 4-6). Besides, it can be observed that the influence of the depth of coring is minor up to an inclination angle of approximately 10°, beyond which the axial stress imbalance appears to increase with the depth of coring. This is in accordance with Cleland's findings [6].

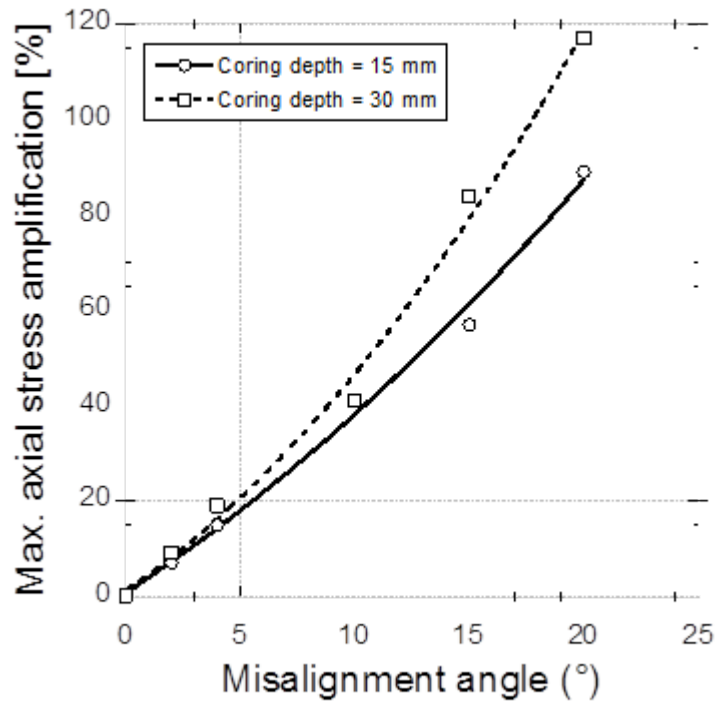


Figure 0-6: Theoretical axial stress (σ_y) amplification as a function of the misalignment angle of inclination and coring depth in a pull-off experiment.

At point A, a misalignment angle of 2° induces maximum axial (σ_y) stress increases of 6 and 9%, for core depths of 15 and 30 mm [0.6 and 1.2 in.] respectively, while a misalignment angle of 4° causes the axial stresses to increase by 14 and 19% for core depths of 15 and 30 mm [0.6 and 1.2 in.] respectively. As a simple first-order assumption, it can be inferred that corresponding the pull-off strength values are reduced by 7 and 13% for a coring depth of 15 mm [0.6 in.] and by 8 and 16% for a coring depth of 30 mm [1.2 in.].

It should be noted that the actual numerical results are dependent on the modelling assumptions and assumed material properties. For instance, the use of different E modulus values would have yielded different results.

4.5 Experimental programs

4.5.1 Pull-off experiments on monolithic substrates (U. of Liège)

Experiments were performed with three types of concrete mixtures: C30/37, C40/50, C50/60.

The concrete mixtures were prepared using the following constituents:

- Portland cement CEM I 52.5N;
- 0-2 mm crushed limestone sand;
- 2-8 mm, 8-14 mm and 14-20 mm crushed limestone coarse aggregates.

A series of six 600×400×100 mm concrete slabs was prepared with each of the three investigated mixtures. During the initial 24-hour period after casting, the slabs were covered with plastic. At 24 hours, they were demolded and stored in lime-saturated water up to 27 more days. Five tests have been realized for each parameters composition.

After 28 days of moist curing, the concrete slab surfaces were prepared by sandblasting for pull-off testing. The surface roughness was then evaluated with the *sand-patch* test method (EN 13036/EN1766/ASTM E965). The *texture depth* values recorded for the three different concrete mixtures were comparable, the overall average being equal to 0.90 mm.

As in the theoretical part of this task, the tensile pull-off tests were conducted on test specimens prepared with different core depths and inclinations. Core depths of 15 mm (0.6 in.) and 30 mm (1.2 in.) and coring axis inclinations of 0°, 2° and 4° were again investigated. The various core inclinations were achieved using the special device shown in Figure 0-7, which allows controlling precisely the inclination of the core drill axis. Taking into account the maximum aggregate size of the concrete mixtures (20 mm), 80-mm diameter cores were drilled for pull-off testing (80 mm diameter and 30 mm thick steel dollies).

During the pull-off test, the load was increased at a constant rate of 0.05 MPa/s up to failure. The average pull-off strength values recorded for the different concrete mixtures are summarized in Table 0-2.

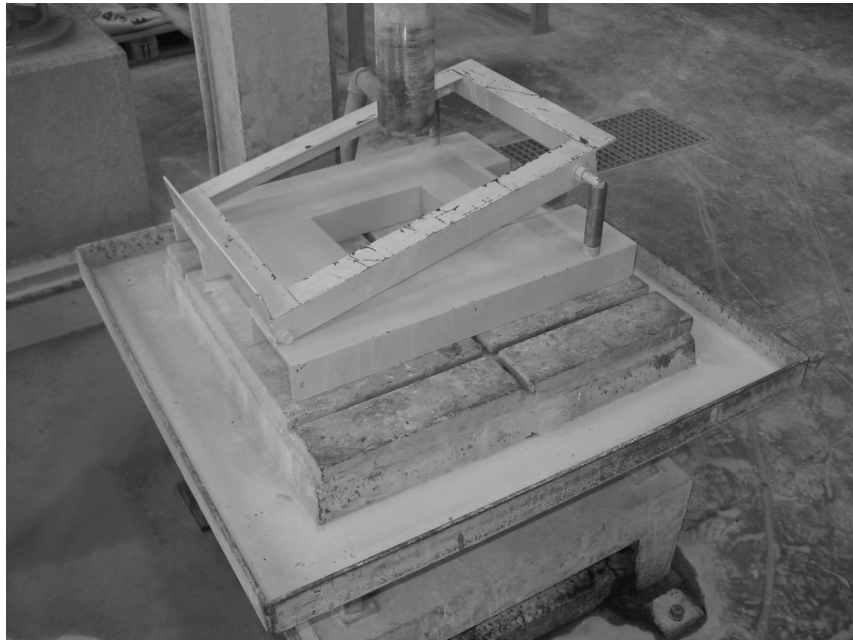


Figure 0-7: Special device for controlling the coring axis inclination at U. of Liège

The pull-off tests yielded results that are actually comparable in magnitude to those obtained in the direct tensile strength tests. Overall, the results reveal that a core misalignment results in slightly lower recorded pull-off strength values, the reduction reaching up to 13% for a 4° inclination. However, owing to the intrinsic pull-off test and material variability, which is reflected by the relatively high coefficients of variation of the results (**Erreur ! Nous n'avons pas trouvé la source du renvoi.**), the observed trends within individual series are not systematic. In fact, the pull-off strength reduction due to misalignment, within the range of inclination angles investigated, is of the same order of magnitude as that of the pull-off result variability. In order to get more consistent trends, a higher number of tests for each series would thus have been required.

Table 0-2: Direct tensile test and pull-off test results

Concrete mixture	Avg. direct tensile strength ¹	Test nr	Pull-off strength [MPa]	
			core depth	
			15mm (0.6 in.)	30mm (1.2 in.)
Misalignment angle				

	[MPa]		0°	2°	4°	0°	2°	4°
C30/37	3.6	1	3.8	3.5	3.2	3.6	3.0	3.6
		2	3.4	3.3	3.2	3.0	2.9	2.4
		3	4.1	3.8	3.8	3.2	3.0	2.8
		4	3.8	3.2	3.6	3.6	3.0	3.4
		5	3.6	3.7	3.8	2.7	2.6	2.5
		6	A.F.	3.2	3.5	2.6	3.0	A.F.
		Avg.	3.8	3.4	3.5	3.1	3.0	2.8
C40/50	3.9	1	3.7	3.3	3.4	2.9	2.9	3.4
		2	4.1	3.9	3.8	3.3	3.1	3.6
		3	4.0	3.2	3.7	3.7	2.9	2.9
		4	A.F.	A.F.	A.F.	3.0	2.5	A.F.
		5	3.6	3.4	2.8	A.F.	3.6	3.3
		6	3.9	3.8	3.3	2.6	3.2	3.2
		Avg.	3.9	3.4	3.4	3.0	3.0	3.3
C50/60	3.5	1	4.0	3.8	3.0	3.5	2.8	2.4
		2	3.7	3.3	3.6	3.6	3.0	2.3
		3	3.9	4.2	3.7	3.7	3.3	3.1
		4	3.3	3.4	3.3	3.2	A.F.	3.4
		5	4.1	4.0	3.5	3.1	2.9	3.3
		6	4.4	4.0	3.3	2.8	3.5	3.1
		Avg.	3.9	3.9	3.4	3.3	3.0	3.1

Besides, while a net decrease in average pull-off strength values is observed for the 30-mm core depth in comparison with the 15-mm core depth results (Table 0-2), there is almost no influence of the concrete type and the recorded strength values are relatively high in all cases (Figure 4-8).

Nearly 90% of the pull-off failures occurred at the bottom of the core, with just a few (6%) being observed in the body of the core. Careful examination of the fracture surfaces revealed interesting information. Irrespective of the type of concrete, through aggregate failure was dominating in 15 mm cores, while aggregate/paste interface failure was more frequent in the case of 30 mm cores. It is consistent with the higher tensile strengths and better superficial concrete behavior observed for 15-mm core depth specimens.

Nevertheless, the type of failure (through vs. around the aggregates) does not seem to be significantly affected by the load or core misalignment, the recorded values differing by less than 3%.

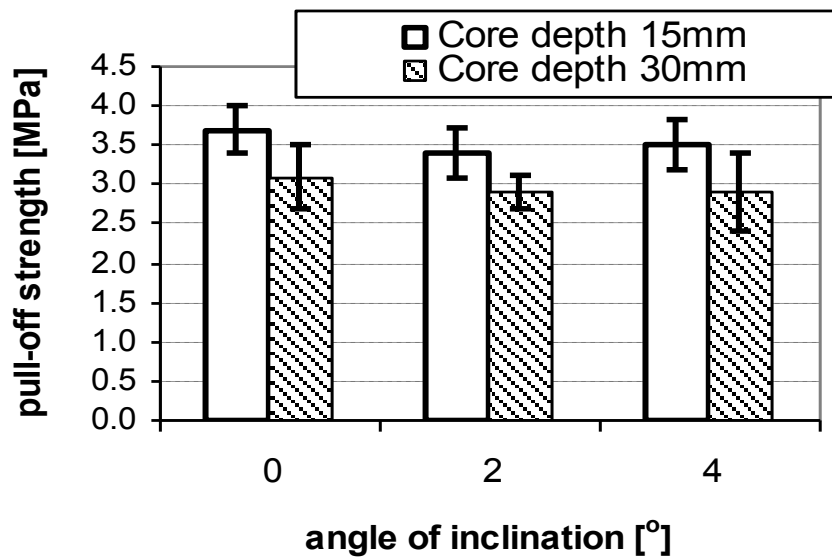


Figure 0-8: Average pull-off strength values for concrete slabs C30/37

4.5.2 Pull-off experiments on repaired substrates (USBR)

That part of Task 3 was handled at the US Bureau of Reclamation in Denver (CO). For the purpose of tasks 1 to 3, a series of twelve 560 × 1170 × 150 mm concrete slabs was manufactured at the US Bureau of reclamation with a 42-MPa (6000 psi) OPC supplied by a ready-mix concrete plant. The slabs underwent a 72 hours moist curing and they were aged and monitored under controlled conditions until volumetric stability was reached.

Afterwards, the top surface of each slab was prepared using different surface preparation methods. Three types of surface preparation methods were used; chipping hammer, water jetting and sandblasting (Figure 4-9). For each surface preparation, four slabs were used. Prior

to the application of a 3-in. overlay, the top surface of each slab was lightly sandblasted to remove any carbonated concrete. The light sandblast should not have affected the original surface preparation.

Figure 0-9: Surface treatment of concrete prior to repair

The concrete mixture used to cast the overlays had similar characteristics to the one used for manufacturing the base slabs. The overlays were moist cured for 72 hours and aged for a minimum of 28 days before bond tests took place.

The base concrete had a 7-d compressive strength (ASTM C33) of 40 MPa, whereas the overlay concrete had a 7-d compressive strength of 34 MPa (Table 4-3). (to replace with 28-d results if available – information from USBR awaited)

Table 0-3: Compressive strength of concrete samples

.....

According to the scope of research program, the tensile pull-off test was conducted for one core depth (100 mm, i.e. 25 mm into the substrate). On the 4 specimens of each surface preparation series, pull-off strength test series were carried out after coring with the following inclinations with respect verticality: 0°, 2° and 4° (36, 18 and 18 tests per surface treatment respectively).

The angle of inclination was obtained by using the experimental setup shown on Figure 0-10: it allowed to core with precisely controlled inclination using mobile drilling machinery. The picture of Figure 0-11 shows an extracted core specimen which was drilled with a 4° angle.



Figure 0-10: Experimental setup for coring under controlled inclination at USBR

Considering the aggregate maximum size of both the base and overlay concrete mixtures (XX mm), a 76.2-mm (3-in.) core diameter was selected for pull-off test with XX mm (X-in.) thick steel dollies). The load was increased at a constant rate of XX kN/s up to failure.



Figure 0-11: View of a 4°-inclined core after pull-off extraction

The results indicate that the average recorded bond strength decreases with the angle of inclination (Table 0-4 and Figure **Erreur ! Nous n'avons pas trouvé la source du renvoi.**).

Within a range of variation of $\pm 2^\circ$, the effect is almost negligible.

Table 0-4: Average pull-off test results - repaired substrates

Surface preparation	Tensile bond strength (MPa)*		
	Core inclination		
	0°	2°	4°
Chipping hammer	1.3 (0.4)	1.4 (0.4)	1.2 (0.3)
Sandblasting	1.6 (0.4)	1.5 (0.3)	1.5 (0.3)
Water jetting	1.9 (0.3)	1.8 (0.3)	1.5 (0.3)

* data in parentheses: standard deviation (MPa)

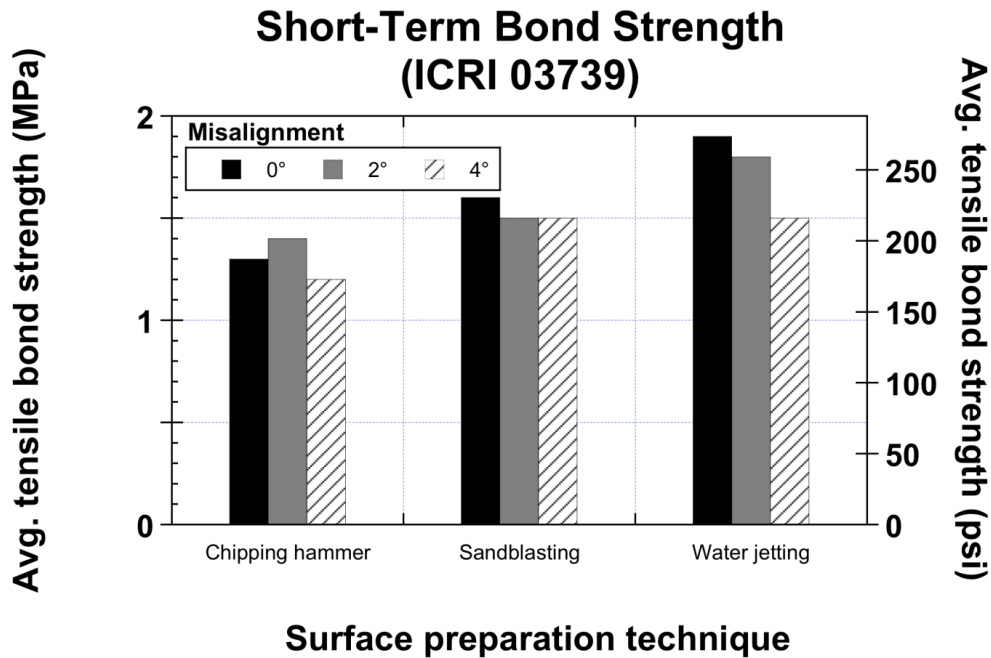


Figure 0-12: Average pull-off test results - repaired substrates

4.6 Conclusions

On the basis of the results of the numerical analysis and experimental results, the following conclusions can be drawn:

- up to a certain misalignment limit angle assumed to be detectable by the average human eye (4° in the present study), load and coring misalignments were not found to yield significantly different stress fields and, for practical calculation purposes, they can be addressed in a similar fashion;
- results of simulations revealed that a distorted stress field is induced by pulling-off testing misalignment, resulting in stress concentrations in an area at the bottom of the core slit: a 2° misalignment yield maximum stress increases of 6 and 9 % respectively for 15 mm

and 30 mm [0.6 and 1.2 in.] coring depths, and the corresponding increases resulting from a 4° misalignment reach 14 and 19%;

- the experimental pull-off test program results are overall consistent with the theoretical calculations, although the observed trends are not as clear, owing to the experimental variability and to the added influence of the coring depth;
- the simulation results provide a conservative but realistic lower bound limit for evaluation the influence of misalignment upon pull-off test results: a 2° misalignment can be expected to yield a pull-off strength reduction of 7 to 9 % respectively for 15 mm [0.6 in.] and 30 mm [1.2 in.] coring depths, and the corresponding decrease resulting from a 4° misalignment reach between 13 and 16%;
- as for the failure mode, it can be concluded that within 4°, testing misalignment does not significantly change the failure mode characteristics.

From a practical standpoint, the results generated in this study indicate that when specifying a pull-off strength limit in the field, the value should be increased (probable order of magnitude: 15%) to take into account the potential reduction due to testing misalignment.

4.7 References

1. **Vaysburd AM, Emmons PH** (2000) How to Make Today's Repairs Durable for Tomorrow – Corrosion Protection in Concrete Repair, *Construction and Building Materials*, 14(4): 189-197.
2. **Long AE** (1983) Review of Methods of Assessing the In-Situ Strength of Concrete, Keynote paper NDT 83 (Heathrow, London, England), Nov. 16-17, 16 p.

3. **Naderi M, Cleland DJ, Long AE** (1986) In Situ Test Methods for Repaired Concrete Structures. Proceedings ISAP 86 Adhesion between polymers and concrete, (H.R. Sasse, Chapman and Hall, London): 707-718.
4. **Hindo KL** (1990) In-Place Bond Testing and Surface Preparation of Concrete, *Concrete International*, 12(4): 46-48.
5. **Vaysburd A, McDonald JE** (1999) An evaluation of equipment and procedures for tensile bond testing of concrete repairs, US Army Corps of Engineers, *Technical Report REMR-CS-61.*, 65 p.
6. **Cleland DJ, Long AE** (1997) The pull-off test for concrete patch repairs, *Proc. Inst. Civ. Engineers Structures & Buildings*, 122(11): 451-460.
7. **Austin S, Robins P, Pan Y** (1995) Tensile bond testing of concrete repairs, *Materials and Structures*, 28: 249-259.
8. **Courard L, Bissonnette B** (2003) Adaptation of the pull-off test for the evaluation of the superficial cohesion of concrete substrates in repair works: analysis of the test parameters, *Materials and structures*, 37(269): 342-350.
9. **Bungey JH, Madandoust R** (1992) Factors influencing pull-off tests on concrete. *Magazine of Concrete Research*, 44(158): 21-30.
10. **Gerard P, Charlier R, Chambon R, Collin F** (2008) Influence of evaporation and seepage on the convergence of a ventilated cavity, *Water Resources Research*, 40(7): W00C02.
11. **Moczulski G, Garbacz A, Courard L** (2008) Evaluation of the Effect of Load Eccentricity on Pull-off Strength, ICCR08 International Congress on Concrete Repair, Reinforcement and Retrofitting (Alexander et al. eds., 2009 Taylor & Francis Group, London), Cape Town: 1017-22.

Table of contents

Table of contents	i
List of tables.....	iii
List of figures	iv
Task 4 – Develop a Field Test to Evaluate the Optimum Moisture Conditioning of the Particular Concrete Substrate.....	1
5.1 General.....	1
5.2 Background information.....	2
5.3 Objectives and methodology	4
5.4 Experimental program	5
5.4.1 Research objectives.....	Erreur ! Le signet n'est pas défini.
5.4.2 Initial Surface Absorption Test (ISAT).....	5
5.4.3 Modified Capillary Suction Test (MCST).....	6
5.5 Specimen preparation and conditioning	7
5.5.1 Concrete design and sample preparation	7
5.5.2 Surface preparation	8
5.5.3 Storage conditions	8
5.6 Analysis of the results.....	10
5.6.1 Results of water absorption tests.....	10
5.6.2 Comparison of the two methods	13

5.7	Adhesion and saturation level	Erreur ! Le signet n'est pas défini.
5.8	Conclusions	18
5.9	References	20

List of tables

Table 0-1: Calculation of work of adhesion for interfaces without (W_A) and with (W_{AL}) water (13).....	4
Table 0-2: Composition of concrete.....	7
Table 0-3: Storage conditions and saturation levels.....	9
Table 0-4: Correlation coefficients for ISAT and MCST methods vs. saturation level..	14
Table 0-5: Adhesion of mortar A on concrete substrate vs. saturation level of concrete substrate and slurry	17
Table 0-6: Adhesion of mortar B on concrete substrate vs. saturation level of concrete substrate and slurry	18

List of figures

Figure 0-1: Water intrusion into concrete, repair system and interface	Erreur ! Le signet n'est pas défini.
Figure 0-3: Wetting of a solid surface by two immiscible liquids (here, the wetting is favourable to liquid B)	3
Figure 0-4: Autoclam system and electronic controller	5
Figure 0-5: Gluing the ring onto the concrete substrate (ISAT)	5
Figure 0-6: Capillary suction test	7
Figure 0-7: Preparation of concrete cylinders for MCST test	7
Figure 0-8: Storage conditions referred to in 4, 5, 6, 7 and 8	9
Figure 0-9: Carbide bomb test	9
Figure 0-10: Comparison of water content of concrete samples, obtained with weight method and carbide bomb method	10
Figure 0-11: Permeability index for the different conditions: concretes, storage conditions (atm) and surface preparation	11
Figure 5-1: Permeability index versus degree of saturation (ISAT)	
Figure 0-13: Capillary absorption coefficients for atmosphere 4 and hydro-jetting	12
Figure 0-14: Capillary absorption rate versus degree of saturation (MCST)	13
Figure 0-15: Comparison between permeability index and capillary absorption	14
Figure 5-2: Permeability index versus degree of saturation (ISAT) after elimination of extreme values	

Section 5 – Develop a methodology for evaluation of the optimum moisture conditioning of a specific concrete substrate

The experimental work in this task was carried out in Belgium at the GeMMe Building Materials Research Unit of the University of Liège's ArGEnCo department, and in the United States at the U.S. Bureau of Reclamation in Denver, Colorado.

5.1 General

The influence of surface moisture on the bond between existing concrete and repair is an issue of significant importance. Moisture condition of the concrete substrate surface at the time of application of repair material has a major influence on the moisture transport mechanism between the freshly applied repair material and existing concrete substrate.

Saturated Surface Dry (SSD) conditioning of the substrate prior to application of cementitious repair materials is usually recommended and used, which underlies the “layman’s” instinctive procedures to avoid problems, rather than achieving the most effective bond. Various investigators came to the conclusion that different substrates and repair materials may require different interface moisture conditions at the time of casting to achieve optimum interfacial bond. The problem is that presently there is no test method to determine the optimum moisture condition for a given combination of substrate and repair material.

Water is one of the critical factors influencing bond development between concrete and repair materials: it may accumulate at the interface or migrate through it in either direction, as a result of mechanical (i.e. gravity), chemical (i.e. hydration) or physical (i.e. temperature gradients) driving forces.

Different moisture transport parameters affect the formation and behavior of the repair interfacial zone, such as diffusion and permeability coefficients, as the interface characteristics are indeed influenced by different forms of water interaction:

- First, moist conditioning of the substrate before the application of the repair system is a key consideration. Partial or total saturation of a concrete substrate is a common situation in repair works. Water along the interface may prevent adhesion to the repair system, with regard to PC, PCC or CC types (5);
- Second, water or aqueous solution movements may appear (3) due to migration and infiltration along the interface (4) or diffusion and capillary absorption from the zones to be repaired (5). Resistance to these water movements will directly depend on the quality of the materials: W/C, porosity, etc.

In most situations, the saturation level at the interface appears to be a predominant factor in promoting the adhesion of the repair system.

5.2 Background information

Saturated Surface Dry (SSD) conditioning of the substrate prior to application of cementitious repair materials is usually recommended and used, and underlies the “layman’s” instinct to avoid problems rather than achieving the most effective bond. Various investigators have come to the conclusion that different substrates and repair materials correspond to different optimum interface moisture conditions at the time of casting. The problem is that presently, there is no methodology to determine the optimum moisture condition for a given combination of substrate and repair material.

When water is present at the interface between repair and the concrete substrate, the thermodynamic equilibrium with respect to the surface free energy of each material is modified (7-9). From a theoretical point of view, this requires a generalization of the Young and Dupré’s equation (10), relative to a new liquid-liquid interface. Contact angle modification is a visible effect

of the interaction between the two liquids and a solid surface. But what happens to the spreading conditions? When equilibrium is attempted and if there is no spreading of one liquid to the detriment of the second (equations 1 and 2), the equilibrium of forces means (Fig. 2):

$$\gamma_{SA} = \gamma_{SB} + (\gamma_{AB} \cdot \cos \theta) \quad (5-1)$$

where γ_{SA} , γ_{SB} , γ_{AB} and θ are the interfacial tension between solid S and liquid A, interfacial tension between solid S and liquid B, interfacial tension between liquids A and B, and contact angle of these liquids on the solid surface, respectively (Fig. 2).

It is possible to show (11) that the liquid with the higher tension of adhesion ($\gamma_x \cdot \cos \theta_x$) will expel the other one from the surface. The calculation of the work of adhesion allows interesting interpretations, taking into account the variation of surface free energies in the presence of water (12).

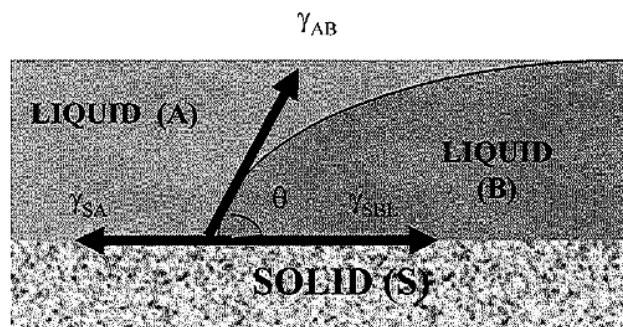


Figure 5-1: Wetting of a solid surface by two non-miscible liquids (wetting effect favorable in this case to liquid B)

The work of adhesion (equation 3) is an “evaluation” of adhesion between the liquids and solids in contact with each other, which is described by the following equation:

$$W_{x(L)} = \gamma_{x(L)} \cdot (1 + \cos \theta_{x(L)}) \quad (5-2)$$

Table 5-1 shows the loss of adhesion when water is present at the interfaces between acrylic-based or epoxy-based resins and concrete.

Table 5-1: Work of adhesion for interfaces without (W_A) and with (W_{AL}) water [13]

Interface	W_A (mJ/m ²)	W_{AL} (mJ/m ²)
Mortar / concrete	87.8	-
Acrylic / concrete	74.1	22.7
Acrylic / acrylic	80.4	53.7
Acrylic / hydrophobic treatment	52.2	66.7
Epoxy / concrete	79.6	21.8
Epoxy / epoxy	92.4	53.0
Epoxy / hydrophobic treatment	56.0	42.2

A high specific work of adhesion value does not automatically *per se* ensures good bond of the repair system to the concrete substrate (14). However, it is an indication that helps determine whether minimum conditions for proper bonding are met: the lower the work of adhesion, the less chance there is of obtaining strong physico-chemical interactions between solid and liquid phases. This is a necessary, but insufficient condition for adequate bond (15).

5.3 Objectives and methodology

The objective of this task was to develop a methodology to evaluate moisture level of the concrete substrate surface and to determine the optimum moisture conditioning for a given concrete surface such as to achieve maximum bond in a composite repair system. The governing criteria for the methodology development was its applicability to practical field use and accuracy. Eight (8) different concrete surface moisture levels and their effect on the bond strength were considered. Two methods were evaluated and compared.

5.4 Experimental program

5.4.1 General

Two concrete surface moisture test procedures were investigated: an “*Initial Surface Absorption Test (ISAT)*”, developed on the basis of a Queen’s University of Belfast testing device (16), and a modified capillary suction test (*MCST*) developed at the University of Liège (17). The first test procedure offers several improvements with regard to other existing techniques, making it an attractive alternative for non-destructive field testing: it is compact, more affordable, and the test duration is short (approximately 10 minutes). More common methods were also used as references.

Finally, the influence of moisture level on bond was evaluated by performing pull-off bond strength tests on concrete base slabs overlaid with two different cement-based repair mortars.

5.4.2 Initial Surface Absorption Test (ISAT)

Autoclam (Table 5-2) is a testing device designed for measuring the air and water permeability of concrete (CNS Electronics). It can be used in the laboratory as well as *in situ*: a metallic ring is fixed to the concrete substrate (Table 5-3), and the amount of fluid (air or water) that penetrates into the concrete at a typical pressure of 0.5 kg/cm² is continuously recorded. Typically, the slope of the linear part of the curve between 5 and 15 minutes is used to determine a permeability index.



Figure 5-2: Autoclam system and electronic controller



Figure 5-3: Gluing of the ring onto the concrete substrate (ISAT)

5.4.3 Modified Capillary Suction Test (MCST)

The most commonly used test to analyze water transfer at the interface is the capillary suction test (18). It is described by several standards, which differ from one another on the water level above the bottom surface of the concrete specimen and the time period of the measurement. Mass change is usually measured after 5, 15, 30 and 45 minutes, as well as after 2, 6 and 24 hours (19). Mass is measured on samples wiped off with a damp tissue. However, capillary forces exist when contact is created between the concrete substrate and the repair material. The liquid phase from the repair material mixture is being absorbed into the capillaries of concrete. In the recently developed MCST test (17), the specimen mass change arising during the process of capillary suction is recorded in a continuous fashion (Table 5-4a).

Specimens are cast concrete cylinders ($\varnothing = 80 \text{ mm}$; $L = \text{XXX mm}$) with the lateral face coated with epoxy resin (Table 5-4b) to avoid moisture penetration and evaporation in the transverse direction: water comes up from the bottom until contact with the sample occurs. Mass change is continuously monitored (1 or 5 seconds), and the measurements obtained from a weighing scale are saved through the use of appropriate computer software.



a) experimental setup



b) test specimen

Figure 5-4: MCST test

5.5 Specimen preparation and conditioning

5.5.1 Concrete substrate and sample preparation

Experiments were performed on three different grades of concrete: C30/37, C40/50 and C50/60, respectively. The concrete mixtures were prepared with ordinary Portland cement and limestone crushed aggregates (Table 5-2).

Table 5-2: Concrete mixture composition

		C30/37	C40/50	C50/60
CEM I 52.5 N	(kg/m ³)	275	325	375
Sand 0/2	(kg/m ³)	765	729	676
Crushed aggregate 2/8	(kg/m ³)	255	230	206
Crushed aggregate 8/14	(kg/m ³)	569	576	601
Crushed aggregate 14/20	(kg/m ³)	390	401	412
Water	(kg/m ³)	192	6	182
W/C	(kg/m ³)	0.70	0.57	0.49
Mean Compressive Strength	(MPa)	42.9	54.3	61.2

Eighteen 800×600×100-mm concrete slabs were cast (6 slabs for each concrete grade). After casting (24 hours), slabs were demolded and stored in water for up to 28 days. The compressive strength of concrete was determined for each mixture using three 150×150×150-mm cube specimens (Table 5-2).

5.5.2 Surface preparation

After 28 days of curing, the concrete slab surfaces were prepared either by sandblasting (SB) or hydro-jetting at a 1000-bar pressure (HD); control slabs without any surface preparation (NT) were kept as reference. In the case of sandblasting (SB), the roughness of the surface was assessed using the Sand Patch Test (EN 13036-1:2002) and an average texture depth value of 0.60 mm was recorded. After thorough observation, only the test specimen prepared by hydro-jetting exhibited some cracking; still, the observed cracks (20) were very small.

5.5.3 Storage conditions

The concrete slabs were then subjected 8 different environmental conditioning, in such a way to obtain saturation levels ranging from 40 to 100% (Table 3). The duration of storage was 3 months (Fig. 7).



Figure 5-5: Storage conditions (see details in Table 5-3)



Figure 5-6: Carbide bomb test

The saturation level is determined by measuring the water content of small-size drilled samples stored in the same conditions as for the specimen slabs.

Table 5-3: Storage conditions and saturation levels.

Storage conditions (SC)	Saturation level (%)
1 Oven-dried (40 °C in oven until constant weight) and stored at 23 °C / 85% RH	32
2 Stored outdoors (in Belgium winter conditions temperature, protected from rain)	64
3 Stored in a climatic room at 20 °C / 100% RH	100
4 Dried, submerged in water for 30 seconds and stored in a plastic bag	41
5 Stored in water, taken out for 3 hours (23 °C / 50% RH) and then stored in a plastic bag	90
6 Stored in water, taken out for 1 hours (23 °C / 50% RH) and then stored in a plastic bag	92
7 Stored in water, taken out for 15 minutes (23 °C / 50% RH) and then stored in a plastic bag	96
8 Stored under standard laboratory conditions at 23 °C / 50% RH	42

The Carbide bomb test (22) (Fig. 8) was also used for comparison with the weighing method (Fig. 9).

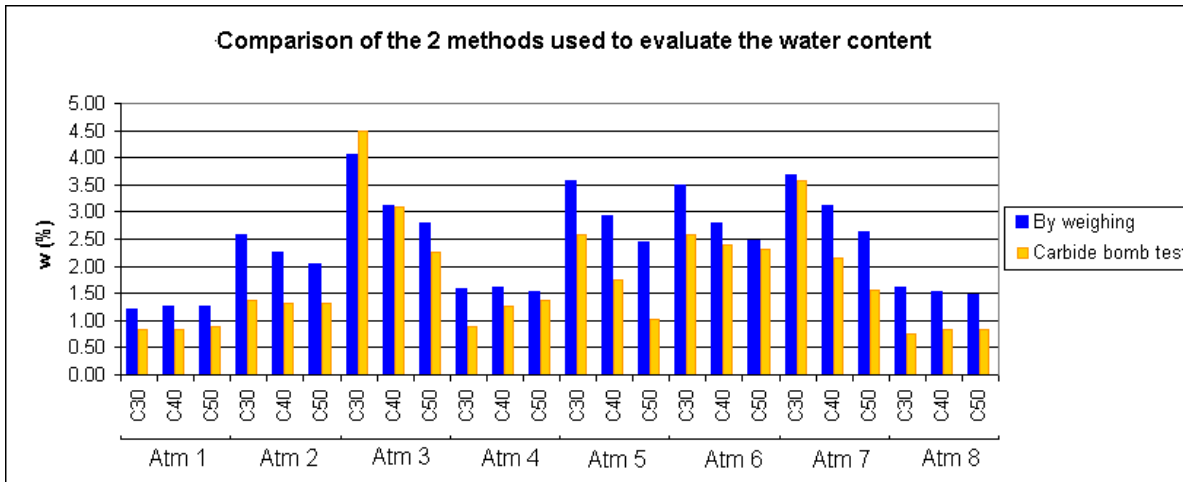


Figure 5-7: Comparison of water content of concrete samples obtained with specimen weight method and Carbide bomb test method

5.6 Test result analysis

5.6.1 Water absorption test results

Water absorption permeability indices (Fig. 10) exhibit relatively high degrees of correlation with the degree of saturation (Fig. 11). Statistically speaking, however, no correlation was found between the absorption permeability indices and compressive strength. It was noted though that absorption rates were higher for surfaces prepared by hydro-jetting (HD) as compared to values obtained for sandblasted surfaces (SB), likely due to the presence of superficial cracking in the former.

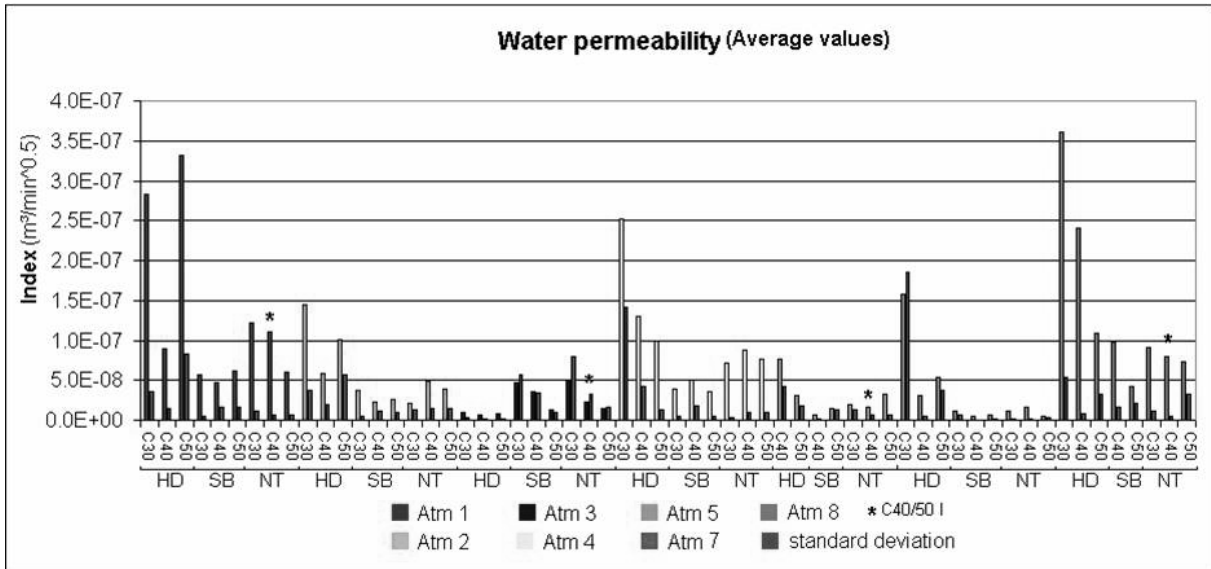


Figure 5-8: Permeability index for the different conditions: concretes, storage conditions (atm) and surface preparation.

A strong correlation between permeability index and the degree of saturation was also observed: the higher the saturation, the higher the permeability index (Fig. 11). The dispersion of the results remains important, however, especially for saturation levels higher than 80% RH.

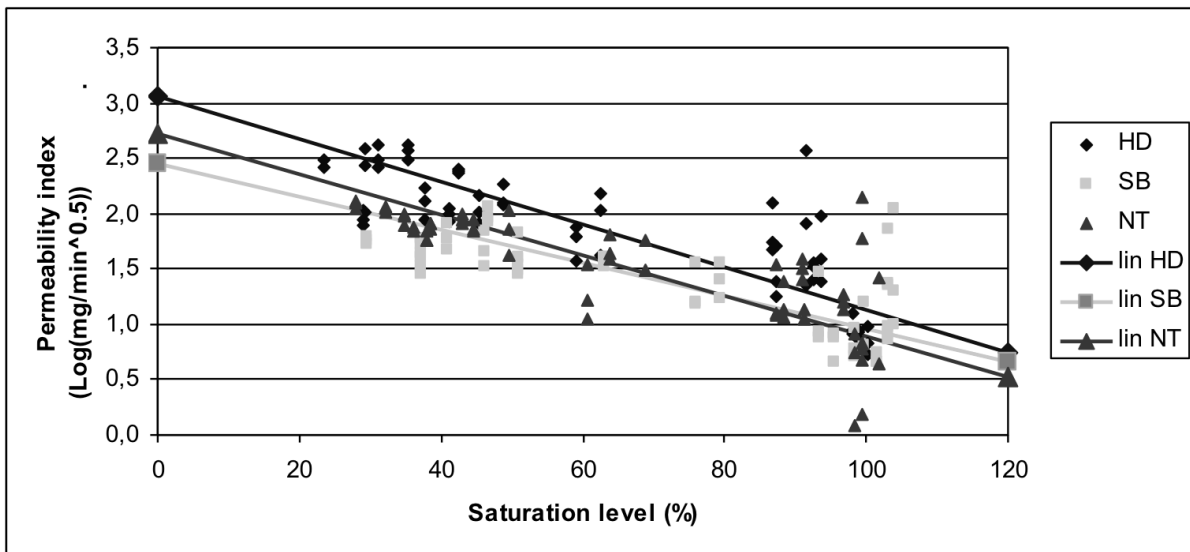


Figure 5-9: Permeability index versus degree of saturation (ISAT)

Water capillary absorption tests (MCST) yield more consistent data and clearer tendencies than ISAT tests (Fig. 12): the stronger the concrete, the lower the absorption coefficient. The parameters influencing the MCST test procedure appear to be more easily controllable.

It can be concluded that the degree of saturation has a direct effect on capillary absorption (Fig. 13). In comparison with sandblasting, it was observed that hydro-jetting induces a higher rate of water capillary absorption, which probably can be attributed to soft microcracking.

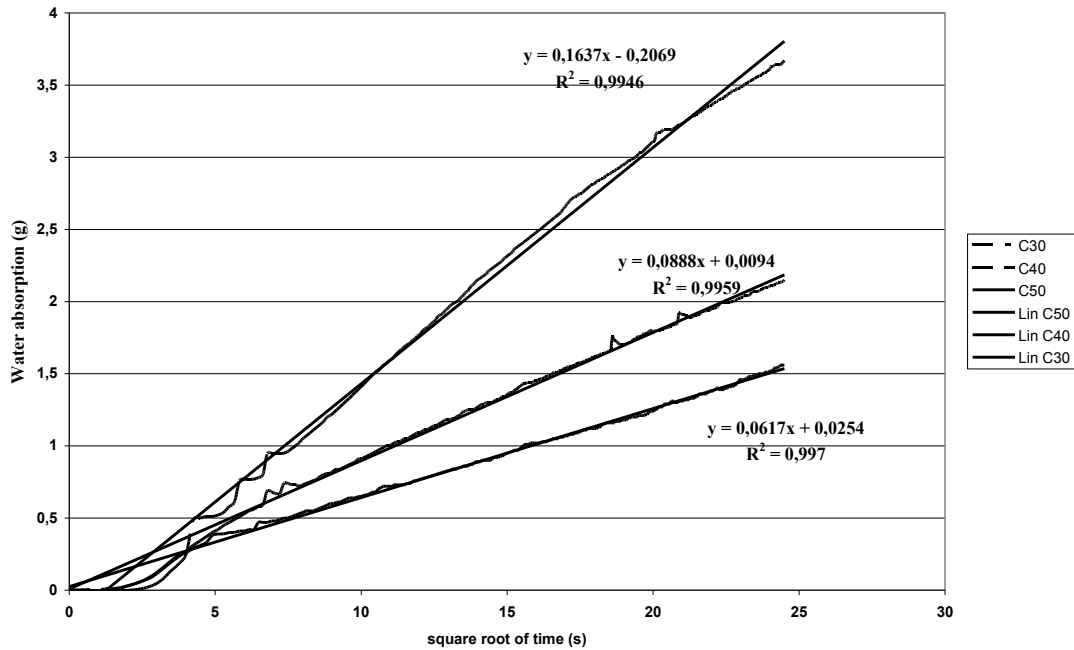


Figure 5-10: Capillary absorption coefficients for atmosphere 4 and hydro-jetting

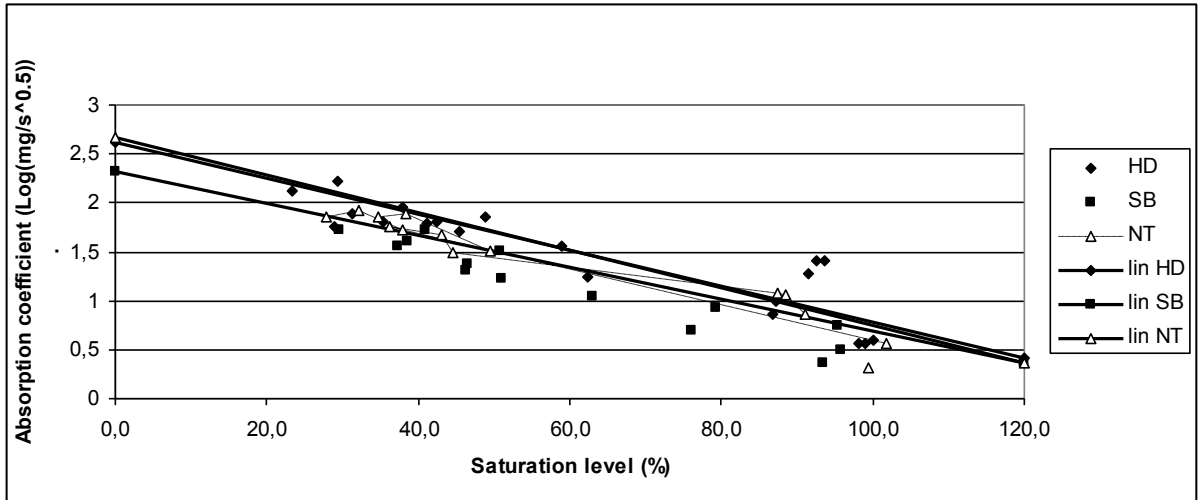


Figure 5-11: Capillary absorption rate versus degree of saturation (MCST)

5.6.2 Comparison of ISAT and MCST test methods

The same trends were observed for the two methods (Fig. 14).

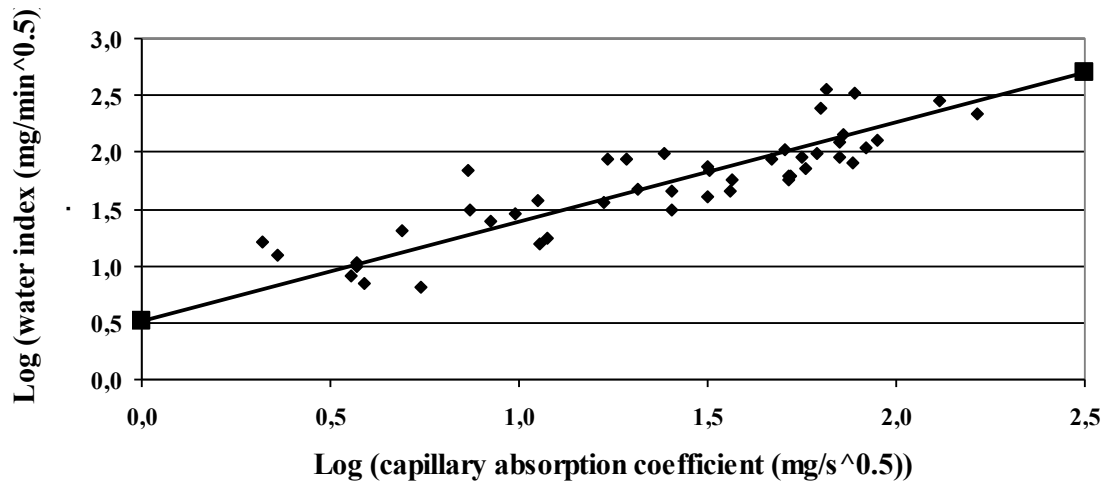


Figure 5-12: Comparison between permeability index and capillary absorption

However, the coefficients of correlation with the degree of saturation are systematically higher with MCST than with ISAT (Table 4).

Table 5-4: Correlation coefficients for ISAT and MCST methods vs. saturation level

Surface preparation		ISAT		MCST		
		r	r ²	r	r ²	
HD	sat/log (index)	-0.80	0.64	sat/log (abs)	-0.90	0.80
SB	sat/log (index)	-0.73	0.53	sat/log (abs)	-0.96	0.91
NT	sat/log (index)	-0.78	0.62	sat/log (abs)	-0.96	0.93

Index = permeability index

Abs = absorption rate

The higher variation and dispersion of results for ISAT may stem from the difficulty of performing the test and, specifically, the waterproofing of the connection between the metallic ring and the substrate (Fig. 7). Moreover, dispersion can be aggravated by the following factors:

- Intrinsic concrete variability: the microstructure of the concrete may vary spatially, especially along the surface;
- Approximation of the evaluation of the degree of saturation: If these are measured on samples stored in the same conditions as concrete slabs, the real saturation level of the concrete is probably not really or precisely known;
- Test conditions: tests are performed under laboratory conditions (50% R.H. and 23 °C). This means that the samples are taken out of their storage conditions during testing time and water vapor exchanges may occur.

If “extreme” values corresponding to specific “out of the range” behaviors to eliminate, relatively good correlations are found, with correlation coefficients of 0.82, 0.73 and 0.90 for HD, SB and NT, respectively (Fig. 15).

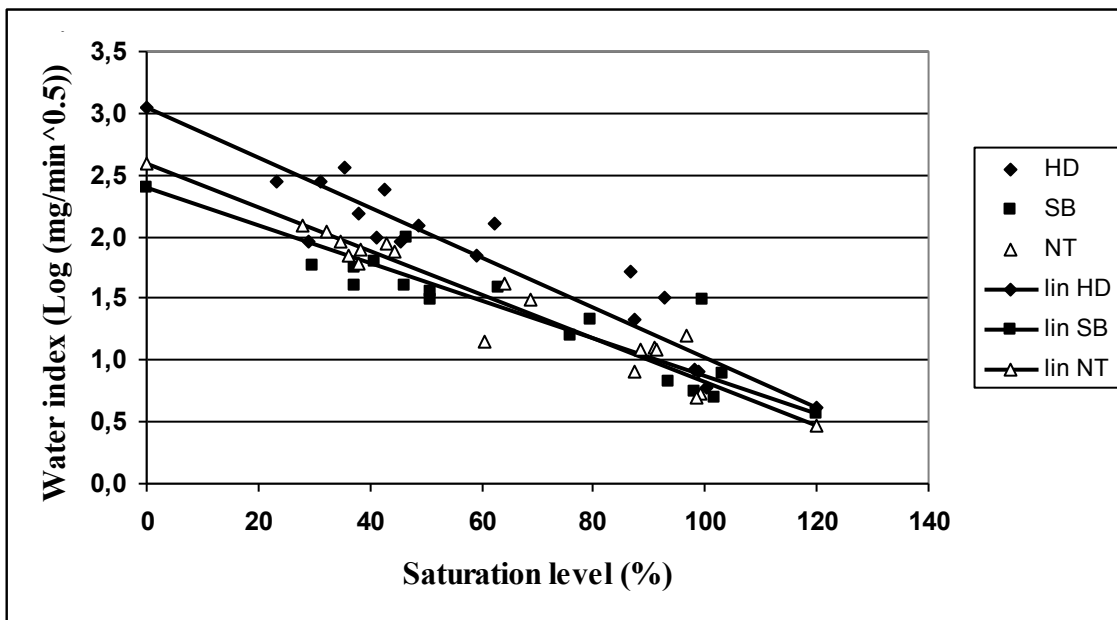


Figure 5-13: Permeability index versus degree of saturation (ISAT) after elimination of extreme values

5.7 Bond test results

The influence of saturation level on bond between repair and substrate was evaluated by conducting series of pull-off tests for 2 types of PCC repair mortars referred to as A and B, with the following characteristics:

- Mortar A is a two-component mortar mixture with a 105/1000 liquid to powder content weight ratio. A bonding layer of acrylic-based slurry was applied prior to mortar placement. The material is acrylic-based with a characteristic bending strength of 11 MPa, a characteristic compressive strength of 54.98 MPa and a density of 1.87;
- Mortar B is a one-component repair mortar with a 95/1000 water to powder content ratio. The mortar is acrylic-based with a characteristic bending strength of 10.94 MPa, a characteristic compressive strength of 48.36 MPa and a density of 2.18.

The repair systems are applied to the sandblasted concrete slabs. The cohesion of concrete is equal to 4.16 N/mm². Concrete slabs are stored as mentioned above (Table 3) in order to reproduce different saturation levels.

The slabs are positioned vertically and a 10-mm thick mortar layer is applied. The slabs are taken out of the bags only when the components are mixed or the slurry is ready to be used. Wet and dry slurries are applied to each half of the slab. The time between the application of the slurry and the application of the mortar is about 30 seconds, according to supplier recommendations. The samples are then stored for 28 days at 20 °C/65% RH. Three core samples of 50 mm in diameter are taken out of each slab half, and bond strength is measured according to EN 1542. For all test specimens, failure occurred within the concrete substrate, just below the surface (quasi-adhesive failures).

Bond strength changes as a function of the water saturation level of the substrate (Tables 6 and 7). Although the recorded bond strength is relatively weak for low saturation levels ($\leq 50\%$), it reaches more typical values for saturation levels ranging between 55 and 75%. Above this ranges,

a decrease in bond strength (> 90%) is observed. Hence, a low saturation level seems to affect negatively the hydration of cement in the repair material, while a moisture content close to saturation influences the attraction/repulsion force balance between the solid particles, the porosity, the kinetics of contact and the adhesion properties, the end result being a lower bond strength in both cases. Optimal moisture of the substrate is 100% RH, which can be easily reached in a laboratory. Consequently, maximum bond strength values can be achieved for a rather wide range of saturation levels, which means that adhesion does not extensively depend on slight variations of water content, with the exception of extreme conditions.

Table 5-5: Bond strength of mortar A as a function of the concrete substrate saturation level

Avg. bond strength (MPa)		
Saturation level (%)	Dry slurry	Wet slurry
50	0.83	2.32
52	2.80	2.14
55	2.09	2.89
70	2.75	2.65
90	3.54	3.36
93	2.13	3.06
97	1.81	2.58
100	1.43	1.48

In the case of mortar A, the influence of the slurry water content upon bond strength seems to be negligible for substrate saturation levels ranging between 70 and 90% (Table 5). Out of this range, the wet slurry yielded better results. For mortar B, the recorded bond strength values with dry slurry are somehow higher than the ones recorded with wet slurry (Table 6), a result which

could be related to the fact that the water-based mortar B (not a polymeric emulsion) potentially increased the effective W/C ratio (and, as a result, increased the porosity) in the interfacial zone.

Table 5-6: Bond strength of mortar B as a function of the concrete substrate saturation level

Bond strength (MPa)		
Saturation level (%)	Dry slurry	Wet slurry
50	1.41	1.34
60	2.90	2.72
70	2.95	1.41
100	1.09	1.43

Establishing the optimum moisture conditioning level for a specific concrete substrate is one of the critical factors affecting the bond strength in the overall quality and, potentially, the longevity of composite repair / overlay systems. Saturation levels of the concrete substrate surface at the time of repair material application in fact had a significant impact on the absorption of moisture and fine particles from the fresh (plastic) repair material, and as a result on the recorded bond strength results.

It should be stressed here that pure cement-based materials and polymer-based materials exhibit different behaviors when affected by water at the interface (21).

5.8 Conclusions

The following conclusions may be reached from the experimental work performed in this task:

1. ISAT is an attractive test method for performing a quantitative test to evaluate the saturation level of a concrete substrate: it is compact, cost-effective and rapid. ISAT results (permeability index) are not sensitive to concrete compressive strength, at least

in the range from 30 to 50 MPa. They are influenced by the substrate surface quality, but it is difficult to conclude whether this is due to surface roughness, microcracking, or a combination of both. The relatively high variation and dispersion characterizing the ISAT test results may stem from the difficulty of performing the test on rough concrete surfaces (for instance after hydro-jetting).

2. The MCST test yielded clearer trends and less dispersed information than the ISAT test, as well as a better correlation with water content measurement (wet and dry weighing measurements).
3. A good correlation was found between the water absorption index and the capillary absorption coefficient determined using both the ISAT and MCST tests.
4. There is a large range of saturation levels (50 to 90%) where bond strength remains high and constant, which seems to limit the influence of environmental conditions on adhesion of cement-based repair systems. The bond strength is relatively low for low saturation levels ($\leq 50\%$), but it reaches higher values for saturation levels comprised between 55 and 90%.
5. When acrylic emulsion is used as a bonding agent, the highest saturation levels induce a water film at the interface, which is incompatible with polymeric material and reduces the effectiveness of adhesion.

These findings evidence the effect of water in the substrate concrete superficial zone and the difficulty encountered in evaluating reliably the actual saturation level. For the repair systems considered in this task, it seems that optimum saturation levels for repair bond strength would lie somewhere between 55 to 90%. Clearly, additional work is required to identify a methodology that could be used in field applications and, furthermore, to assess what are the optimum moisture ranges for cement-based repair materials.

5.9 References

1. **Courard, L., Degeimbre, R., Darimont, A., and Wiertz, J.** (1995) Influence of composition of repairing mortars on adhesion. In: Proceedings of the VIII International Congress on Polymers in Concrete (Ed. D. van Gemert, KULeuven en KVIV), Oostende, pp. 119-124.
2. **Pareek, S. N.** (1993) Improvement in adhesion of Polymeric Repair and Finish Materials for reinforced Concrete Structures. Doctoral Dissertation, Nihon University, College of Engineering (Japan), p. 182.
3. **Courard, L., Degeimbre, R., Darimont, A., and Wiertz, J.** (2003) Hygro-thermal application conditions and adhesion. In: Proceedings of the Fifth International Colloquium Industrial Floors '03 (Ed. P. Seidler, Technische Akademie Esslingen), Ostfildern/Stuttgart, pp. 137-142.
4. **Courard, L., and Darimont, A.** (1998) Appetency and adhesion: analysis of the kinetics of contact between concrete and repairing mortars. In: Proceedings of the RILEM International Conference, Interfacial Transition Zone in Cementitious Composites (Eds A. Katz, A. Bentur, M. Alexander and G. Arliguie, E&FN Spon), Haïfa, pp. 185-194.
5. **Courard, L., Degeimbre, R., Darimont, A., and Wiertz, J.** (1999) Effects of sunshine/rain cycles on the behaviour of repair systems. In: ISAP 99, Proceedings of the 2nd International RILEM Symposium on Adhesion between Polymers and Concrete (Ed. Y. Ohama and M. Puterman), Dresden, pp. 511-521.
6. **Bissonnette, B., Courard, L., Vaysburd, A., and Bélaïr, N.** (2006) Concrete removal techniques: influence on residual cracking and bond strength. *Concrete International* 28(12): 49-55.
7. **Courard, L.** (1999) How to analyse thermodynamic properties of solids and liquids in relation with adhesion? In: ISAP 99, Proceedings of the 2nd International RILEM

- Symposium on Adhesion between Polymers and Concrete (Ed. Y. Ohama and M. Puterman), Dresden, pp. 9-20.
8. **Courard, L.** (2000) Parametric Study for the Creation of the Interface between Concrete and Repair Products. *Mater. Struct.* 33: 65-72.
 9. **Courard, L., Degeimbre, R., and Wiertz, J.** (1998) The behaviour of coatings on concrete substrates in relation with different forms of water attack. In: CONSEC '98, Proceedings of the 2nd International Conference on Concrete under Severe Conditions (Eds. O.E. Gjorv, K. Sakai and N. Banthia, E&FN Spon), Tromso, pp. 997-1006.
 10. **Comyn, J.** (1992) Contact angles and adhesive bonding. *International Journal of Adhesion and Adhesives* 12(3): 145-49.
 11. **Courard, L., Degeimbre, R., Darimont, A., and Wiertz, J.** (2003) Effects of environment on Repair Materials: Results of a Five-Year Research Project. In: Proceedings of the Sixth Canmet/ACI International Conference on Durability of Concrete (Ed. V. M. Malhotra, SP212-57), Thessaloniki, pp. 921-940.
 12. **Courard, L., Degeimbre, R., Wiertz, J., and Van de Put, M.** (1998) Analysis of the resistance to water of the interface between concrete and repairing systems: experimental approach. In: CONSEC '98, Proceedings of the 2nd International Conference on Concrete under Severe Conditions (Eds. O.E. Gjorv, K. Sakai and N. Banthia, E&FN Spon), Tromso, pp. 988-996.
 13. **Courard, L.** (2002) Evaluation of thermodynamic properties of concrete substrates and cement slurries modified with admixtures. *Mater. Struct.* 35: 149-155.
 14. **Gutowski, W.** (1987) The relationship between the strength of an adhesive bond and the thermodynamic properties of its components. *International Journal of Adhesion and Adhesives* 7(4): 189-98.

15. **Posart, W. and Kamuzewitz, H.** (1993) The thermodynamics and wetting of real surfaces and their relationship to adhesion. *International Journal of Adhesion and Adhesives* 13(2): 77-84.
16. Permeability testing of site concrete. A review of methods and experience. *Concrete Society Technical Report*, 31, Concrete Society Working Party, London, 1987.
17. **Courard, L. and Degeimbre, R.** (2003) A capillary suction test for a better knowledge of adhesion process in repair technology. *Can. J. Civil Eng.* 30(6): 1101-1110.
18. Saturation level of the superficial zone of concrete and adhesion of repair systems. L. Courard, J. F. Lenaers, F. Michel and A. Garbacz. *Construction and Building Materials* 25(5), May 2011, 2488-2494.
19. **Justnes, H.** (1995). Capillary suction of water by polymer cement mortars. In: Proceedings of the RILEM Symposium on Properties and Test Methods for Concrete-Polymer Composites (Ed. D. van Gemert, KULeuven en KVIV), Oostende, pp. 29-37.
20. **Courard, L., and Lenaers, J. F.** (2008) Evaluation of saturation and microcracking of the superficial zone of concrete: new developments. In: Proceedings of the ICCRRR08 International Congress on Concrete Repair, Reinforcement and Retrofitting (Alexander et al (eds), 2009 Taylor & Francis Group, London), Cape Town, pp. 977-82.
21. Evaluation and quality assessment of industrial floors (Chapter 4). RILEM TC 184 – IFE Industrial floors for withstanding environmental attacks, including repair and maintenance. **Coordinator: L. Courard – Authors: L. Courard, A. Garbacz (Poland) and L. Wolff (Germany).** Rilem Report 33 (Ed. P. Seidler, Rilem Publication), pp. 59-89 (August 2006).
22. **Vaysburd, A.M. and Bissonnette, B.** (2009) Methods to Measure Near Surface Moisture Content of Concrete and Mortar, Technical report, U.S. Bureau of Reclamation, Denver (CO), 47 p.

Table of contents

Table of contents	i
List of tables.....	ii
List of figures	iii
Task 5 – Evaluate the effect of carbonated substrate concrete on bond strength	1
6.1 General	Erreur ! Le signet n'est pas défini.
6.2 Background information	Erreur ! Le signet n'est pas défini.
6.3 Objectives and methodology.....	3
6.4 Experimental program.....	Erreur ! Le signet n'est pas défini.
6.5 Conclusions	10
6.6 References.....	11

List of tables

Table 5-1: Compressive strength test results	8
Table 5-2: Tensile strength test results	8

List of figures

Figure 5-1:	Slabs after surface preparation.....	7
Figure 5-2:	Carbonation depth measurement	7
Figure 5-3:	Coring template.....	7
Figure 5-4:	Pull-off bond test apparatus	8
Figure 5-5:	Bond strength results for the chipping hammer surface preparation	8
Figure 5-6:	Bond strength results for the sandblast surface preparation	9

- Task 5 – Evaluation of the effect of substrate concrete carbonation upon bond strength

This part of the report is related to Task 5, as described in the original research program. The experimental work has been carried out at the U.S. Bureau of Reclamation, Denver (CO).

6.1 Introduction

ACI defines “carbonation” as the “*reaction between carbon dioxide and a hydroxide or oxide to form carbonate, especially in cement paste, mortar or concrete; the reaction with calcium compounds to produce calcium carbonate* (ACI 116R, Cement and Concrete Terminology).” The alkalinity of the concrete initially rises to a pH of 12.8 and higher due to the calcium hydroxide released during the cement hydration. However, alkalis in concrete exposed to the atmosphere react with acidic components of the atmosphere, particularly with carbon dioxide (CO₂). As a result, the calcium hydroxide is converted to calcium carbonate. The reaction of carbon dioxide with the calcium hydroxide in concrete is called “carbonation”. Carbonation as a process mainly affects the capability of concrete to protect embedded steel reinforcement from corrosion. Therefore, the attention with regard to carbonation in reinforced concrete is essentially paid to its electrochemical effects.

One of the issues sometimes ignored or overlooked is the fact that carbonation also alters a number of physical properties of concrete (Vaysburd, A.M., Sabnis, G.M. and Emmons, P.H., 1997). Carbonation has an effect of strengthening and densification of cement-based materials, such strengthening and densification of the structure is associated with forming calcium carbonate, and depends on type of cement used in concrete. In Portland cement-based concrete, carbonation can lead to an increase in compressive strength exceeding 50 %. When using cements incorporating natural pozzolans or supplementary-cementing materials such as

silica fume, fly ash and slag, the changes in strength by carbonation are only marginal (Meyer 1987).

Another very important consequence of carbonation is a change in the void space and the permeability of carbonated concrete. The calcium carbonate fills the fine pores around the larger voids within the pore structure (Vaysburd, A.M., Sabnis, G.M. and Emmons, P.H., 1997). Blocked pores on a concrete surface may affect the wetting and suction of repair materials.

The term “adhesion” describes the condition in the boundary layer between two connecting materials with a common interface. Adhesion mechanisms can be divided basically into mechanical interaction, thermodynamic mechanisms, and chemical bonding (Beushausen, 2005). Mechanical adhesion in repaired concrete members relies on the hardening of the repair material mixture inside the open cavities, pores and asperities of the substrate surface, and the physical anchorage resulting therefrom. The cement paste absorption into open pores of the substrate concrete plays an important role in the anchoring effect, as it draws paste into the substrate. Thus, the phenomenon of carbonation, by producing a denser surface layer with so-called “clogged” pore system, which reduces the absorptivity of the substrate concrete, might affect negatively the bond strength in repair systems.

Through proper surface preparation the carbonated concrete surface can usually be removed, thereby exposing a “fresh” non-carbonated surface. However, in some cases it involves extensive removal of otherwise sound concrete. Also, long periods of time between concrete surface preparation and repair placement may result in carbonation of the exposed substrate surface.

The influence of carbonation of the concrete substrate surface upon bond strength of concrete repairs has not been investigated extensively. In addition, from the limited published research data, there is no consensus regarding the effects of carbonation in the scientific community. For instance, test results from Gulyas, Wirthlin and Champa (1995) show that carbonation may decrease the bond strength significantly. Block and Porth (1989), on the contrary, found in their studies that carbonated substrate does not affect pull-off bond strength. The conflicting results prompted the experiments performed in this task.

The objective of the task reported in this chapter was to evaluate the effect of carbonation of the concrete substrate upon tensile bond strength of repairs.

6.2 Methodology

In order to evaluate the effect of carbonation of the concrete substrate upon tensile bond strength of repairs, the following basic variables were selected for investigation:

- Concrete surface preparation technique;
 - ✓ Chipping hammer;
 - ✓ Sandblasting;
- Conditioning prior to repair;
 - ✓ No carbonation (control specimens);
 - ✓ Carbonation.

The experimental test program carried out at the U.S. Bureau of Reclamation (USBR), Denver (CO) is summarized in Table 6-1. Further details pertaining to the test variables, the specimen sizes, the preparation and conditioning of these specimens, and the bond tests are disclosed in the subsequent paragraphs.

Table 0-1: Concrete mixture characteristics and mechanical properties (USBR)

Material	Test slab concrete mixture	Repair concrete mixture
Nominal strength	27.5 MPa (4000 psi)	27.5 MPa (4000 psi)
Mixture characteristics	ASTM Type I cement 14-mm (½ in.) coarse agg.	ASTM Type I cement + black pigments (6% of C wgt.) 10-mm (3/8 in.) coarse agg.
Fresh concrete properties ¹		
Slump (mm)	125-175	125-175
Air content (%)	4-7	5-8
Compressive strength ² (MPa)		
7 d	20.9	21.9
28 d	28.3	27.5
Splitting-tensile strength ³ (MPa)		
7 d	n/a	2.34
28 d	n/a	2.92 ⁵
Elastic modulus ⁴ (GPa)		
7 d	n/a	21.3
28 d	n/a	22.9

¹Specified values; ²ASTM C39, ³ASTM C496, ⁴ASTM C469; ⁵at 10 days.



Figure 0-1: Base slabs after surface preparation

In each set of prepared test slabs, four (4) control slabs were protected from carbonation (control), and five (5) slabs underwent controlled carbonation in a laboratory carbonation chamber. Throughout the conditioning period, the control slabs were covered with polyethylene sheets sealed with duct tape to prevent carbonation. The carbonation chamber used to condition the test specimens has a storage capacity of ten (10) slabs, thus accommodating five specimens of each set. The slabs were conditioned for 10 weeks, such as to reach a carbonation depth of at least 3 mm, which was assessed through phenolphthalein measurements performed on cores (Figure 6-3). As a matter of fact, as seen on the picture, the carbonation front had reached a depth of the order of 10 mm.

All slabs were then overlaid (75-mm thick overlay) with a 27.5-MPa ready-mix concrete mixture similar to the one used originally for the base slabs, except for the maximum aggregate size (10 mm instead of 14 mm).

The repair concrete mixtures characteristics and properties are also provided in Table 1. The repaired specimens were moist-cured for 3 days, after what they were air-dried for at least 28 days, until the bond strength tests were carried out. For bond strength evaluation, nine (9) pull-off bond tests were performed on each repaired slab.

The pull-off bond test layout and apparatus used in the program are shown in Figure 6-5. The repair material and the substrate had reached respectively 3 months and one year at the time the pull-off tests were performed. The average bond strength values recorded for the different test specimen series are summarized in Figures 6-6 and 6-7.



Figure 0-2: Carbonation depth measurement on a freshly exposed concrete section using phenolphthalein

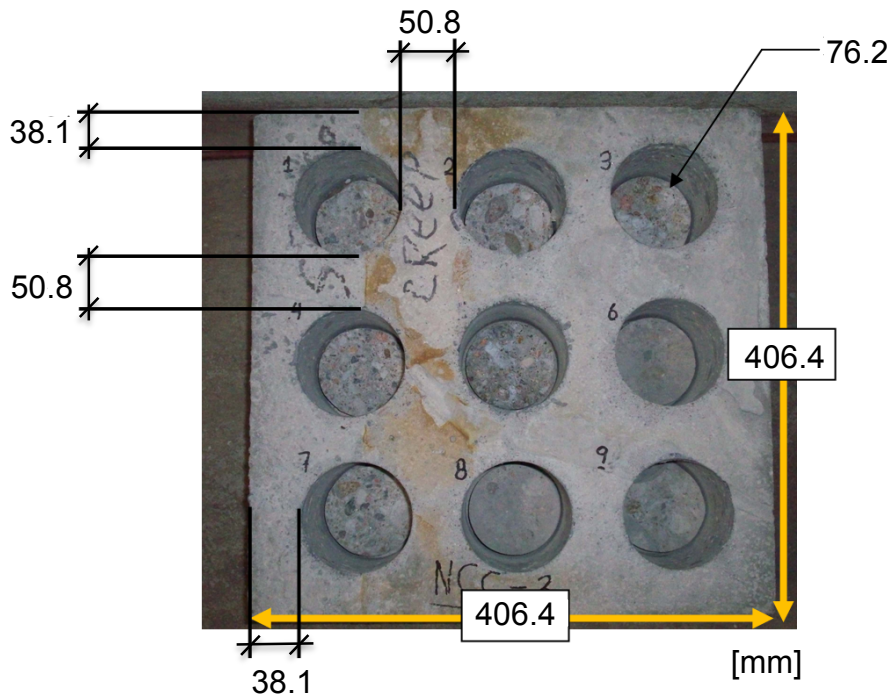


Figure 0-3: Slab coring template



Figure 0-4: Pull-off bond test apparatus

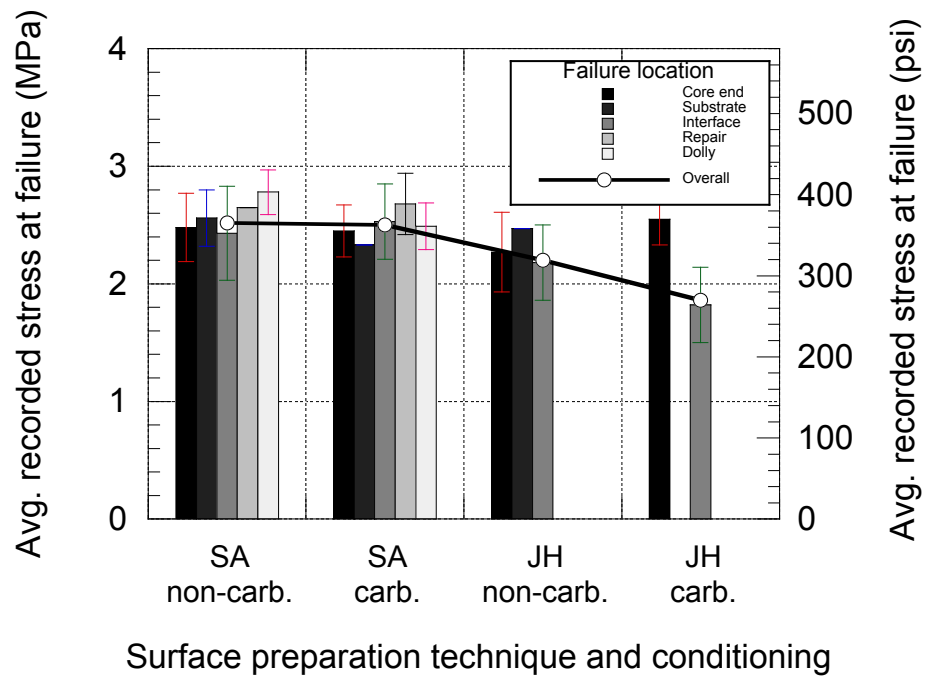


Figure 0-5: Bond strength results for the chipping hammer surface preparation

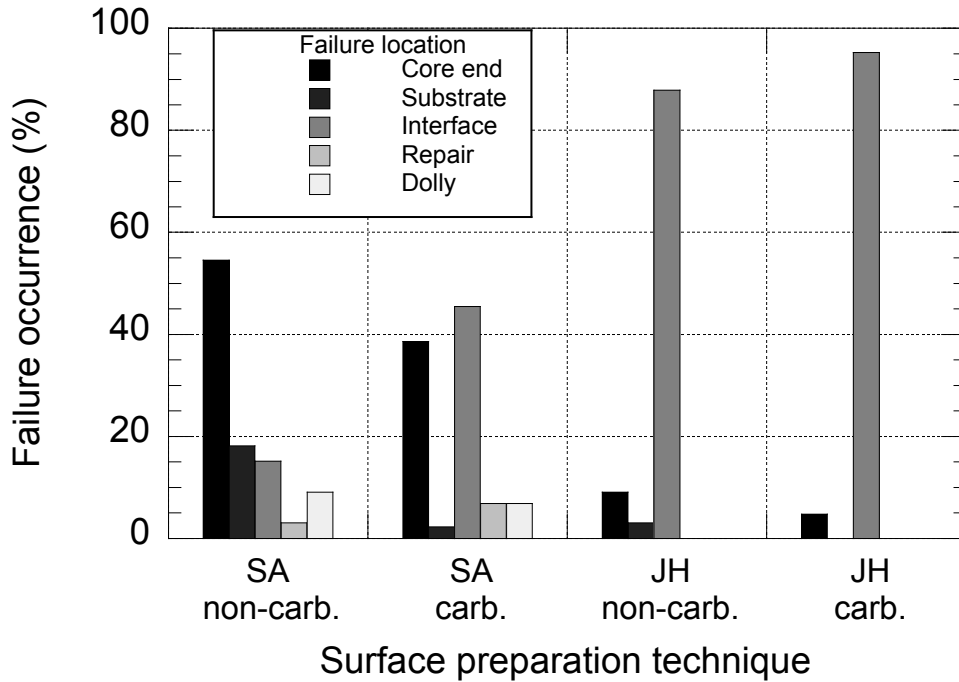


Figure 0-6: Bond strength results for the sandblast surface preparation

All failure modes displayed on the bar charts referred to the actual types of failures observed during the test. In the present case, three types of failures were observed: 88% of the failure occurred at the interface, 3% in the substrate, and 9% at the bottom. In this case, four different failures were observed: at the bottom of the core, in the substrate, at the interface and in the repair/top of the core. 15% of the failure occurs at the interface, 55% at the bottom, 18% in the substrate and 12% at the repair/top of the core.

With regard to figure 5-4 and 5-5, the effect of carbonation seems to be more significant with the chipping hammer surface preparation than with sandblasting. For the chipping hammer

preparation, a loss of bond strength around 16% was measured while no effect of the carbonation was recorded with the slabs sandblasted prior to repair.

6.3 Conclusions

The effects of concrete substrate carbonation have on the tensile bond strength of the repair material to the substrate were investigated. The results obtained allowed for the following conclusions.

1. There was no difference found in tensile bond strength between carbonated and non-carbonated concrete surfaces, prepared by sandblasting.
2. There was a significant difference in tensile bond strength between carbonated and non-carbonated concrete surfaces, prepared utilizing chipping hammer. The bond strength of repair to carbonated concrete surface prepared by chipping was about 16% lower than to the non-carbonated concrete surface prepared by the same method.
3. Such difference in the tensile bond strength developed between repair material and carbonated concrete substrates prepared by sandblasting and chipping most likely can be attributed to the light bruising of the concrete surface caused by the chipping hammer operation. The difference between bond of repair to non-carbonated concrete surfaces prepared by sandblasting and chipping (the bond to the sandblasted surface was 13% stronger than to the surface prepared by chipping).
4. It also must be concluded that only one type of repair material - regular concrete - was used in the experiments, and different cement-based materials may behave differently in tensile bond development to the carbonated concrete surfaces.

The effects of concrete substrate carbonation on the tensile bond strength for surfaces prepared by sandblasting and chipping techniques were investigated and analyzed.

The following basic conclusions were drawn:

- For substrate surfaces prepared by sandblasting there was no difference in bond strength found between carbonated and non-carbonated concrete surfaces;
- For substrate surfaces prepared by chipping a significant reduction (16%) of bond strength was documented for carbonated surfaces compared to non-carbonated;
- Such different effects of carbonation were attributed to the possible micro defects (bruising) of the surface prepared by chipping hammer.
-

It should be added that the limited amount of tests performed using only one type of a repair material does not allow for conclusions on the overall effect of carbonation on the tensile bond strength. Different repair materials may behave not necessarily the same way in bond development to the carbonated surfaces.

6.4 References

1. **ACI 116R-00**. Cement and Concrete Terminology. ACI manual of concrete practice, American concrete institute, 2000, pp. 11

2. **ACI Committee 201.** Guide to durable concrete. *ACI 201.2R-01*, American concrete institute, 2000, 41 p.
3. **ASTM C 39.** Standard Test Method for Compressive Strength of Cylindrical Concrete Specimens. *Annual Book of ASTM Standards*. 2009, Vol. 04.02, pp. 1-7.
4. **ASTM C 496.** Standard Test Method for Splitting Tensile Strength of Cylindrical Concrete Specimens. *Annual Book of ASTM Standards*. 2009, Vol. 04.02, pp. 1-5. 4.
5. **Beushausen, H-D.** Long-term performance of bonded concrete overlays subjected to differential shrinkage. *Ph D. Thesis presented at University of Cape Town*, South Africa, February 2005, 265 p.
6. **Block, K., and Porth, M.** Spritzbeton auf carbonatisiertem Beton. *Beton*, 1989, No. 7, pp. 299-302.
7. **Gulyas, R.J., Wirthlin, G.J., and Champs, J.T.** Evaluation of Keyway Grout Test Methods for Precast Concrete Bridges. *PCI Journal*, 1995, Vol. 40, No. 1, Jan – Feb., pp. 44-57.
8. **Meyer A.** The importance of surface layer for durability of concrete structures, *ACI special publication*, 1987, SP 100, pp.49-62
9. **Vaysburd, A. M., Sabnis, G. M. and Emmons, P. H.** Concrete carbonation - A fresh look. *Indian Concrete Journal*. 1997, Vol.67, No. 5, pp. 215-220.

Table of contents

Table of contents i

**Section 7 – Guide Specifications for Surface Preparation of Concrete Surface
for Repair 2**

7.1 General introduction 2

7.2 Concrete removal 5

 7.2.2 Structural safety 6

 7.2.3 Precautions prior to concrete removal 6

 7.2.4 Concrete removal geometry..... 7

 7.2.5 Saw cutting 8

 7.2.6 Chip cutting 9

 7.2.7 Concrete removal techniques 10

 7.2.7.1 General10

 7.2.7.2 Impacting methods.....10

 7.2.7.3 Waterjetting12

 7.2.8 Treatment of reinforcing steel 15

 7.2.9 Concrete surface roughness..... 16

7.3 Evaluation of adhesion 17

7.4 Evaluation of optimum moisture content 18

7.5 Perspectives 19

Section 7 – Guide Specifications for Surface Preparation of Concrete Surface for Repair

This part is intended to provide guidance on the surface preparation of concrete prior to repair and overlay. It can be used by the individuals involved in developing project specifications who are competent to analyze the significance and limitations of these guide specifications' content and who will accept responsibility for the application of the material and provisions it contains.

Guide Specifications were developed for surface preparation of existing concrete for repair/overlay with Portland cement concrete and pre-packaged cement-based materials.

The document is developed based on the previous results and the review of best practices and knowledge in the area of concrete repair.

7.1 General introduction

These guide specifications contain design and construction recommendations for surface preparation of concrete for repair and overlay. The document summarizes current knowledge, best practices and results of the research concerning the surface preparation of concrete prior to application of repair/overlay materials. The guide specifications are applicable to repairing damaged or deteriorated concrete structures, correcting design or construction deficiencies, or upgrading a structure for new uses, or to meet more restrictive code requirements.

The specification details removal of concrete, preparation of the concrete substrate surfaces for repair and quality control/quality assurance of the work performed. These guide specifications are recommended for design engineers and personnel who face task of introducing the best practices for concrete surface preparation on repair and rehabilitation projects. These guide specifications are recommended for use after they have been modified to reflect specific local conditions.

To achieve the goal of durable repaired concrete structure the specifier of a specific structure shall use equipment, techniques and procedures that are appropriate for the project objectives, deterioration mechanism(s), environmental conditions, structural circumstances and other local conditions and limitations which exist for the specific structure or part of the structure under consideration.

Repair geometries, locations, access, amount and spacing of reinforcement, climatic conditions, available equipment, local engineering and labour skills, local regulations, etc. have to be analyzed and addressed in properly tailored specifications.

The success of concrete repairs is dependent on determining the cause and extent of concrete distress or deterioration establishing realistic repair objectives and developing a repair strategy to address the problem. Typical steps of a systematic repair are as follows.

1. A condition survey with a scope consistent with the perceived condition of the structure and the owner's repair objectives, performed by qualified individuals, to document and evaluate visible and non-visible defects and damage as well as potential damage.
2. An assessment of the application and service conditions to which the concrete repair is, or will be, exposed.
3. Determination of the cause of the damage or deterioration necessitating the repair; for example, mechanical damage such as impact or abrasion; design, detailing or construction deficiencies; chemical damage, such as alkali-aggregate reaction; physical damage related to cycle of freezing and thawing or thermal movements; and corrosion of the steel reinforcement caused by improper placement, carbonation of the concrete, or chloride ingress into the concrete.
4. Determination of the repair objectives, including desired service; and durability planning including service life modeling.
5. Design of a repair project including appropriate specification for a particular project.

6. In the specific repair project, the specifier should consider outside constraints such as limited access to the structure; the operating schedule of the structure; any limitation imposed by the owner of the structure, including the cost; the required useful life of the repaired structure.
7. Consideration shall be given to the physical, chemical and electrochemical condition of the existing concrete substrate, the ability of the structure to carry loads, movement and vibration during repair, ambient conditions, and the characteristics of substrate materials and those of the repair materials and systems.
8. Safety and structural stability before, during and after repair shall be maintained in accordance with the specific project specifications and design.

The following requirements shall be met:

1. The achievement of the required condition of the substrate regarding cleanliness, roughness, cracking, tensile and compressive strength, chlorides and other aggressive agents, depth of carbonation, moisture content and temperature.
2. The achievement of the compatibility of the existing concrete and reinforcement with the repair and protection materials and systems, and compatibility between different repair and protection products, including avoiding the risk of creating conditions which may cause acceleration of corrosion.
3. The achievement of the specified requirements, characteristics and properties of repair materials and systems and the composite repair system regarding the fulfilment of their purpose to prolong the useful service life of the structure.
4. The achievement of the required repair application conditions regarding ambient temperature, humidity, wind force and precipitation and any temporary protection when needed.

This Guide Specifications provides commentaries with background information to the normative text to facilitate specific requirements and decisions when particular project specifications are designed.

7.2 Concrete removal

7.2.1 Description

This section specifies procedures, equipment and requirements for the removal of concrete in areas designated for repair. The process of concrete preparation for repair is the process by which sound, clean, and suitably roughened surfaces are produced on concrete substrates. This process includes the removal of unsound and, if necessary, sound concrete and bond inhibiting foreign materials from the concrete and reinforcement surfaces, opening the concrete pore structure, reinforcement damage verification and repair, if necessary.

Unsound or deteriorated concrete shall be defined as: concrete affected by spalling, delamination, disintegration and concrete in areas with severe cracking where active corrosion of reinforcing steel has been detected. “Unsound” concrete suggests that the material is in a reduced physical condition and hence relatively easy to remove. Alternatively “sound” concrete in all probability may be in physically good condition and involves considerable effort for its removal. Contaminated with chlorides and/or carbonated concrete is usually physically sound concrete.

Concrete removal usually involves unsound material. However, some sound concrete is also removed to permit for adequate repair geometry, to remove contaminated concrete, to prepare embedded reinforcement, and to permit structural modifications. The effectiveness of various concrete removal techniques may differ for unsound and sound concrete and a combination of techniques may be necessary.

Proper attention to surface preparation is essential for a durable repair. Regardless of the cost, complexity and quality of the repair material and application method selected, the care with

which concrete is removed and concrete reinforcement surfaces are prepared will often determine whether a repair project will be successful.

The methods used to remove the deteriorated or contaminated concrete and prepare the concrete and reinforcement to receive the repair material shall not weaken the surrounding sound concrete and reinforcement.

7.2.2 Structural safety

Before starting removal of existing concrete, the effect of the removal on the structural integrity should be reviewed. In cases where removal of deteriorated concrete and/or severely corroded reinforcing steel can affect the load carrying capacity of the structure or its elements, a temporary shoring system should be provided to relieve the loads from the structure or its member being repaired. Caution needs to be exercised in order that the safety of the structure is not jeopardized by repair activities.

Details of shoring to be used shall be provided by the Contractor and shall be designed and sealed by a Professional Engineer; this does not, however, in any way relieve the Contractor of his responsibility for the safety and adequacy of the shoring system.

The limitations for concrete removal such as the depth, reduction of cross section, the amount of concrete removed from the top surface, etc. shall be subject to the restrictions described in the contract.

7.2.3 Precautions prior to concrete removal

The areas where concrete is to be removed shall be examined to determine if there are electrical conduits, utility lines, or other embedments which may be damaged during removal.

If required, the Contractor shall enclose work area with a plastic barrier to confine dust and debris inside the work areas. The enclosures shall be securely constructed-and inspected by the Contractor each working day to ensure that there are no holes or tears.

The Contractor shall ensure that the level of equipment exhaust fumes (such as from air compressors or portable generators) is within acceptable limits. If the fume level cannot be kept at an acceptable level using the existing garage exhaust fans, then the Contractor shall use other equipment or relocate the equipment so that the fumes can be properly exhausted away from occupied areas.

All necessary precautions shall be taken to ensure that dust or falling debris does not constitute a hazard to personnel, equipment, the structure, its occupants and the general public. Effective means of clearing dust and debris away from the working area shall be continuously implemented.

The extent and depth of concrete removal required shall be measured and recorded on drawings by the Contractor and agreed with the Engineer as the work proceeds.

7.2.4 Concrete removal geometry

The location, number, and extent of defects shown in the Contract are indicative only. The true location, number, and extent of defects requiring repair can only be assessed properly by close inspection and other testing during the course of concrete removal. The limits of each repair shall be marked with chalk or paint by the Contractor as a series of straight lines on the surface. The limits of each repair shall be subject to agreement by the Engineer.

Areas requiring repair shall be modified to provide for simple layouts. The layouts shall be designed to reduce boundary edge length and eliminate acute angles. Excessive or complex edge conditions are usually produced by trying to closely follow the shape of the deteriorated concrete. Such edge conditions often result in shrinkage stress concentrations and cracking.

The perimeters of repairs that involve concrete removal shall provide right angle cuts to the concrete surface by saw cutting, chipping or hydrodemolition.

7.2.5 *Saw cutting*

A saw cut along the perimeter of the area where concrete is to be removed shall be provided to reduce edge spalling and to provide a sound edge surface against which the repair material will be placed. The saw cuts shall be made to a depth of approximately ½ inch (13 mm). Where the cover to the reinforcing steel is low, disk cutting will have to be omitted in order to avoid damage to reinforcement.

The saw cut surfaces shall be roughened prior to application of a repair material. It is best achieved by sand or grit blasting at the same time as cleaning of exposed reinforcement. Care needs to be exercised when roughening the disc-cut surfaces to avoid damage to the repair cavity edges.

The advantages of the saw cutting procedure include the following:

- The saw leaves vertical edge faces;
- The forces experienced by the pavement during chipping are isolated within the sawed boundaries;
- Very little spalling of the remaining pavement occurs;
- Removing the deteriorated concrete within the sawed boundaries is usually easier and faster when the boundaries are sawed than when they are not sawed;
- Most crews are familiar with the method.

The disadvantages of the saw cutting procedure include the following:

- More workers are required than in the other procedures;
- Since water is used when sawing, the repair area is saturated for some time, possibly delaying the repair;
- Saw overcuts weaken the repair area and must be cleaned and sealed;
- The polished, vertical repair boundary faces may lead to poor bonding;

- If more unsound concrete is later found beyond the sawed boundaries, the operation should be repeated to saw new boundaries causing extra work and further delays.

7.2.6 *Chip cutting*

The boundaries in chip procedure are the same as in the saw cut procedure, except the repair boundaries are not sawed. The concrete in the center of the repair area is removed using a light jackhammer with a maximum weight of 15 lb (6.8 kg). The concrete near the repair borders is then removed using a light jackhammer with a maximum weight of 15 lb (6.8 kg) and hand tools. The work should progress from the inside of the repair toward the edges, and the chisel point should be directed toward the inside of the repair.

The advantages of the chip cutting procedure include the following:

- The rough vertical edge produced promotes bonding;
- There are no saw overcuts;
- It has fewer steps than the saw cut method;
- Spalling is controlled by using light hammers at the edges.

The chip and patch procedure may be faster because it has fewer steps; the patch boundaries are not sawed, and there are no saw overcuts to be cleaned and sealed. Once joint sawing is complete, the saw is not needed again, even if more unsound concrete is later found beyond the boundaries.

The disadvantages of the chip cutting procedure include the following:

- Sound concrete may be damaged by chipping hammers;
- Hammers can cause feathered patch edges;
- Vertical sides are difficult to achieve.

7.2.7 *Concrete removal techniques*

7.2.7.1 General

Concrete removal methods are categorized by the way in which the process acts on concrete. The general categories are impacting, blasting, cutting, milling, pre-splitting, and abrading. ACI 546R Concrete Repair Guide provides a description of these categories, lists the specific removal techniques, and provides a summary of information on each technique.

Only impacting and hydrodemolition (waterjetting) concrete removal methods are addressed in this section.

7.2.7.2 Impacting methods

Impacting methods are the most commonly used concrete removal systems. They generally employ the repeated striking of a concrete surface with a high energy tool to fracture and spall the concrete. Impacting methods include hand-held breakers and scabblers.

The hand-held breaker or chipping hammer is probably the best known of all concrete removal devices. Hand-held breakers are available in various sizes with different levels of energy and efficiency. The smaller hand-held breakers (15 pounds) are commonly specified for use in partial removal of unsound concrete or concrete around reinforcing steel, because they do little damage to surrounding concrete. The larger hand-held breakers (30-90 pounds) are used for complete removal of large volumes of concrete. Care shall be exercised when selecting the size of breakers to minimize the damage to existing concrete and its bond to embedded reinforcing steel.

Chipping hammers are typically classified by weight, even though breakers of similar weight do not necessarily generate the same impact force.

The percussive force used by pneumatic breakers to fracture concrete is primarily determined by the impact energy and the frequency at which the impacts occur. The impact energy is based

on the mass of the piston, the size of the cylinder, and the inlet port diameter. Impact energy ranges from approximately 15 lb (7 kg) per blow for small tools to more than 180 lb (82 kg) per blow for large tools. The frequency of impact, or blows per minute, ranges from 900 blows per minute to more than 2,000 blows per minute, depending on the valve design.

Various cutting tools are available for use with hand-held pneumatic breakers. The shank end, which is inserted into the tool-retaining mechanism, is common to all. The cutting or working end can vary from a broad spade like blade to a sharp well-honed point. The vast majority of concrete removal work is done with a pointed tool, although a relatively narrow (3 in. to 4 in. [7.5 cm to 10 cm]) blade-type tool is sometimes used to remove cracked and deteriorated concrete.

Effect of the breaker concrete removal operation must be monitored to ensure minimal impact on surrounding environment. The primary issues of concern are noise, dust, and flying debris.

The first step in the removal procedure is saw cutting the repair boundaries. The deteriorated concrete in the center of the repair is then removed using a light jackhammer with a maximum weight of 15 lb (6.8 kg). The work should progress from, the inside of the repair toward the edges. When all unsound concrete in the repair area is removed and repair geometry is established the final procedure is to remove the concrete near the repair borders using a light jackhammer and/or hand tools.

Removal near the repair boundaries must be completed with hammers fitted with spade bits as gouge bits can damage sound concrete. Jackhammers and mechanical chipping tools should be operated at an angle less than 45 degrees from the vertical.

Water-wash equipment shall be used to remove sawing slurry from the repair area before it dries.

7.2.7.3 Waterjetting

The waterjetting procedure uses a high pressure water jet to remove deteriorated concrete. A high-pressure water jet uses a small jet of water driven at high velocities commonly producing pressure of 10,000 to 45,000 psi (69 to 310 MPa) and above.

High-pressure water jetting (hydrodemolition) may be used as a primary means for removal of concrete when it is desired to preserve and clean the steel reinforcement for reuse and to minimize damage to the concrete remaining in place. Hydrodemolition disintegrates concrete, returning it to sand and gravel-sized pieces. This process works preferentially on unsound or deteriorated concrete and leaves a rough profile. Care must be taken not to punch through thin slabs or decks if unsound concrete exists in an area to be repaired.

High-pressure water jets in the 10,000 psi (70 MPa) range require 35 to 40 gal/min (130 to 150 L/min). As the pressure increases to 15,000 to 20,000 psi (100 to 140 MPa) the water demand will vary from 20 to 40 gal/min (75 to 150 L/min). The equipment manufacturer should be consulted to confirm the water demand. Ultra-high-pressure equipment operating at 25,000 to 35,000 psi (170 to 240 MPa) has the capability of milling concrete to depths of $\frac{1}{8}$ inch to several inches (3 mm to approximately 50 mm).

Waterjetting (hydrodemolition) should not be allowed for concrete removal if there is a possibility that unbonded post-tensioned systems are within the concrete removal zone. The only viable method of concrete removal in this situation is concrete removal using lightweight chipping hammers.

Two trial areas, one of sound concrete and one of deteriorated concrete, are then used to determine the appropriate waterjetting operating parameters. These parameters include speed, pressure, and the number of overlapping passes. Using trial and error in the test areas, the waterjet must be programmed, removing sound concrete unnecessarily. In the sound area, consistent concrete removal depth of $\frac{3}{4}$ inch behind the reinforcing bar shall be obtained. After

successful cutting of the above test area, with specified depth control, the operation shall be moved to the deteriorated concrete and remove all deteriorated concrete. If a result is obtained which meets the specified requirements, these parameters shall be used as a basis for the production removal. If not, the Contractor shall repeat the trial process and recalibrate the equipment or replace the equipment until a result which meets the specified requirements is obtained. Once properly calibrated, the operating parameters should not be changed while waterjetting the rest of the spalls, unless the concrete changes (for example, a harder aggregate has been used in one section of the structure). If the concrete does change, the waterjetting machine must be recalibrated using two new trial areas in the section with the different concrete.

All concrete within a marked for repair area should be removed to a minimum depth of 2 in (51 mm) with neat vertical faces. Then the repair area must be tested again for soundness. Any additional unsound concrete must be removed by continued waterjetting.

The debris and slurry that result from the waterblasting operation must be removed using a low-pressure water stream before the slurry dries and hardens on the surface of the cavity. If this is not done, the repair area may have to be refaced. Once dried, sandblasting may or may not be able to remove the dried slurry residue. Some moisture-sensitive materials may require the repair area be completely dry before placing the material.

The advantages of waterjetting include the following:

- It requires fewer workers than the other procedures;
- Once an experienced operator adjusts the operating parameters, only weak concrete is removed;
- The cavity surfaces produced are vertical, rough, and irregular, and enhance bonding;
- No hauling is required.

The disadvantages of waterjetting include the following:

- The finished surfaces are saturated. Placement must be delayed until the area dries unless the repair material is not moisture-sensitive;

- The fine slurry laitance remaining after the procedure requires careful attention during cleaning;
- A protective shield must be built around the repair area traffic if the patch is next to occupied areas;
- It can be difficult to control the depth of removal;
- Equipment rental is expensive;
- It can be difficult to obtain a good production rate; performance of waterjetting equipment has been variable;
- The waste water and debris must be handled in an environmentally acceptable manner as prescribed by local regulations.

Remark

Although hydrodemolition will not physically damage steel tendons, it is not considered to be a viable concrete removal technique if there is a possibility of the high- pressure water coming into contact with tendons, anchorages, or both. Reasons why hydrodemolition is not considered to be a viable technique include:

- 1) Hydrodemolition of post-tensioned concrete elements may cause a safety problem. It is potentially dangerous because it may accidentally undercut embedded anchors and result in explosive release of prestressing force.
- 2) If any part of the tendon is exposed to high water pressure, water may penetrate into the tendon. The water jets will likely destroy the sheathing on the tendons, whether it is wrapped in paper, plastic, tubing, or extruded plastic. If the sheathing is damaged, the water has a direct path to the prestressing strand or wire, and corrosion may result.
- 3) Concrete repair projects commonly include replacement of post-tensioning strand. The water pressure used in hydroremoval equipment can force slurry into the sheathing. When slurry and other debris exist within the sheathing, installation of a new strand becomes very difficult. When the new strand is pushed into the existing sheathing, debris

within the sheathing builds up ahead of the advancing strand. This buildup of debris can cause the sheathing to rip and “ball up” in front of the leading edge of the strand. This scenario makes strand replacement very difficult and compromises the corrosion protection or sheathing over the prestressing steel.

More information can be found in ACI 423.4R.

7.2.8 Treatment of reinforcing steel

The most frequent cause of concrete deterioration is the corrosion of embedded reinforcing steel; the evaluation of condition of reinforcing steel exposed in the repair area and proper reinforcement treatment steps will ensure that the repair will not fail prematurely.

The first step in preparing reinforcing for repair or cleaning is the removal of deteriorated concrete or sound chloride contaminated concrete surrounding the reinforcement. Extreme care should be exercised to insure that further damage to the reinforcing or prestressing steel is not caused by the process of removing the concrete. Impact breakers can damage reinforcing steel if the breaker is used without regard to the location of the reinforcement. Once the larger areas of unsound concrete have been removed, a smaller chipping hammer (15 lbs. Type) should be used to remove the concrete in the vicinity of the reinforcement. Care should be taken not to vibrate the reinforcement or otherwise cause damage to its bond to concrete adjacent to the repair area.

All unsound concrete shall be chipped away. If during the removal operation, reinforcing steel is exposed, then concrete removal around the bar shall continue to provide a minimum $\frac{3}{4}$ inch clear space between the rebar and surrounding concrete or $\frac{1}{4}$ inch larger than the maximum size aggregate in the repair material, whichever is greater.

Additional concrete removal shall be carried out along corroded exposed bars until a continuous length of 50 mm (2 in) of bar free from corrosion is exposed. The limit of activity corrosion shall be assessed on a visual basis. The edges of any additional areas removed shall

be cut square as specified above. The extent of concrete removal shall be agreed by the Engineer before any commences.

An additional length of uncorroded bar will have to be exposed out if couplers or lap splices are to be used for replacement reinforcement.

7.2.9 Concrete surface roughness

Interface roughness depends to a large extent on the method of substrate surface preparation. Mechanical methods of concrete removal normally leave the substrate surface much rougher than blast methods. The magnitude of surface roughness for concrete repairs is commonly measured in mm.

Unacceptably rough of flat substrate profiles after concrete removal may be reduced through additional work using properly selected surface preparation technique.

The decisions about surface preparation and its roughness in particular, cannot be made without knowing the properties and application requirements of the selected repair/overlay material. Material manufacturer shall be consulted.

For selecting, specifying and evaluating the concrete surface profile, follow the ICRI Guideline No. 03732, "Selecting and Specifying Concrete Surface Preparation for Sealers, Coatings, and Polymer Overlays": the nine concrete surface profile chips provide benchmarks profiles to aid in achieving the desired results. Each profile carries a CSP number ranging from a base line of CSP 1 (nearly flat) through CSP 9 (very rough).

Recently, various techniques were developed for concrete surface profile characterization. The combination of different methods can yield a very accurate description of the "roughness" at various scale levels, depending on the roughness range to be analysed. For instance, mechanical and laser lab-profilometers allow a more accurate micro-roughness characterization, while the investigated interferometrical (optical) method provides a better description of the shape of the profile. Nevertheless, investigations of a range of concrete surface treatments with

very precise laser and mechanical profilometers clearly indicated that the surface treatment technique does not have much influence on micro-roughness (high-frequency waves). This indicates that only the waviness parameters actually need to be determined for assessing surface roughness prior to repair.

Among the techniques available today, the best suited method for field assessment appears seems to be the Concrete Surface Profile developed by ICRI: it is rapid, easy to use and yields reliable information, irrespective of the surface orientation. However, its use is limited right now to surface up to 6 mm in terms of profile height, for which it was actually designed for: it is clearly not suitable for water jetting or jack hammering evaluation.

The advantages of Sand Patch Test method are the speed and its applicability in situ on a surface that has to be protected from wind and rain. The biggest limitations are range of validity (from 0.25 to 5 mm), which usually exclude surface with high holes and peaks and possibility of application only on horizontal surfaces. It gives however good correlations with statistical parameters like W_a .

Considering the fact that surface preparation essentially influences waviness, the optical method based on Moiré's pattern, which offers significant advantages in terms of production rate and surface area treatment capability, could in fact be used alone to perform the whole surface roughness characterization. The method directly yields a handful of reliable quantitative data, but the equipment available today is not adapted to daily field applications. Nevertheless, with the rapid technological development in that field, the availability of suitable optical devices can be foreseen in a near future. This would allow even more rapid and objective assessment.

7.3 Evaluation of adhesion

.....

7.4 Evaluation of optimum moisture content

For bonded overlays it is commonly specified that the substrate surface has to be pre-wetted but surface-dry prior to overlay application. However, little evidence is provided in the literature suggesting that this actually improves the quality of the bond. If pre-wetting is done then it needs to be ensured that the substrate surface has dried out completely before the overlay is applied as any water in the substrate surface pores will prevent mechanical interlock between substrate and overlay.

The moisture condition of the substrate will determine the rate of movement of water from the repair mortar to substrate concrete due to the moisture imbalance between the two layers. Both the surface moisture condition and the moisture distribution inside the substrate are important.

The optimum moisture condition will vary from substrate to substrate in otherwise equal conditions because the performance of the bond depends on the way the substrate will affect the direction and rate of water movement between phases of the composite repair system.

Investigations concerning the measurement of water saturation levels and their effect on the adhesion of cement and polymer cement concrete repair systems have shown that the Modified Capillary Suction Test (MCST) gives clearer, more accurate and lower dispersive information than the Initial Surface Absorption Test (ISAT), with a higher correlation for water content measurement (wet and dry weighing). Moreover, there is a very good correlation between the water absorption index and the capillary absorption coefficient determined using the ISAT and MCST tests, respectively.

MCST requires to core a sample of concrete and to test it in the laboratory. ISAT is an attractive option for performing a quantitative test to evaluate the saturation level of a concrete substrate: it is compact, cost-effective and quick. The higher variation and dispersion of results for ISAT may stem from the difficulty of performing the test with a rough concrete surface (after

hydro-jetting). Procedures are influenced by the surface quality, but it is difficult to conclude whether this is due to cracking or roughness.

Evaluation of humidity content remains a challenge and no clear recommendations can be proposed.

There is a large range of saturation levels (50 to 90%) where adhesion remains high and constant, which seems to limit the influence of environmental conditions on adhesion of hydraulic binder-based repair systems. The adhesion is relatively weak for low saturation levels (< 50%), but it reaches classical values for saturation levels between 55 and 90%;

When acrylic emulsion is used as a bonding layer, the highest saturation levels induce a water film at the interface, which is incompatible with polymeric material and artificially reduces the effectiveness of the adhesion.

This clearly points to the effect of water in the concrete superficial zone and the difficulty of accurately evaluating the saturation level. Saturation levels from 55 to 90% must be attempted for cement concrete and polymer cement concrete repair systems.

7.5 Perspectives

Extend the CSP ICRI plates

To evaluate humidity